Wayne State University Dissertations

1-1-2013

Progress Towards Development Of Multifunctional, Dopamine D2/d3 Receptor Agonists As Symptomatic And Disease-Modifying Therapeutic Agents For Parkinson's Disease

Mark Andrew Johnson
Wayne State University,

PROGRESS TOWARDS DEVELOPMENT OF MULTIFUNCTIONAL, DOPAMINE D2/D3 RECEPTOR AGONISTS AS SYMPTOMATIC AND DISEASE-MODIFYING THERAPEUTIC AGENTS FOR PARKINSON'S DISEASE

by

MARK JOHNSON

DISSERTATION

Submitted to the Graduate School

of Wayne State University,

Detroit, Michigan

in partial fulfillment of the requirements

for the degree of

DOCTOR OF PHILOSOPHY

August 2013

MAJOR: PHARMACEUTICAL SCIENCES
(Medicinal Chemistry)

Approved by:

_____
Advisor   Date

_____

_____

_____

DEDICATION

I dedicate this dissertation to my parents and grandparents, who worked so hard to provide me the opportunity to pursue my dreams. I especially dedicate this to my late father, who dedicated his life to his family and made me the person I am today. The love that my father has shown me is the true inspiration behind this work.

My wife Caitlyn and our two beautiful children, Noah and Julia, have been a guiding light for me over the course of my graduate studies. Through failures and setbacks, their constant love and support reminded me that success is worth the struggles. I love each of them more than words can describe and this work is equally dedicated to them. I am not able to say enough words to describe the appreciation I have for my parents, grandparents and family for their love and support over the years. I have had the chance to pursue my dreams in something that I love and am passionate about, an opportunity that not every child is granted. My parents sacrificed and sometimes struggled in order to offer me the bright future they envisioned for me. I have been fortunate to be raised in a family that put love for each other above all else. This is the greatest gift I have been given and for it, I am forever grateful.

TABLE OF CONTENTS

LIST OF TABLES

LIST OF FIGURES

LIST OF SCHEMES

*CHAPTERS 1 & 3 CONTAIN MATERIAL FROM PUBLISHED WORK IN WHICH I WAS THE FIRST AUTHOR. THE CO-AUTHORS OF THESE PUBLICATIONS AGREE TO THE USE OF THE PUBLISHED DATA IN THIS DISSERTATION.

CHAPTER 1

INTRODUCTION

1.1   Parkinson's Disease

Parkinson's disease (PD) is a progressive, neurodegenerative disorder that arises primarily through the loss of dopaminergic neurons in the substantia nigra pars compacta (SNc), resulting in a diminished level of the neurotransmitter dopamine (DA) in the nigrostriatal pathway and ensuing loss of motor function {Braak, 2003}. Common symptoms of PD include resting tremor, muscular rigidity, bradykinesia (slowness and decreased amplitude of movement), along with postural instability and cognitive psychiatric complications {Paulus, 1991; Sherer, 2001}. PD affects 1% of the population ≥ 65 and is the second most prevalent neurodegenerative disorder next to Alzheimer's disease. {Hoehn, 1998; Recchia, 2004}. The neuropathological hallmarks of PD are intracellular inclusions termed, Lewy bodies (LB) and Lewy neurites (LN), composed primarily of insoluble aggregates of ubiquitin and α–synuclein {Gomez-Tortosa, 1999; Spillantini, 1998a; Spillantini, 1998b}.

It is estimated that seven to ten million people worldwide are currently living with PD. The financial burden of treating PD is significant and especially troublesome for elderly, low-income patients. Medication expenses average approximately $2,500 per patient annually and the cost of therapeutic surgery can reach as much as $100,000. Additionally, when considering direct and indirect expenditures for PD treatment,

including payment of social security benefits and lost income from the inability to work, the cost soars to nearly $25 billion annually.

1.2 Pathogenesis of PD

In PD, the progressive loss of dopaminergic neurons, mainly in the SNc and ventral tegmental area, results in a depletion of DA in the basal ganglia and striatum. Low DA levels cause dysregulation of the motor circuits that project through this brain region, leading to the clinical manifestations of the disease. Although the etiology of PD is not yet clear and may be multifactorial, oxidative stress and mitochondrial dysfunction are thought to play a central role in the pathology of the disease {Cavalli, 2008}. A reduction in natural antioxidant defenses (glutathione, catalase, superoxide dismutase) has also been correlated with disease progression and susceptibility. In addition, increased iron concentration and protein aggregation, namely that of α–synuclein, are thought to be intimately associated with disease pathogenesis. These hypotheses have been strengthened by post-mortem studies of the PD brain, in which evidence of mitochondrial dysfunction, oxidative damage and elevated iron concentration and α–synuclein aggregation have been observed (Figure 1) {Jenner, 2003b; Mandel, 2003}.
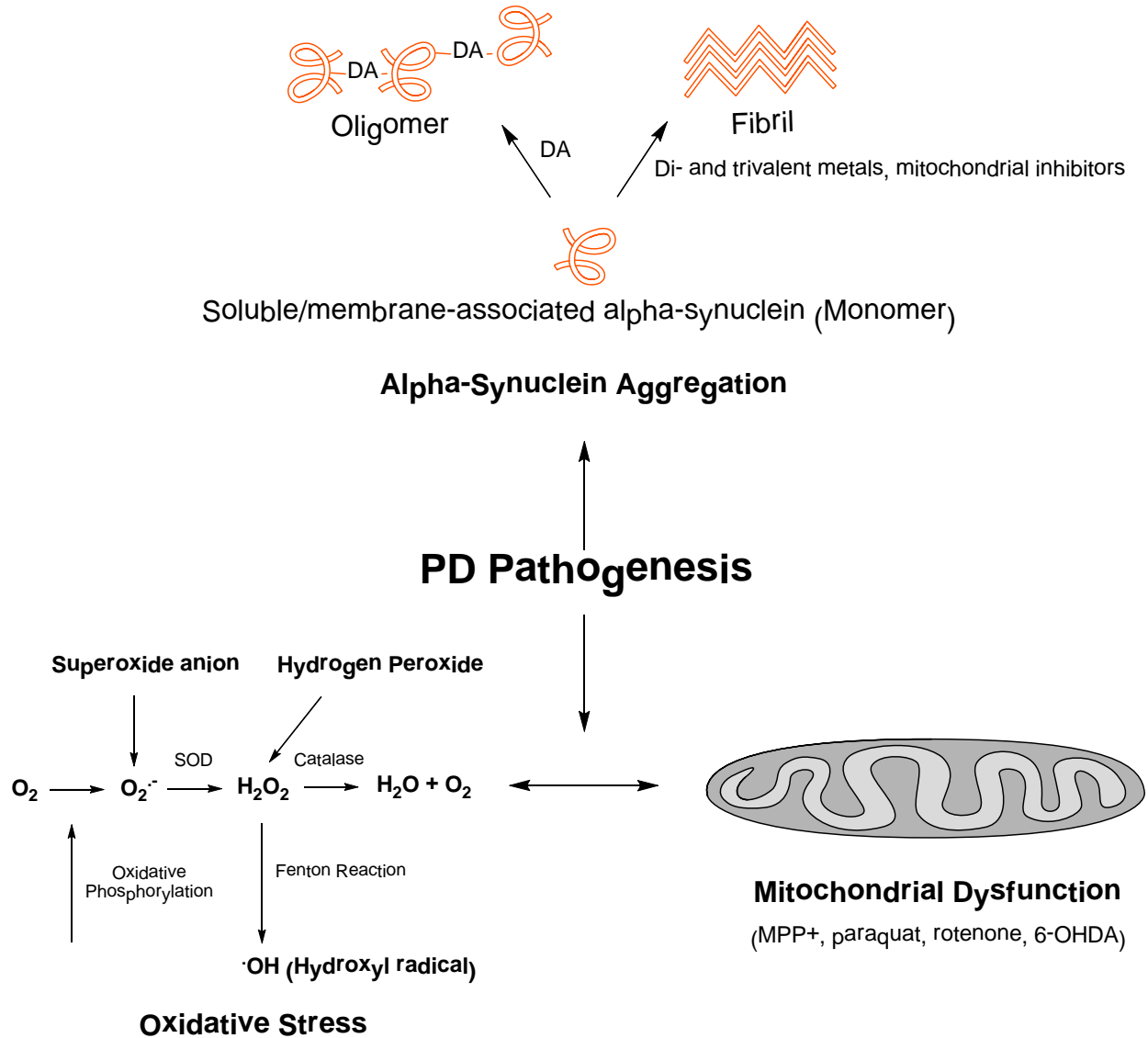
Figure 1. Multiple factors contributing to PD pathogenesis.

1.2.1 Mitochondrial Dysfunction and Oxidative Stress

Mitochondrial dysfunction is thought to be the leading source of increased oxidative and nitrosative stress observed in the brains of sporadic PD patients. Mounting evidence suggests a role for mitochondrial dysfunction in the pathogenesis of PD, specifically, defects in mitochondrial complex-I of the respiratory chain. Complex-I

deficits could be theorized to produce neuronal degeneration by way of decreased adenosine triphosphate (ATP) synthesis and damage caused by increased reactive oxygen species (ROS) production {Van Der Walt, 2003}. Genetic evidence that alterations in complex-I activity may play a role in the pathogenesis of sporadic PD is provided by the observation that a single nucleotide polymorphism in the gene encoding the nicotinamide adenine dinucleotide (NADH)-dehydrogenase 3 enzyme of complex I leads to a significantly lowered risk of developing PD in Caucasians {Sherer, 2002}. Epidemiological studies have indicated that environmental toxins and pesticides that inhibit complex-I activity are implicated in the pathogenesis of sporadic PD {Langston, 1983a}. MPTP (1-methyl-4-phenyl-1,2,3,6-tetrahydropyridine), a by-product of the manufacture of a synthetic opiate, inhibits complex-I activity and replicates nearly all features of PD in human and animal models {Dauer, 2003; Forno, 1988}. MPTP is converted by the enzyme monoamine oxidase B (MAO-B), in astrocytes, to its metabolite MPP+ (1- methyl-4-phenyl pyridinium). MPP+ is taken into DA neurons via affinity for the dopamine transporter (DAT), where it inhibits complex-I and leads to cell death {Forno, 1988}. In aged, nonhuman primates, MPTP treatment has been found to produce intracellular proteinaceous inclusions that bear a resemblance to immature LB, which are filamentous in nature and comprised of α-synuclein {Manning-Bog, 2002}. Paraquat, a known complex-I inhibitor with structural similarity to MPP+, induces selective degeneration of DA neurons along with aggregation of α–synuclein in the SNc of mice {McCormack, 2002; Savitt, 2006}. Systemic treatment of rats with rotenone, a known inhibitor of mitochondrial function, has been found to effect selective nigrostriatal

dopaminergic degeneration with coupled inclusion of α–synuclein fibrils {Eisenhofer, 2004}.

Mitochondria are exposed to an oxidative environment, as oxidative phosphorylation is coupled to the formation of ROS. Post-mortem analyses have consistently implicated oxidative damage in the pathogenesis of PD and oxidative damage to lipids and DNA has been found in the SNc region of the PD brain. Increased oxidative stress in PD may be attributed to one, or a combination, of the following processes: mitochondrial dysfunction, enzymatic and auto-oxidative DA metabolism, elevated free iron levels and compromised antioxidant defense pathways {Jenner, 2003b}.

1.2.1.1 Enzymatic and Auto-Oxidative DA Metabolism

DA is theorized to play a role in the neurodegenerative process via both enzymatic and auto-oxidative metabolism (Figures 2 & 3). DA is known to undergo nonezymatic, auto-oxidation, leading to reactive quinones and cytotoxic free radicals {Eisenhofer, 2000}. Additionally, DA is metabolized catalytically by MAO-B within astrocytes. MAO-B levels have been found to increase with age and in association with neurodegenerative disease in humans {Shapira, 1990}. MAO-B-catalyzed DA metabolism leads to production of a highly reactive catecholaldehyde metabolite, 3,4-dihydroxyphenylacetaldehyde (DOPAL), as well as hydrogen peroxide (H_2O_2) {Mallajosyula, 2008}. Furthermore, neurotoxicity of DOPAL has been demonstrated in both cell culture and animal models {Eisenhofer, 2000}. Hydrogen peroxide, a common by-product of both auto-oxidative and enzymatic DA metabolism, has further

implications, as it is converted by iron in the Fenton reaction to hydroxyl radical and other toxic free radical species that can contribute to the degenerative process.
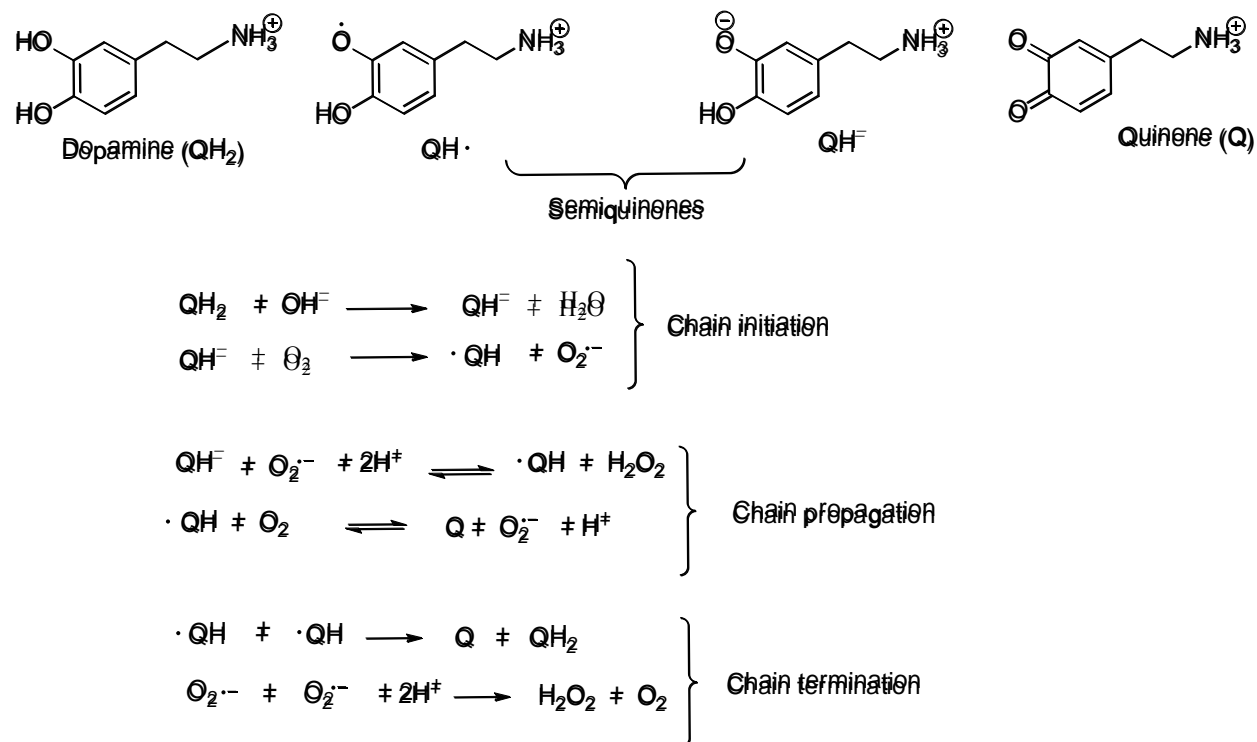
Figure 2. Auto-oxidative metabolism of DA.
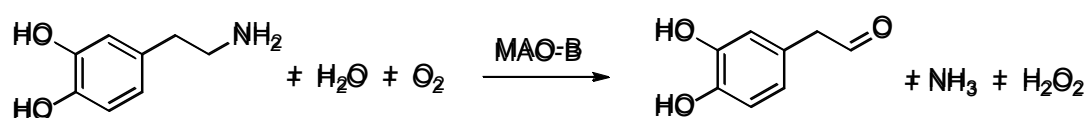
Figure 3. Enzymatic oxidation of DA by MAO-B, yielding toxic metabolites.

1.2.1.2 Increased Free Iron

Studies have shown that free iron ($Fe^{2+/3+}$) concentrations are considerably increased in parkinsonian SNc and within DA neurons. Under basal conditions, iron is

stored intracellularly in a non-toxic form by the ubiquitous protein, ferritin. Ferritin contains 24 α-helical subunits, comprised of both heavy(H)- and light(L)-chains. A significant reduction in the amount ferritin L-chains has been found in parkinsonian SNc. Due to the role of L-chains in iron storage within the shell of the protein, their decrease may lead to efflux of free iron from the protein complex. It is well established that free iron induces oxidative stress via initiation of the Fenton reaction (Figure 4), resulting in amplified hydroxyl radical production among other oxidative species. Hydroxyl radical is highly reactive and known to damage DNA, lipids and proteins, leading to further production of free radicals and propagation of the neurodegenerative process {Friedman, 2012}.

$$H_2O_2 + Fe^{2+} \longrightarrow OH^- + OH^. + Fe^{3+}$$

$$Fe^{3+} + O_2^{.-} \longrightarrow Fe^{2+} + O_2$$

$$\overline{O_2^{.-} + H_2O_2 \longrightarrow O_2 + OH^- + OH^.}$$
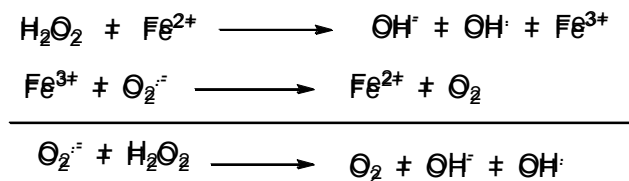
Figure 4. Fenton reaction. Fe^{2+} and Fe^{3+} catalyze the conversion of hydrogen peroxide and superoxide anion to molecular oxygen, hydroxide anion and hydroxyl radical.

1.2.1.3 Compromised Antioxidant Defense Pathways

An impairment of the antioxidant defenses posed by the cell can lead to increased oxidative stress. Under normal conditions, the generation of oxidative species is compensated by the action of endogenous antioxidants, including: reduced glutathione, glutathione reductase, glutathione peroxidase, catalase and superoxide dismutase (SOD) (Figure 5). Superoxide dismutases are a group of enzymes that

catalyze the conversion of superoxide to molecular oxygen and hydrogen peroxide. Additionally, hydrogen peroxide is decomposed to water by reduced glutathione, with the help of glutathione peroxidase at low concentration and by catalase at high concentrations. In PD, low levels of both glutathione and catalase have been found in the SNc region of the brain. Particularly, as glutathione is the major endogenous antioxidant produced by the cell (up to 5 mM), its significant reduction in the effected PD brain region leaves the DA neuron incapable of neutralizing oxidative species that are produced and oxidative stress remains unchecked {Fahn, 1992}.

$$2\ GSH\ +\ H_2O_2\ \xrightarrow{\text{Glutathione peroxidase}}\ GSSG\ +\ 2\ H_2O$$

$$GSSG\ +\ NADPH\ +\ H^+\ \xrightarrow{\text{Glutathione reductase}}\ 2\ GSH\ +\ NADP^+$$

$$2\ H_2O_2\ \xrightarrow{\text{Catalase}}\ O_2\ +\ 2\ H_2O$$

$$2\ O_2^{\cdot-}\ +\ 2\ H^+\ \xrightarrow{\text{SOD}}\ O_2\ +\ H_2O_2$$
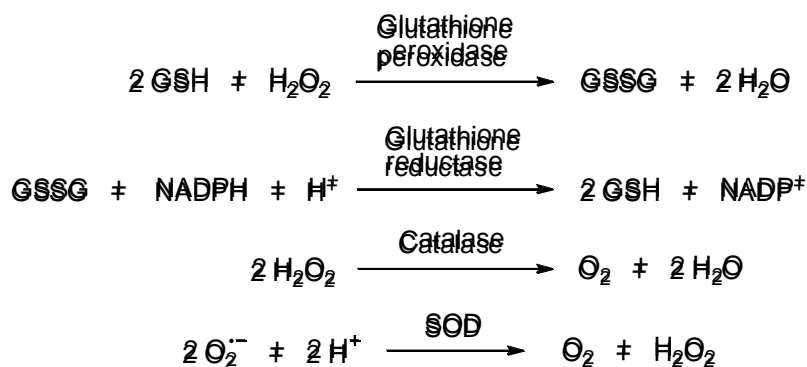
Figure 5. Decomposition of oxidative species via endogenous antioxidant defenses.

1.2.2 α-Synuclein Aggregation

A critical biomolecular event in PD pathogenesis is the aggregation of α–synuclein. Alpha-synuclein is a pre-synaptic, natively unfolded, neuronal protein that has been located to the cytoplasm and associated with cellular phospholipid membranes. However, the structure and function of α–synuclein in the cell remains

heavily debated. Aggregation of α-synuclein has been found to occur in a nucleation-dependent manner, in which elongation to the fibrillar form of the protein is preceded by smaller, oligomeric aggregates (Figure 6) {Wood, 1999}. Recent studies have demonstrated the oligomeric form of α–synuclein to be chiefly responsible for its neurotoxicity {Winner, 2011}. The mid-region of α–synuclein contains a hydrophobic, non-Aβ component (NAC) of Alzheimer's disease amyloid domain, which is thought to enable the protein to undergo conformational change from random coil to the β-sheet structure found in fibrillar forms of the protein {Serpell, 2000}. The findings that fibrillar α-synuclein is the major constituent of LB and the A30P and A53T mutated forms of the protein, which are associated with autosomal dominant forms of PD, have increased rates of self-aggregation compared to wild-type, has led to speculation that α-synuclein aggregation has a prominent role in PD {El-Agnaf, 1998}. Studies have demonstrated aggregation of α-synuclein in the presence of oxidative stress-inducing compounds and metals including: Al^{3+}, Fe^{3+}, Cu^{2+}, Co^{3+}, MPTP, DA, pesticides and lipids {Uversky, 2001a; Kowall, 2000; Cappai, 2005; Uversky, 2001b; Jo, 2000}.

However, α-synuclein is non-toxic in nondopaminergic human cortical neurons, suggesting its toxicity is DA-dependent. It is hypothesized that oxidative species produced via DA metabolism, such as hydrogen peroxide, superoxide and dopamine quinones, may be involved along with iron in the oxidation and aggregation of α-synuclein {Andersen, 2004}. Oligomeric α-synuclein is hypothesized to bind and permeabilize synaptic vesicles, releasing DA and leaving the protein more susceptible to oxidation {Volles, 2002; Lotharius, 2002}. Additionally, studies have uncovered a role for α-synuclein in regulation of DA biosynthesis via modulation of tyrosine hydroxylase

activity {Perez, 2002}. Interestingly, in embryonic midbrain cultures, α-synuclein-induced cell death is attenuated by depleting intracellular DA or antioxidant treatment. The attenuation of cell death in the absence of DA or in the presence of antioxidants indicates that loss of cell viability caused by α-synuclein is due to DA-dependent, oxidative events {Xu, 2002}.
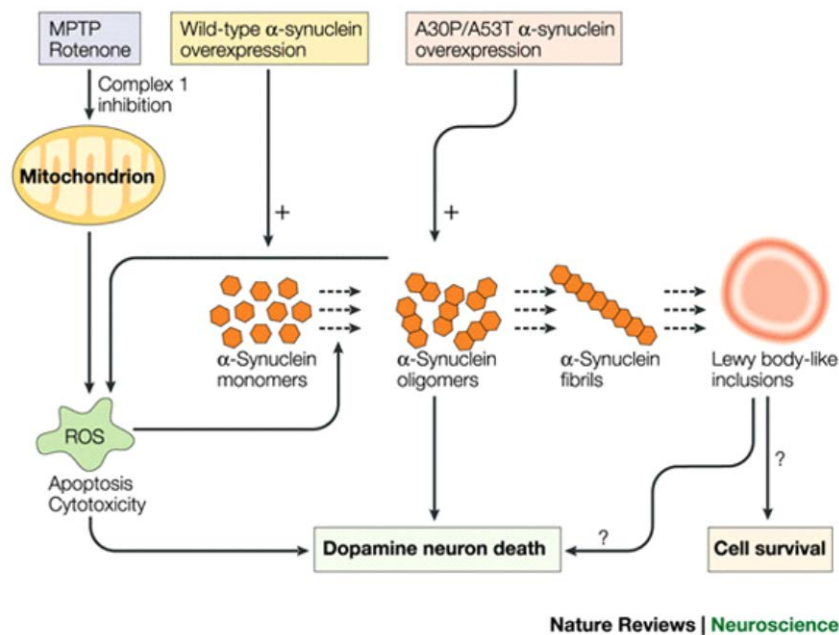
Figure 6. Multiple factors influencing α-synuclein aggregation and contributing to the neurodegenerative process.

1.3   Therapuetic Strategies for PD Treatment

1.3.1 Symptomatic Treatment

A range of therapeutic approaches have been used to treat the symptoms associated with PD. Since its discovery approximately 40 years ago, L-3,4-dihydroxyphenylalanine (L-dopa) has been the "gold standard" in PD treatment. L-dopa

is the biosynthetic precursor to endogenous DA and most often is given in combination with the aromatic-L-amino acid decarboxylase inhibitor, carbidopa, which prevents peripheral metabolism and increases L-dopa bioavailability {Birkmayer, 2001}. Although L-dopa is the most effective treatment option available for reducing motor symptoms, chronic use and disease progression cause motor complications, such as dykinesia and "on-off" episodes {Tuite, 2003}. Disease progression causes an increased loss of dopaminergic nerve terminals and L-dopa can no longer be stored, resulting in motor fluctuations dependent upon circulating plasma levels of the drug {Münchau, 2000}. Additionally, due to the metabolism of L-dopa to DA and subsequent oxidative stress-inducing metabolites, it has been speculated that chronic L-dopa use may be toxic to DA neurons and exacerbate the neurodegenerative process. Although the toxic effect of L-dopa has not been fully substantiated *in vivo*, nevertheless, additional medications have been utilized in order to: sustain a therapeutic benefit of L-dopa, alleviate L-dopa-induced motor fluctuations and delay the onset of L-dopa treatment {Lipski, 2011; Tuite, 2003; Münchau, 2000}. Common alternative/adjuvant PD therapies include DA agonists, selective MAO-B inhibitors and catechol-O-methyltransferase (COMT) inhibitors (Table 1).

The selective and irreversible MAO-B inhibitors, selegiline (deprenyl) and rasagiline, prevent oxidative DA metabolism, thereby increasing synaptic DA levels and providing symptomatic benefit. Selegiline monotherapy in early PD delays the need for additional treatment by approximately one year {Parkinson Study Group, 1989}. In addition, selegiline can potentially reduce the necessary L-dopa dose by 30% and reduce symptomatic fluctuations observed with L-dopa therapy {Münchau, 2000}.
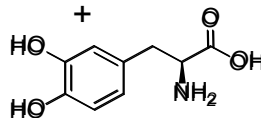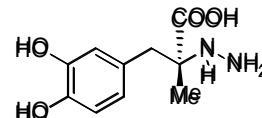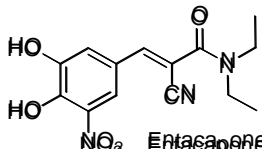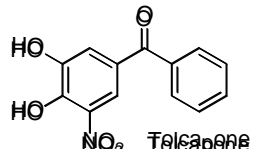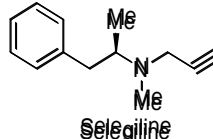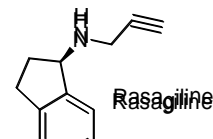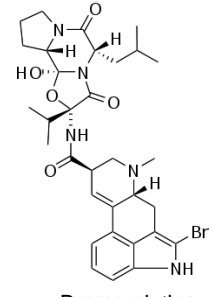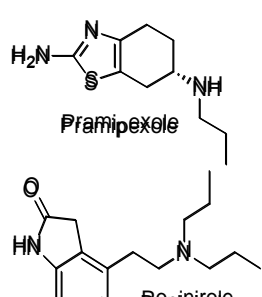
Although selegiline has been shown to reduce PD symptoms, potential side effects, including enhanced L-dopa-induced dykinesia (LID) and psychiatric problems have been reported {Churchyard, 1997}. In Phase III clinical trials of advanced PD with motor fluctuations, rasagiline/L-dopa combination therapy significantly reduced the amount of "off" time {Nayak, 2008}. A recent study that examined the effect of rasagiline as monotherapy concluded that it may delay the progression of PD, an effect that cannot be explained by anti-symptomatic effects alone and may represent an early disease-modifying effect {Schapira, 2006}.

COMT inhibitors, entacapone and tolcapone, delay the metabolism and elimination of L-dopa by inhibiting the enzyme, catechol-O-methyltransferase, leading to increased L-dopa bioavailability and stable plasma levels. Entacapone/L-dopa combination therapy extends the half-life of L-dopa elimination by 85% and increases plasma levels by 50% {Schrag, 2005; Nutt, 1994}. Furthermore, evidence suggests that in addition to the degree of striatal denervation, pulsatile and intermittent stimulation of DA receptors contributes significantly to motor fluctuations observed during L-dopa therapy. In MPTP-lesioned monkeys, combination L-dopa/entacapone therapy was found to reduce motor fluctuations compared to L-dopa treatment alone {Jenner, 2003a; Smith, 2005}. Randomised, controlled trials have demonstrated that in PD patients with L-dopa-induced motor fluctuations, addition of entacapone resulted in a reduction of motor variability and the required L-dopa dose {Schrag, 2005}.

DA agonists are frequently used in the management of early PD based on their low potential for inducing dyskinesia {Parkinson Study Group, 2000}. Pramipexole or ropinirole/L-dopa adjuvant therapy in PD patients with motor fluctuations can reduce

''off'' time by 1.0-1.5 h/day {Lieberman, 1998; Pinter, 1999}. In addition to reducing motor fluctuations, DA agonists partially alleviate LID, an effect most likely due to a 30% reduction in the needed L-dopa dose {Stocchi, 2008}. Recent studies indicate that novel DA agonists may slow disease progression. In a clinical study of PD patients, pramipexole was compared to L-dopa in terms of their effect on disease progression. In this regard, a decreased loss of striatal DAT, a marker for PD progression, was seen in the case of D3 receptor-preferring pramipexole {Parkinson Study Group, 2002}. In patients with advanced PD, pramipexole improves motor function during "on" and "off" periods, reduces total "off" time and decreases the severity of "off" time {Lieberman, 1997}. Furthermore, pramipexole and D3 receptor-preferring agonist, D-264, have demonstrated the ability to both improve motor dysfunction and provide a neuroprotective benefit in a variety of *in vivo* PD models {Li, 2010}. These findings indicate the use of D3 receptor-preferring agonists as a symptomatic and neuroprotective, disease-modifying treatment option for PD.

Table 1. Pharmacological treatments used in PD therapy.

Mechanism of Action	Drugs
DA replacement	L-dopa, Carbidopa
COMT inhibition	Entacapone, Tolcapone
MAO-B inhibition	Selegiline, Rasagiline
DA receptor agonism	Bromocriptine, Pramipexole, Ropinirole

1.3.2 Neuroprotective Treatment

Neuroprotective therapy aims to modify disease pathogenesis, thereby slowing or halting the degenerative process. Standard PD treatment options, such as L-dopa, are unable to slow its progression. Although no currently available drugs have been convincingly proven to be neuroprotective in PD, MAO-B inhibitors and DA agonists have demonstrated neuroprotection in both *in vitro* and *in vivo* PD models. In cellular models of PD, rasagiline protects against cell death induced by 6-hydroxydopamine (6-

OHDA), MPTP and nerve growth factor deprivation {Nayak, 2008; Carvey, 2001; Li, 2010}. The neuroprotective effect of rasagiline has been extended to the *in vivo* system, where in a rodent model of PD it was shown to protect DA neurons from the toxic effects of 6-OHDA. In this case, pretreatment with rasagiline prevented the loss of tyrosine hydroxylase (TH)-positive DA neurons in the SNc and DA terminals in the striatum by approximately 35% {Blandini, 2004}.

Pramipexole has demonstrated protection against several neurotoxins *in vitro*, including 6-OHDA, MPP^+ and H_2O_2. In these models, the neuroprotective effect of pramipexole was independent of DA receptor stimulation and thought to be related to ROS scavenging properties {Fujita, 2006; Le, 2000; Abramova, 2002}. Recently, in both MPTP- and lactacystin-lesioned mouse models of PD, D-264 demonstrated significant neuroprotection; an effect that correlated with both D3 receptor activation and up-regulation of brain-derived neurotrophic factor (BDNF) and glial-cell derived neurotrophic factor (GDNF) expression {Li, 2010}. Mechanistic studies suggest that the neuroprotective effect of DA agonists, specifically D3 receptor-preferring agonists, relies on their ability to: reduce DA turnover via activation of pre-synaptic DA autoreceptors and decreasing L-dopa dose, decrease ROS load through radical scavenging activity and activate post-synaptic DA receptors to induce expression of BDNF and GDNF {Carvey, 2001; Du, 2005}.

1.3.2.1 Mechanisms of Neuroprotection

The progression of PD causes an increasing number of DA neurons in the SNc to die. As a result, compensatory DA synthesis and metabolism in surviving neurons

cause increasing ROS production and a so-called "domino-effect" in DA neuron death {Chiueh, 1994}. MAO-B inhibitors are known to inhibit oxidative DA metabolism, thus reducing DA turnover and cell death {Marsden, 1990}. DA D2 and D3 receptors are expressed both pre- and post-synaptically. In this case, whereas post-synaptic D2 or D3 receptor activation results in modulation of motor activity, pre-synaptic activation down-regulates DA biosynthesis. DA agonists are hypothesized to protect DA neurons by reducing DA biosynthesis and metabolism via activation of pre-synaptic autoreceptors in conjunction with striatal-nigral feedback inhibition {Carvey, 2001; Carter, 1991}. As mentioned previously, DA agonist therapy reduces the needed dose of L-dopa by up to 30%, thereby protecting DA neurons from ROS production caused by DA metabolism. *In vivo* studies demonstrate that levels of DA and related metabolites are significantly reduced in animals treated with DA agonists compared to L-dopa {Fahn, 2005}. Due to the role of ROS in the degenerative process, antioxidant properties of direct-acting DA agonists, such as pramipexole and ropinirole, are thought to contribute to their neuroprotective effect. Pramipexole is a potent ROS scavenger with spin trapping properties in the low micromolar range, although is neuroprotective in the low nanomolar range, suggesting multiple mechanisms involved in its neuroprotection {Carvey, 1997; Vincenzi, 1998}.

Striatal neurotrophic activity functions as a regulatory feedback mechanism designed to maintain the cytoarchitectural integrity of the nigrostriatal pathway {Carvey, 1993a; Carvey, 1993b}. Neurotrophic factors, BDNF and GDNF, have been shown to protect DA neurons exposed to neurotoxins 6-OHDA and MPP$^+$ {Krobert, 1997; Kirschner, 1996}. The mechanism by which neurotrophic factors exert their protective

effect is proposed to involve alterations in pro-apoptotic signal transduction {Yang, 1998}. Expression of the anti-apoptotic proteins, Bcl-2 and Bcl-X_1, increases in response to oxidative stress, inhibiting cell death {Bredesen, 1995}. Treatment of primary mesencephalic cultures with pramipexole was found to increase the expression of Bcl-X_1 and reduce the neurotoxicity of L-dopa {Carvey, 2001}. Evidence suggests that via increased Bcl-X_1 expression, pramipexole is able to stabilize the mitochondrial transition pore {Bennett Jr., 1999}. Signal-mediated apoptosis has been shown to be associated with DA neuron loss in PD. Several *in vitro* and *in vivo* studies have indicated the ability of propargylamines, such as rasagiline, to block apoptosis {Blandini, 2004; Yi, 2006; Olanow, 2006}. Mechanistically, rasagiline has been found to: stabilize mitochondrial membrane potential, reduce levels of cytochrome c and caspase-3 and prevent DNA fragmentation and chromatin clumping {Youdim, 2001}.

1.4 DA Receptor System

The DA receptors are phylogenetically classified as members of the biogenic amine receptors and part of the "rhodopsin-like" sub-family. Further classification places DA receptors in the super-family of membrane-bound proteins, termed G-protein coupled receptors {Boeckler, 2006}. Until 1990, the DA receptor population of the brain and periphery was believed to consist solely of the D1 and D2 subtypes {Seeman, 1987}. Cloning of these two receptors led to the discovery of several additional, low-abundance DA receptors, including the D3, D4 and D5 subtypes {Bunzow, 1988; Monsma Jr., 1990; Zhou, 1990}. The D1-D5 subtypes are further classified on the basis of their inherent biochemical and pharmacological characteristics. The D1-like

receptors, D1 and D5, have low nanomolar affinity for DA and are stimulatory in nature, thereby activating the second messenger enzyme adenylyl cyclase to produce cyclic adenosine monophosphate (cAMP). The D2-like receptors, D2, D3 and D4, have nanomolar affinity for DA and are negatively coupled to adenylyl cyclase, decreasing cAMP production. Additionally, D2-like receptors are associated with other signal transduction systems, such as potassium channels and the phosphoinositide cascade {Levant, 1997}. The cloning of the D_3 receptor in 1990, initially undertaken by Sokoloff and colleagues, became of particular interest due to new hypotheses that proposed the D_3 receptor as a therapeutic target for neuropsychiatric disorders and PD {Sokoloff, 1990}.
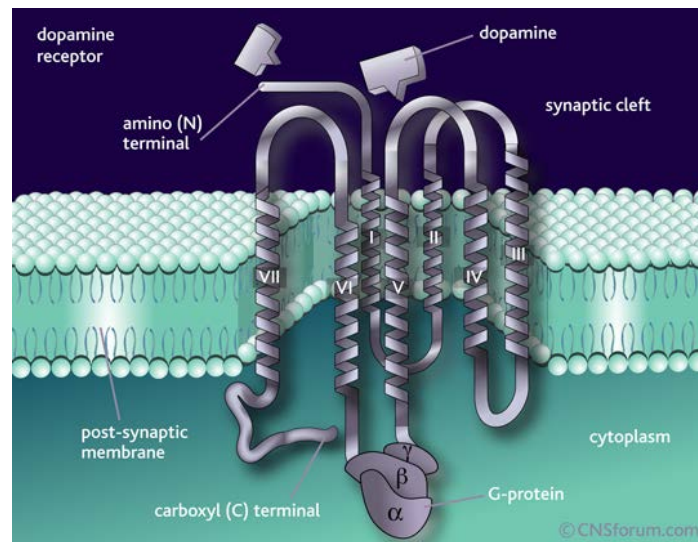
Figure 7. Generalized structure of the DA receptor.

1.4.1 Comparison of D2 and D3 Receptor Subtypes

Although D2 and D3 receptors share biochemical and pharmacological similarities, their localizations within the CNS set them apart. Unlike D2 receptors, which are widely distributed among dopaminergic brain regions with highest density in the striatum, nucleus accumbens, olfactory tubercle and SNc, D3 receptors are found predominantly in limbic brain regions {Levant, 1997}. Three splice variants of the D2 receptor have been identified to date and include $D2_{short}$, $D2_{long}$ and $D2_{longer}$ {Seeman, 2000}. These splice variants give rise to differences in size of intracellular loop 3 (IL 3), which is involved in G-protein-coupling and impacts signal transduction. Several truncated forms of D3 receptor have been reported including $D3_{nf}$, which contains a deletion in the C-terminal region of IL3 and is nonfunctional. Studies suggest that some DA agonists, including DA and quinpirole, possess higher affinity for D3 receptor, whereas antagonists, such as haloperidol, spiperone and domperidone display higher affinity for D2 receptor {Sokoloff, 1990}. Although several studies have suggested a lack of functional coupling of D3 receptor to G-proteins, this is thought to result from D3 receptors maintained in a low-affinity state under basal conditions and may have implication to the PD condition {Levant, 1997}.

The development of selective pharmacological tools to probe the pathophysiological significance of the D_3 receptor in PD has been uniquely challenging due to the sequence similarity between D2 and D3 receptors. Sequence alignment studies reveal a 50% sequence identity between D2 and D3 receptors, along with 63% sequence similarity. Moreover, when comparing the agonist binding sites of D2 and D3

receptors, a sequence identity of 79% and sequence similarity of 90% are reported. {Boeckler, 2005}.

1.4.2 Potential of D3 Receptor as Therapeutic Target in PD

The D3 receptor has gained attention as a potential therapeutic target in the treatment of PD. The following characteristics of D3 receptor suggest its potential role in PD treatment: unique CNS distribution, high affinity of DA agonists for D3 receptor, neuroprotective effect of D3 receptor stimulation and its role in both the development and modulation of LID.

The D3 receptor has a unique distribution in the limbic and nigrostriatal brain regions, making it a promising target to treat neurological diseases, including PD. The D3 receptor contributes to the control of movement, emotion and cognition, each of which becomes significantly altered in PD. Additionally, while playing a role in the control of motor activity under normal conditions, D3 receptor may have an expanded and more significant role in the parkinsonian brain, in which its expression and distribution patterns have been found to be markedly altered {Joyce, 2001a}.

Although it has been assumed that D2 receptor stimulation is necessary for the relief of motor dysfunction in PD, DA agonists have in many cases, as high or higher affinity for the D3 receptor. It is thought that mesolimbic D3 receptors may play a role in relief of PD symptoms as the limbic striatum is known to be involved in aspects of movement, such as goal-directed behaviors and locomotor activity {Joyce, 2001b}. Interestingly, locomotor stimulation is observed in 6-OHDA-lesioned rats at doses of D_3 receptor-preferring agonists that are inhibitory in normosensitive rats, suggesting that

D_3 receptor-preferring agonists may be a viable option for antiparkinsonian treatment of DA-depleted animals {Van den Buuse, 1993}.

D3 agonists have been shown to produce their neuroprotective effects by a variety of mechanisms, including: direct scavenging of free radicals, upregulating activity of radical scavenging enzymes, stabilizing mitochondrial membrane potential and apoptosis inhibition {Zou, 1999; Le, 2001}. Clinical studies utilizing positron emission tomography (PET)-imaging of nigrostriatal terminals demonstrate that D3 receptor-preferring agonists, pramipexole and ropinirole, reduce PD disease progression {Clarke, 2002}.

In monkeys rendered parkinsonian with MPTP, D3 receptor expression has been found to decrease significantly (68%) in the caudate nucleus. MPTP-intoxicated monkeys receiving chronic doses of L-dopa for several months resulted in LID symptoms in five of nine cases. Interestingly, D3 receptor expression was found to be higher in the putamen (+154%) of MPTP-intoxicated monkeys with LID compared to non-dyskinetic and normal monkeys. Furthermore, D3 receptor density in the putamen correlated with the incidence and severity of LID. PD-like symptoms and LID were associated with down- and up-regulation of D3 receptor expression. D3 receptor-selective ligands have been investigated for their potential in reducing LID. Recently, D3 receptor-selective, mixed agonist/antagonist, BP 897, was studied *in vivo* to evaluate its ability to reduce LID. BP 897 was administered to dyskinetic, MPTP-intoxicated monkeys in combination with L-dopa. Interestingly, BP 897 reduced LID by 66%, while having no effect on the motor recovery provided by L-dopa {Bézard, 2003}. Additionally, in the unilaterally lesioned rat, simultaneous administration of L-dopa and

D_3 receptor-selective agonist, PG01042, caused attenuation of abnormal involuntary movements (AIMs) in a dose-dependent manner without deleterious motor side effects {Riddle, 2011}. Results such as these suggest that D3 receptor-selective ligands are able to normalize D3 receptor function in the caudate putamen of dyskinetic animals, thereby treating LID symptoms.

1.5   Evolution in the Development of DA Agonists

Early PD therapeutics consisted largely of the ergoline class of DA agonists. The ergot agonists are each derived from ergoline, a chemical substructure of alkaloids found in fungi of the genus *Claviceps*. The ergoline class of DA agonists display preferential affinity for D2-like receptors and include bromocriptine, pergolide, lisuride and cabergoline. Despite the early success of ergoline DA agonists in the treatment of PD, side effects associated with serotonergic activity and drug-drug interactions have limited their use and indicate the need for novel DA agonists {Kvernmo, 2006}.

In the words of French biologist, François Jacob, "Evolution consists largely of molecular tinkering." A great deal of effort has been directed towards the development of novel DA agonists {Boeckler, 2006}. DA binds promiscuously to each of the DA receptor subtypes, although slightly higher affinities (30-40 nM) are reported at D1 compared to D2 receptors (80-120 nM) in their high affinity states {Ross, 1991}. Additionally, DA has been found to bind preferentially to D3 over D2 receptor {Levant, 1997}. Initial efforts toward the development of novel DA agonists focused on determining the bioactive confirmation of DA. Rigidization of the rotatable, aminoethyl side chain of DA produced the 2-aminotetralins, including (S)-(-)-5-hydroxy-2-(N,N-di-n-

propylamino)tetralin [(S)-(-)-5-OH-DPAT] and (R)-(+)-7-hydroxy-2-(N,N-di-n-propylamino)tetralin [(R)-(+)-7-OH-DPAT] {McDermed, 1976; Damsma, 1993}. Furthermore, these conformationally constrained analogs correspond to the α- and β-rotamers of DA, each lacking the *p*-OH group (Figure 8). Structure-activity-relationship (SAR) studies of the 2-aminotetralins at DA receptors concluded that only the *m*-OH group of DA was necessary for binding and agonist recognition, and thus, 5- or 7-OH groups were sufficient for agonist activity {Cannon, 1983; McDermed, 1976; Seiler, 1982}. Studies have indicated moderate D3 selectivity for both (*S*)-5-OH- and (*R*)-7-OH-DPAT (D2/D3 = 26 and 60, respectively) {Van Vliet, 1996}.

Computer models indicate the spatial orientation of conserved amino acids nearly identical between D2 and D3 receptors {Livingstone, 1992}. Computational studies have identified several amino acid residues important for agonist binding to D3 receptors. Conserved amino acid residues, Ser-193 and Ser-196, located in transmembrane domain V, likely interact with the hydroxyl groups of catechols through hydrogen bonding, while Asp-110 of transmembrane domain III is hypothesized to participate in a salt-bridge with the amine group of monoamines {Sokoloff, 1990; Malmberg, 1994}. Moreover, the location and spatial orientation of Ser-193 and Asp - 110 appear to allow for optimal bonding to 2-aminotetralins, such as 7-OH-DPAT, which may confer higher affinity of these ligands at D3 compared to D2 receptor {Malmberg, 1994}.
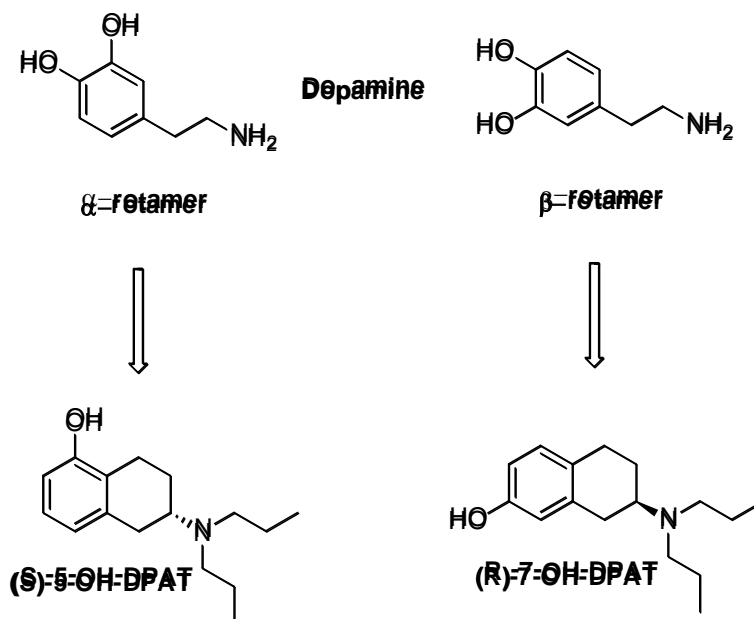
Figure 8. Rigidization of α- and β-rotamers of DA, producing 2-aminotetralins, (S)-(-)-5-OHDPAT and (R)-(+)-7-OHDPAT.

1.5.1 D3 Receptor-Selective Agonists

The pathophysiological significance of D3 receptor in PD underscores the importance of developing novel DA agonists with increased selectivity for the D3 receptor subtype. Further rigidization of 7-OH-DPAT led to the tricyclic, D3 receptor agonist, (+)-PD 128907, which binds to D_3 receptor with high affinity (1 nM) and selectivity (D2/D3 = 1000) {Akunne, 1995}. Bioisosteric mimicry of the DA catechol nucleus has been used in an effort to obtain DA agonists with improved bioavailability, along with selectivity for D3 receptor. Introduction of the catechol bioisostere, 2-aminothiazole, led to the identification of pramipexole, a preferential D3 receptor agonist that displays high affinity (0.5 nM) and selectivity (D_2/D_3 = 193) for D3 receptor {Sautel, 1995; Mierau, 1995; Perachon, 1999}. Mitogenesis assays indicate the intrinsic activity of pramipexole to be 100% at D2 and 80% at D3 receptor {Perachon, 1999}.

Furthermore, bioisosteric replacement with a pyrazole ring system produces quinpirole, a high affinity (0.96 nM), D3 receptor-selective agonist (D2/D3 = 133) {Boeckler, 2006}. Quinpirole demonstrates full agonism at both D2 and D3 receptor in mitogenesis assay {Pilon, 1994}. The pyrimidine ring system has also been utilized as a catechol bioisostere with several analogs displaying high affinity and selectivity for D3 receptor {Avenell, 1999}.

1.5.2 Hybrid Structure Approach: Design of D3 Receptor-Selective Agonists Towards Disease-Modifying Therapeutic Agents for PD.

As indicated previously, the high degree of structural homology shared between D2 and D3 receptors is a major challenge in the development of D3 receptor-selective agonists. Our group has devised a hybrid structure approach to the design of D3 receptor-selective agonists {Dutta, 2002}. In this approach, 2-aminotetralins or bioisosteric equivalents have been tethered to aryl piperazine fragments via a suitable methylene linker (Figure 9). The 2-aminotetralins (5-OH- or 7-OH-DPAT) or bioisosteric (2-aminothiazole, pyrazole, pyrimidine etc.) equivalents impart preferential D3 agonist activity to the molecule, interacting with critical amino acid residues in the D3 agonist binding site. The adjacent aryl piperazine fragment is designed based on known D3 antagonists and interacts with accessory binding sites within D3 receptor, thereby increasing D3 subtype selectivity.
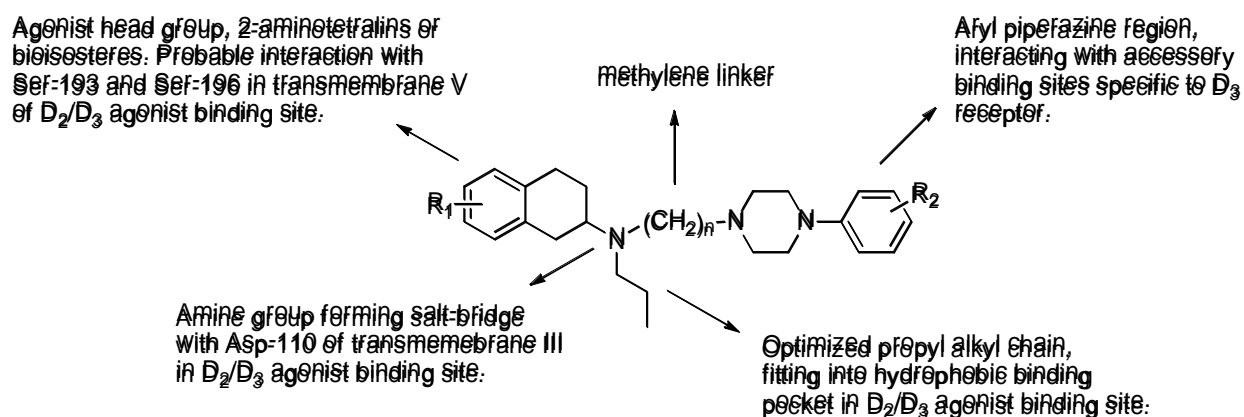
Figure 9. Hybrid structure approach to the design of D3 receptor-selective agonists.

Initial SAR studies utilizing our hybrid structure approach led to the discovery of 7-OH-DPAT derivative, D-74. In the case of D-74, D2 and D3 receptor affinity, as well as D3 receptor selectivity were found to be comparable to that of 7-OH-DPAT. After resolution of D-74, binding and functional evaluation identified *S*-(-)-D-74 as the more biologically-active and selective enantiomer at D3 receptor. The *in vivo* agonist activity of *S*-(-)-D-74 was studied using the 6-OHDA-lesioned rat model of PD, where it displayed contralateral rotations with long duration of action {Dutta, 2004}. The 5-OH derivative of *S*-(-)-D-74, *S*-(-)-D-237, was also developed and displayed higher affinity (Table 2) and potency for D2 and D3 receptors compared to *S*-(-)-D-74. Moreover, *S*-(-)-D-237 demonstrated significantly higher intrinsic activity in functional assays compared to *S*-(-)-D-74 and produced prolonged rotational activity in the 6-OHDA-lesioned rat model {Biswas, 2008a}.

Further efforts at exploring our hybrid template have focused on replacing 2-aminotetralins with bioisosteric equivalent moieties in order to improve D3 selectivity, *in*

vivo bioavailability and antioxidant capacity of the molecule. Extension of the aryl piperazine fragment of *S*-(-)-D-237 to produce a biphenyl structure yielded the 2-aminothiazole derivative, *S*-(-)-D-264 (Figure 10). This lead compound displayed high D3 affinity and selectivity, as well as potent D3 receptor agonist activity in binding and functional assays. Additionally, *S*-(-)-D-264 possesses comparable affinity, although significantly higher selectivity for D3 receptor compared to previous lead compounds and 7-OH-DPAT. Moreover, in terms of functional activity, *S*-(-)-D-264 maintained higher D3 selectivity and intrinsic activity (full agonist, E_{max} = 102%) compared to previous lead compounds and 7-OH-DPAT, which each displayed weak or partial agonist activity at D3 receptor (Table 3). In the 6-OHDA-lesioned rat, *S*-(-)-D-264 induced contralateral rotations with long duration of action, suggesting efficient CNS penetration and antiparkinsonian effect {Biswas, 2008b}. Numerous other analogs have been synthesized by us in order to explore and optimize the following features of our hybrid template: methylene linker length, aromatic group in the aryl piperazine fragment, n-alkyl group and agonist head group. Data collected thus far indicate that compounds derived from our hybrid template have the potential for high affinity, potency and selectivity at D3 receptor with full agonist activity.
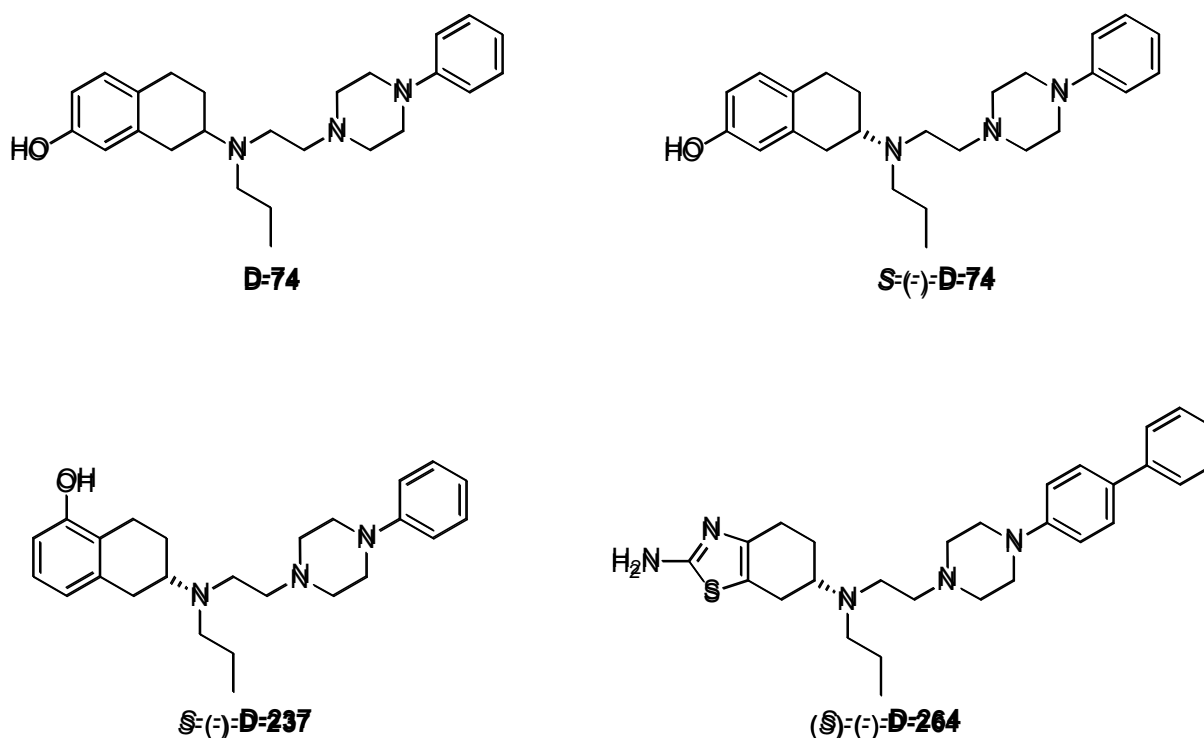
Figure 10. Development of lead compounds utilizing our hybrid template.

Table 2. Affinity of lead compounds for cloned D2L and D3 receptors expressed in HEK-293 cells measured as inhibition of [^{3}H]spiperone binding.

Compound	K$_i$ (nM)　D2L [^{3}H]spiperone	K$_i$ (nM) D3 [^{3}H]spiperone	D2L/D3
7-OH-DPAT	202 ± 34	2.35 ± 0.29	86
D-74	142 ± 23	1.56 ± 0.36	91
(*S*)-(-)-D-74	241 ± 7	1.88 ± 0.42	128
(*S*)-(-)-D-237	26 ± 7.5	0.82 ± 0.13	31.5
(*S*)-(-)-D-264	264 ± 40	0.92 ± 0.23	253

Table 3. Potency of lead compounds in stimulating [^{35}S]GTPγS binding to cloned hD2 receptor expressed in CHO cells and cloned hD3 receptor expressed in AtT-20 cells.

Compound	CHO-D2		AtT-20-D3		
	EC$_{50}$ [^{35}S]GTPγS (nM)	E_{max} (%)	EC$_{50}$ [^{35}S]GTPγS (nM)	E_{max} (%)	D2/D3
7-OH-DPAT	39.8 ± 19.4	61.4 ± 8.6	0.531 ± 0.042	45.3 ± 2.3	74.95
D-74	12.2 ± 0.9	32.1 ± 2.8	0.69 ± 0.39	40.5 ± 7.5	17.6
(*S*)-(-)-**D-237**	2.22 ± 0.27	63.4 ± 3.5	0.12 ± 0.002	78.5 ± 9.5	18.3
(*S*)-(-)-**D-264**	19.9 ± 0.9	119 ± 6	0.085 ± 0.016	102 ± 19	248

A foremost goal of our PD project is to develop compounds based on our hybrid template that are multifunctional, not only relieving motor symptoms, but also modifying progression of the disease. The design of our compounds reflect the multifactorial nature of PD and incorporate functionality in order to achieve a molecular entity that addresses many of the important factors involved in disease pathogenesis. We have demonstrated the ability of these compounds to act as full agonists at both D2 and D3 receptor, along with achieving high binding and functional selectivity for D3 receptor. Additionally, *in vivo* studies in PD animal models have demonstrated that these compounds are able to penetrate the CNS and alleviate motor dysfunction involved with the disease. The neuroprotective action of D3 receptor-selective agonists is well documented and via neurotrophic factor induction and inherent antioxidant capacity, our D3 receptor-selective agonists have potential as a neuroprotective therapy for PD.

In this work, a series of compounds were synthesized based on our well-established hybrid template. In order to study the consequence of varying the agonist head group, these molecules include those containing the 5-OH-aminotetralin head group, in addition to those incorporating the bioisosteric equivalent moiety, 2-aminothiazole. In the aryl piperazine region of the template, indole functionality has been utilized as previous studies have demonstrated its tolerability within accessory binding regions of D3 receptor. In addition, indole is a well known antioxidant and along with 2-aminothiazole, should work synergistically to produce a potent radical scavenger. Within this series, the effect of linker length and the nature and position of indole substitution on piperazine was examined in order to delineate key factors that influence interaction of the molecule within accessory binding pockets of the D3 receptor. Synthesized compounds were evaluated for their binding affinity at both D2 and D3 receptors and molecules of interest were studied further for functional activity at these receptors. Based upon affinity, selectivity and potency measures, lead compounds were taken for *in vivo* examination in PD animal models. An *in vitro* antioxidant assay was then performed in order to confirm the antioxidant capacity of lead compounds. Next, lead compounds were evaluated *in vitro* for their ability to protect dopaminergic cells from neurotoxic insults. Lead compounds were also assessed for their ability to alter the aggregation process of α-synuclein. Finally, the neuroprotective effect of the compounds was examined in greater detail, identifying potential mechanisms involved in their anti-apoptotic and protective action.

CHAPTER 2

SPECIFIC AIMS AND HYPOTHESES

Dopaminergic receptor systems have been targeted in the development of pharmacotherapeutic agents for a number of CNS related disorders, including Parkinson's disease, schizophrenia and drug addiction. Several diseases of the CNS have been shown to involve an imbalance in the dopaminergic system. Compelling evidence has suggested the use of pharmacotherapy acting via agonism, partial agonism or antagonism of the DA receptors to treat such imbalances. DA receptor agonists have been employed more extensively in the treatment of Parkinson's disease than any other type of pharmacotherapy. Although the etiology of PD is still not fully understood, several key pathogenic factors have been identified and such discoveries have indicated the need for multifunctional therapy in order to treat both symptoms and disease progression. Our short term goals are each directed toward the development of multifunctional, DA D2/D3 receptor agonists with the capability of acting both as symptomatic and disease-modifying therapeutic agents for PD.

2.1 Specific Aims

1. Design and synthesis of DA D2/D3 receptor agonists with preferential affinity for D3 receptor and pharmacological characterization of these compounds using *in vitro* binding and functional assays.

2. Perform SAR analysis to determine preference of D3 receptor for the geometry and substitution pattern of indole, along with optimal methylene linker length that results in most favorable interaction of the aryl piperazine

fragment within accessory binding sites of D3 receptor.

3. Evaluate multifunctional properties of lead compounds using *in vitro* antioxidant, neuroprotection and anti-aggregation assays. Elucidate possible mechanisms involved in neuroprotection.

4. Assess *in vivo* efficacy of lead compounds to relieve motor dysfunction in PD animal models.

2.1.1 Hypotheses

1. The combination of 2-aminothiazole and indole within our hybrid template should produce DA agonists with preferential D3 affinity and potency, as well as provide synergistic antioxidant capacity that will aid in the neuroprotective ability of our compounds.

2. Our design of DA D2/D3 receptor agonists with preferential binding and functional potency for D3 receptor has the potential to both treat PD symptoms and modify disease progression.

CHAPTER 3

RESULTS AND DISCUSSION

3.1   Overview

The primary goal of this work is to develop DA D2/D3 agonists with multifunctional properties in order to modify the symptoms and progression of PD. In our efforts toward this goal, we designed and synthesized a series of molecules containing indole within the aryl piperazine fragment, while the agonist head group was varied between 5-OH-aminotetralin and 2-aminothiazole. The length of the methylene linker, along with the geometry and substitution pattern of indole within the aryl piperazine fragment were varied in order to further explore accessory binding sites within D3 receptor. A benzamide moiety was utilized in the aryl piperazine region of our hybrid template in order to increase D3 receptor selectivity, as D3 antagonists are known to contain such functionality. These compounds were then evaluated *in vitro* to determine their D2 and D3 receptor binding affinity and selectivity. Based upon binding results, selected compounds were evaluated for functional properties to determine their potency in stimulating D2 and D3 receptors. Next, lead compounds were subjected to *in vitro* antioxidant, neuroprotection and anti-aggregation assays in order to study their multifunctional properties. Finally, the efficacy of lead compounds in reducing motor dysfunction was evaluated using PD animal models. This chapter will describe the following:

1. Synthesis of all compounds and *in vitro* binding and functional assays.

2. Evaluation of multifunctional properties of lead compounds using *in vitro* antioxidant, neuroprotection and anti-aggregation assays.

3. Assessment of *in vivo* efficacy of lead compounds in PD animal models.

All experimental detail, including synthesis procedures and spectroscopy data, binding and functional assay procedures and protocols pertaining to antioxidant, neuroprotection, anti-aggregation and *in vivo* studies will be described in the Materials and Methods section.

3.2   Chemistry

3.2.1 Synthesis of 6-((2-(4-((1H-indolyl)methyl)piperazin-1-yl)ethyl)(propyl)amino)-5,6,7,8-tetrahydronaphthalen-1-ols

Scheme 1 outlines the synthesis of **9a**, **9b** and **9c**. 5-methoxy-2-tetralone **1** was first condensed with n-propyl amine under reductive amination conditions to yield secondary amine **2**. In preparation of intermediate **7**, Boc-piperazine **4** was *N*-alkylated using 2-bromoethanol to yield **5**. Under Swern oxidation conditions, alcohol **5** was converted to its aldehyde derivative **6**. Aldehyde **6** was subsequently condensed with amine **2** under reductive amination conditions to yield **7**. Treatment of intermediate **7** with aq. HBr (48%) gave amine **8**. Finally, condensation of secondary amine **8** with properly substituted indole-carbaldehydes afforded final compounds **9a-c**.

Scheme 1. Synthesis of 6-((2-(4-((1H-indolyl)methyl)piperazin-1-yl)ethyl)(propyl)amino) 5,6,7,8-tetrahydronaphthalen-1-ols
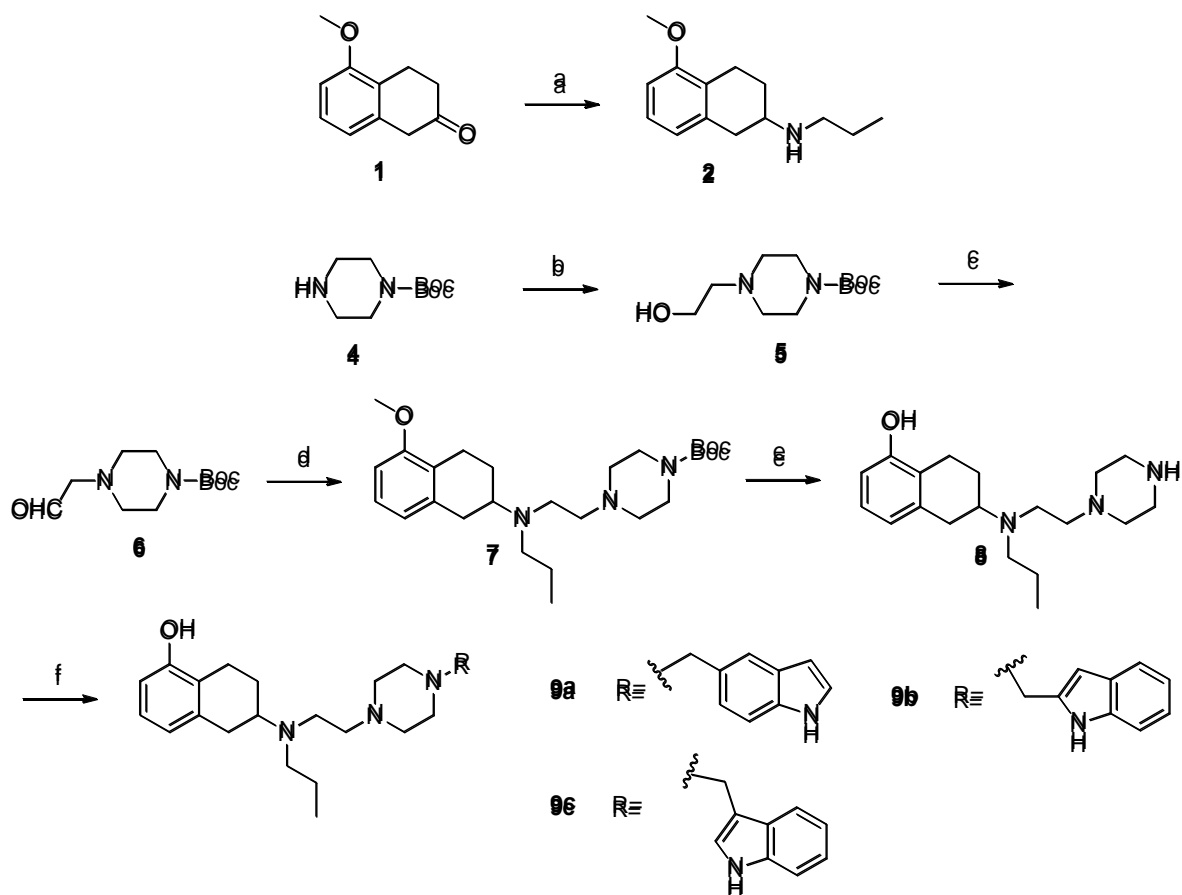
Reagents and conditions: (a) *n*-propyl amine, NaCNBH$_3$, AcOH, CH$_2$Cl$_2$; (b) 2-bromoethanol, K$_2$CO$_3$, CH$_3$CN reflux; (c) (COCl)$_2$, DMSO, Et$_3$N, CH$_2$Cl$_2$, -78 °C-rt; (d) **2**, Na(OAc)$_3$BH, CH$_2$Cl$_2$; (e) aq. HBr (48%), reflux; (f) indole-5-, -2-or -3-carbaldeyde, Na(OAc)$_3$BH, CH$_2$Cl$_2$.

Scheme 2. Synthesis of 6-((2-(4-(4-chloro-1H-indole)piperazin-1-yl)ethyl)(propyl)amino)-5,6,7,8-tetrahydronaphthalen-1-ol and corresponding 2-aminothiazole derivative
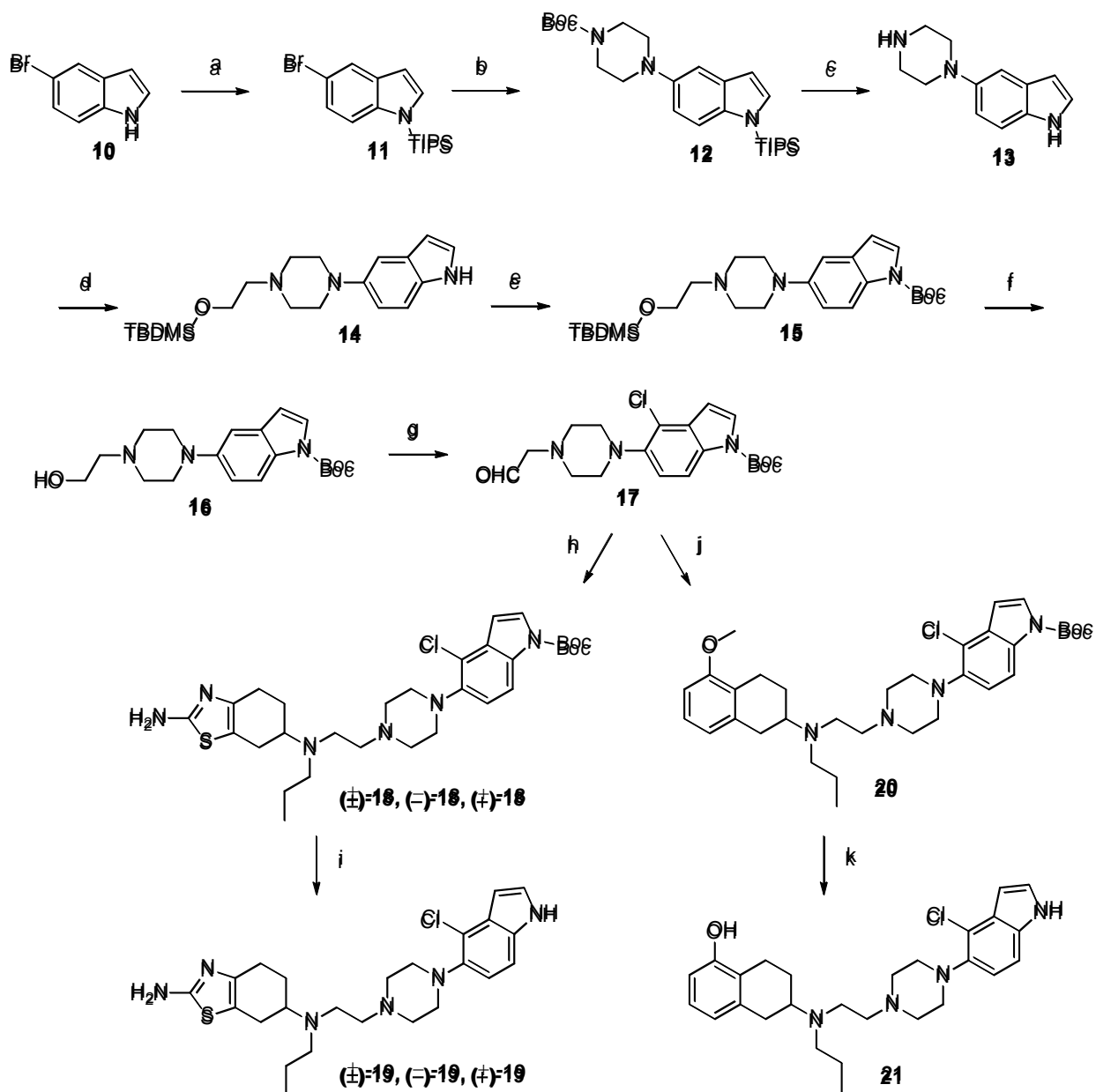
Reagents and conditions: (a) triisopropylsilyl chloride, NaH, THF; (b) **4**, PdCl$_2$[P(o-tol)$_3$]$_2$, NaOtBu, xylenes, reflux; (c) CF$_3$COOH, CH$_2$Cl$_2$; (d) (2-bromo-ethoxy)-*tert*-butyl-dimethyl-silane, K$_2$CO$_3$, CH$_3$CN, reflux; (e) (Boc)$_2$O, DMAP, THF; (f) *n*-Bu$_4$NF, THF; (g) (COCl)$_2$, DMSO, Et$_3$N, CH$_2$Cl$_2$, -78 °C-rt; (h) (±), (-) or (+)-pramipexole, Na(OAc)$_3$BH, CH$_2$Cl$_2$; (i) CF$_3$COOH, CH$_2$Cl$_2$; (j) **2**, Na(OAc)$_3$BH, CH$_2$Cl$_2$; (k) aq. HBr (48%), reflux.

3.2.2 Synthesis of 6-((2-(4-(4-chloro-1H-indole)piperazin1-yl)ethyl)(propyl)amino)-5,6,7,8-tetrahydronaphthalen-1-ol and corresponding 2-aminothiazole derivative

Scheme 2 describes the synthesis of final compounds (±)-**19,** (+)-**19,** (-)-**19** and **21**. Initially, bromo-indole **10** was *N*-protected using triisopropylsilyl chloride in the presence of NaH to give intermediate **11**. Palladium-catalyzed cross-coupling of **11** with amine **4** using PdCl$_2$[P(*o*-tol)$_3$]$_2$ and NaO*t*Bu in xylenes yielded **12**. Successive deprotection of **12** in trifluoroacetic acid gave amine **13,** which on selective, *N*-alkylation with (2-bromo-ethoxy)-*tert*-butyl-dimethyl-silane yielded compound **14**. The indole moeity of **14** was then *N*-protected to give compound **15**, which on selective TBDMS deprotection yielded alcohol **16**. Intermediate **16** was converted to its aldehyde derivative **17**, under Swern oxidation conditions. Aldehyde **17** was subsequently condensed with either (±), (-) or (+)-pramipexole to yield intermediates (±)-**18**, (-)-**18** and (+)-**18**, which were each treated with trifluoroacetic acid to afford final compounds (±)-**19**, (-)-**19** and (+)-**19.** Aldehyde **17** was further condensed with 5-methoxy-1,2,3,4-tetrahydro-naphthalen-2-yl)-propyl-amine under reductive amination conditions and subsequently treated with aq. HBr (48%) to furnish **21**.

3.2.3 Synthesis of (4-(2-((2-amino-4,5,6,7-tetrahydrobenzo[d]thiazol-6- yl)(propyl)amino)ethyl) piperazin-1-yl)(1H-indol-2-yl)methanones

Scheme 3 depicts the synthesis of (±)-**40**, (+)-**40**, (-)-**40**, (±)-**41** and (±)-**42**. Indole-2-carboxylic acid was first coupled to amine **4** using EDCI as coupling reagent. Deprotection of piperazine, followed by selective, *N*-alkylation with appropriately substituted TBDMS-protected alkyl halides afforded intermediates **25**-**27**. Protection of

Scheme 3. Synthesis of (4-(2-((2-amino-4,5,6,7-tetrahydrobenzo[d]thiazol-6- yl)(propyl) amino)ethyl) piperazin-1-yl)(1H-indol-2-yl)methanones

22   **23**   **24**

25: n=1; **26**: n=2; **27**: n=3   **28**: n=1; **29**: n=2; **30**: n=3

31: n=1; **32**: n=2; **33**: n=3   **34**: n=1; **35**: n=2; **36**: n=3

(±)-**37**: n = 1; (+)-**37**: n = 1; (-)-**37**: n = 1
(±)-**38**: n = 2; (±)-**39**: n = 3

(±)-**40**: n = 1; (+)-**40**: n = 1; (-)-**40**: n = 1
(±)-**41**: n = 2; (±)-**42**: n = 3
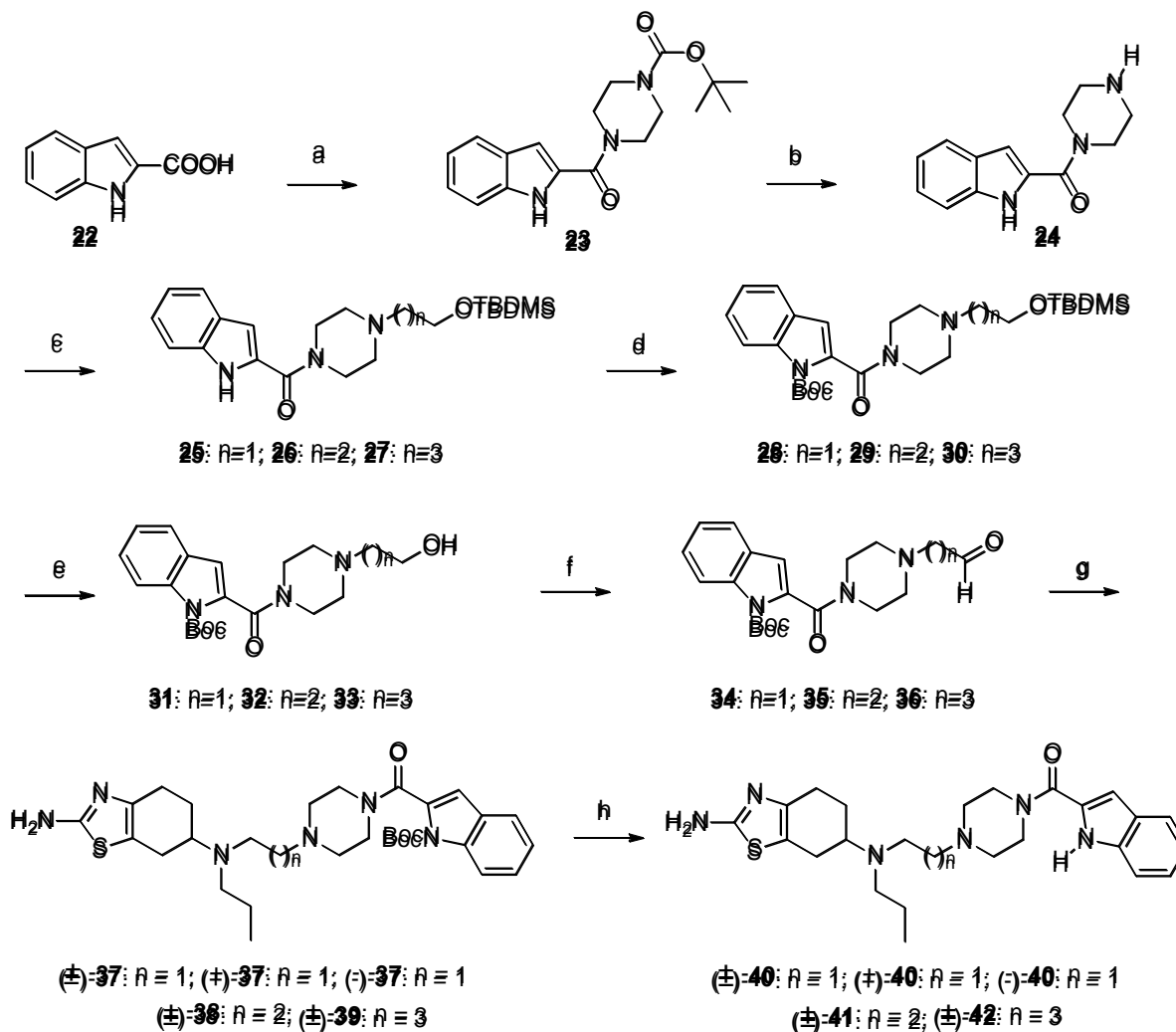
Reagents and conditions: (a) **4**, EDCI, HOBT, Et$_3$N, CH$_2$Cl$_2$; (b) CF$_3$COOH, CH$_2$Cl$_2$; (c) (2-bromoethoxy)(tert-butyl)dimethylsilane, (3-bromopropoxy)(tert-butyl)dimethylsilane or (4-bromobutoxy)(tert-butyl)dimethylsilane, K$_2$CO$_3$, CH$_3$CN, reflux; (d) (Boc)$_2$O, 4-DMAP, THF; (e) n-Bu$_4$NF, THF; (f) (COCl)$_2$, DMSO, Et$_3$N, CH$_2$Cl$_2$, -78 °C-rt; (g) (±), (+) or (-)-pramipexole, Na(OAc)$_3$BH, CH$_2$Cl$_2$; (h) CF$_3$COOH, CH$_2$Cl$_2$.

the indole nitrogen, followed by selective deprotection of the hydroxyl group using *n*-Bu₄NF gave alcohols **31**-**33**. Alcohols **31-33** were subsequently converted to their aldehyde derivative using Swern oxidation conditions to yield aldehydes **34**-**36**.

Scheme 4. Synthesis of (4-(2-((2-amino-4,5,6,7-tetrahydrobenzo[d]thiazol-6-yl)(propyl)amino)ethyl)piperazin-1-yl)(1H-indolyl)methyl and methanone analogs
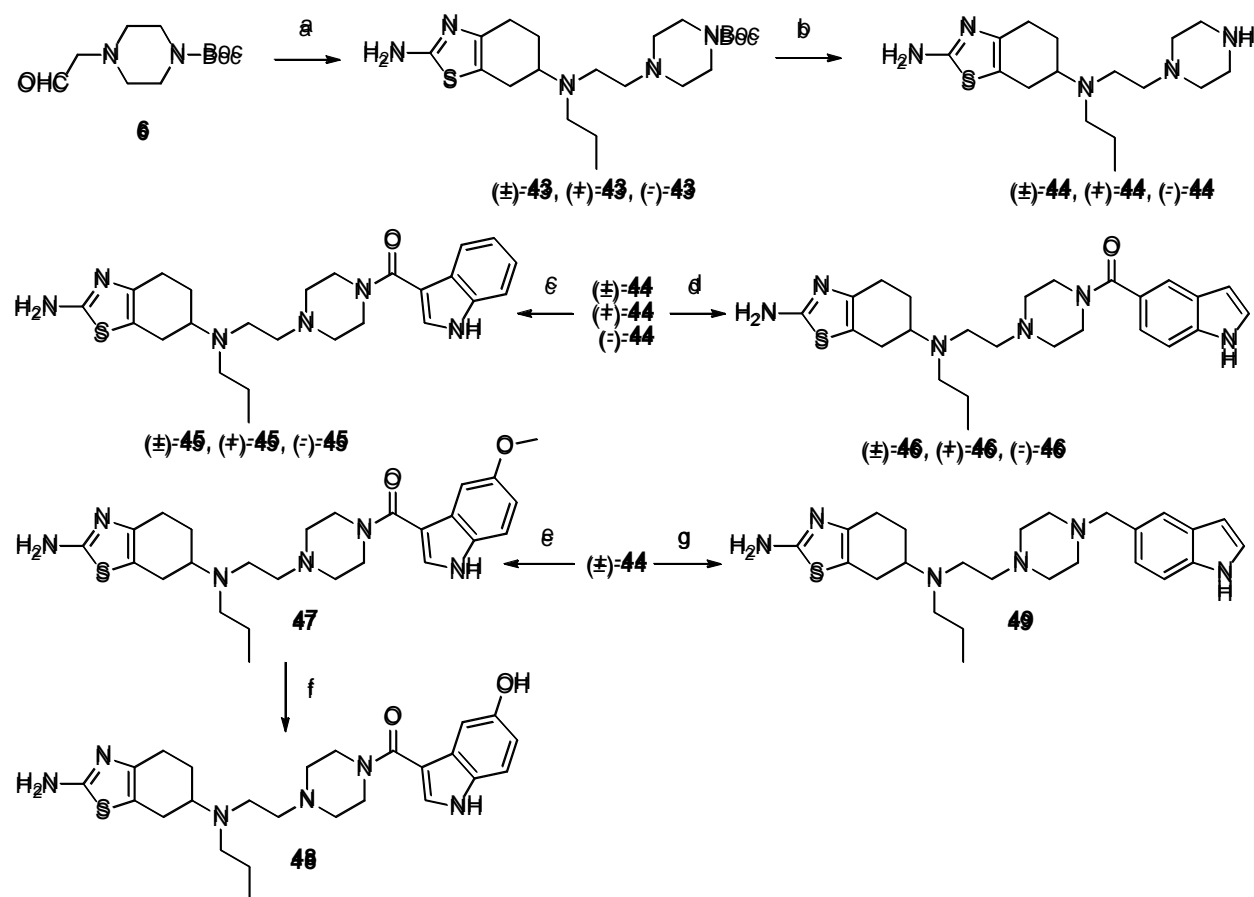
Reagents and conditions: (a) (±), (+) or (-)-pramipexole, Na(OAc)₃BH, CH₂Cl₂; (b) CF₃COOH, CH₂Cl₂; (c) indole-3-carboxylic acid, EDCI, HOBT, Et₃N, CH₂Cl₂; (d) indole-5-carboxylic acid, EDCI, HOBT, Et₃N, CH₂Cl₂; (e) 5-methoxy-1*H*-indole-3-carboxylic acid, EDCI, HOBT, Et₃N, CH₂Cl₂; (f) BBr₃, CH₂Cl₂, -78 °C-rt; (g) 1*H*-indole-5-carbaldehyde, Na(OAc)₃BH, CH₂Cl₂.

Aldehyde **34** was coupled with (±), (+) and (-)-pramipexole under reductive amination conditions to give condensed products (±)-**37**, (+)-**37** and (-)-**37**. Finally, deprotection of the indole nitrogen afforded final compounds (±)-**40**, (+)-**40** and (-)-**40**. Aldehydes **35** and **36** were similarly condensed under reductive amination conditions with (±)-pramipexole to yield intermediates (±)-**38** and (±)-**39**, which were deprotected under acidic conditions to afford (±)-**41** and (±)-**42**.

3.2.4 Synthesis of (4-(2-((2-amino-4,5,6,7-tetrahydrobenzo[d]thiazol-6-yl)(propyl)amino)ethyl)piperazin-1-yl)(1H-indolyl)methyl and methanone analogs

Scheme 4 outlines the synthesis of (±)-**45**, (+)-**45**, (-)-**45**, (±)-**46**, (+)-**46**, (-)-**46**, **48** and **49**. Aldehyde **6** was condensed with (±), (+) or (-)-pramipexole to yield products (±)-**43**, (+)-**43** and (-)-**43**, which were subsequently treated with acid to yield intermediates (±)-**44**, (+)-**44** and (-)-**44**. Separately and under amide coupling conditions, (±)-**44**, (+)-**44** and (-)-**44** were each reacted with either indole-3- or indole-5-carboxylic acid to yield (±)-**45**, (+)-**45**, (-)-**45**, (±)-**46**, (+)-**46**, (-)-**46**. Reaction of (±)-**44** with either 5-methoxy-1*H*-indole-3-carboxylic acid under amide coupling conditions, or 1*H*-indole-5-carbaldehyde under reductive amination conditions, afforded intermediate **47** and **49**. Finally, demethylation of **47** with boron tribromide furnished **48**.

3.2.5 Synthesis of di-acetyl and mono-(*R*)-lipoic acid prodrugs of (-)-45

Scheme 5 illustrates the synthesis of prodrugs (-)-**50** and (-)-**51**. Acetylation of primary and secondary amine groups of (-)-**45** was accomplished with acetic anhydride

and catalytic DMAP, affording (-)-**50**. Additionally, amide coupling of (-)-**45** to (*R*)-lipoic acid, using DCC as coupling reagent, yielded (-)-**51**.

Scheme 5. Synthesis of N-acetyl and -(*R*)-lipoic acid prodrugs of (-)-**45**
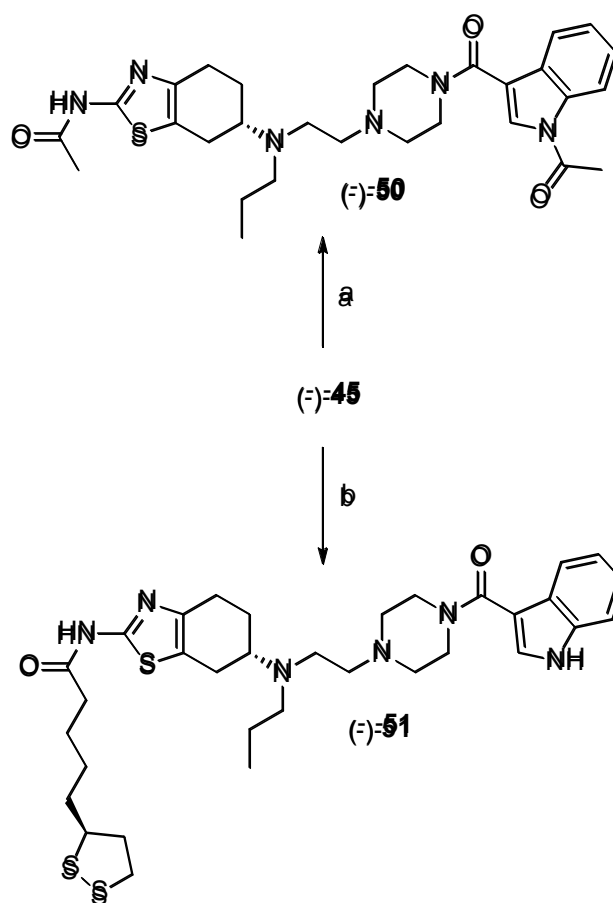
Reagents and conditions: (a) Ac₂O, DMAP, CH₂Cl₂; (b) (*R*)-lipoic acid, DCC, DMAP, CH₂Cl₂.

3.3   *In vitro* binding and functional studies

The present series of compounds comprise various indole derivatives, as our previous studies have indicated an indole substituent in the arylpiperazine region to be

well tolerated, producing molecules with high D2/D3 affinity and preference for D3 receptor {Brown, 2009}. We have carried out our binding studies with rat D2 and D3 (rD2 and rD3) receptors expressed in HEK-293 cells and functional characterization with human D2 and D3 receptors (hD2 and hD3) expressed in CHO cells. In our own findings, we did not observe any significant difference in interaction with receptors when comparing rat and human D2 and D3 receptors. A high degree of homology exists between the two species, with 95% for D2 and 78% for D3, due to a somewhat shorter IL3 in the human version of the D3 receptor {Giros, 1990; Grandy, 1989}.

Table 3 summarizes the binding data for analogues that were synthesized. Compounds **9a−c**, which incorporate the 5-hydroxyaminotetralin head group and a methylene unit connecting piperazine to indole at various positions, displayed high affinity for D3 and moderate affinity for D2 receptors. Among this series of analogues, the 5-substituted indole derivative, **9a**, displayed the highest selectivity (K_i, D2 = 269 nM, D3 = 4.17 nM, D2/D3 = 64.5), while **9c** (K_i, D2 = 82.1 nM, D3 = 3.20 nM, D2/D3 = 25.6) proved to be the most potent and least selective for D3 receptor. Analogues **9a−c** exhibited lower affinity for D2 and in the case of **9a**, higher selectivity for D3 compared to parent compound D-237 (**9a** K_i, D2 = 269 nM, D2/D3 = 64.5 vs D-237 K_i, D2 = 26.0 nM, D2/D3 = 31.5). A similar 5-substituted indole derivative, **21**, displayed low selectivity and lost some potency (K_i, D2 = 76.4 nM, D3 = 10.4 nM, D2/D3 = 7.3) for D3 receptor compared to counterparts **9a−c**. Compound **49**, analogous to **9a−c**, with 2-aminothiazole substitution in the agonist head group, maintained D2 receptor affinity within the range displayed by **9a−c**, while D3 affinity decreased by approximately 2-fold (K_i, D2 = 132 nM, D3 = 8.07 nM, D2/D3 = 16.4).

Previous and current results consistently demonstrate that in the 2-aminothiazole series of hybrid compounds, the (−)-isomeric version exhibits the highest affinity and selectivity for D3 receptor. Bioisosteric equivalent molecules were synthesized with the aminotetralin headgroup replaced with 2-aminothiazole. The first of these analogues incorporated a bond that linked piperazine directly to the indole moeity. The most active optical isomer of this molecule, (−)-**19**, displayed the highest affinity for D2 receptor among compounds in our study, along with low D3 selectivity (K_i, D2 = 39 nM, D3 = 2.19 nM, D2/D3 = 17.8). Parent compound, D-301, displayed lower D2 affinity and higher D3 selectivity (K_i, D2 = 269 nM, D3 = 2.23 nM, D2/D3 = 121) compared to (-)-**19**. This suggests that the indole moiety alone does not give rise to selectivity for either receptor subtype. Next, in an attempt to increase D3 subtype selectivity, we incorporated a benzamide moiety into the aryl piperazine fragment. The benzamide moiety is found in a number D3 receptor-selective ligands {Boeckler, 2006}. Therefore, we synthesized analogues that incorporate an amide bond between the piperazine nitrogen atom and various positions of indole. In these molecules, D3 receptor affinity was maintained in the low nanomolar range, while D2 affinity dropped significantly to the low micromolar range. The 2-aminothiazole derived, 3-indoleacyl, (−)-**45**, displayed the highest D3 receptor selectivity (K_i, D2 = 902 nM, D3 = 1.09 nM, D2/D3 = 828) in our current series of molecules. A more than 3-fold increase in D3 receptor selectivity was observed for (−)-**45** when compared to previous lead and parent compound D-264 (D2/D3, 828 vs 253 for (−)-**45** and D-264, respectively). Our next goal was to synthesize the isomeric, 2-indoleacyl derivative. The most active enantiomer, (−)-**40**, exhibited high affinity and selectivity for D3 receptor (K_i, D3 = 1.84 nM, D2/D3 = 583). The most active

enantiomer of the 5-indolacyl dertivative, (−)-**46**, produced a similar high affinity and selectivity profile for D3 receptor (K_i, D3 = 1.40 nM, D2/D3 = 736). Thus, affinity and selectivity for D3 receptor were similar in isomeric compounds (−)-**40**, (−)-**45** and (−)-**46**.

In order to determine the impact of linker length on D3 receptor binding, we varied the length of the two-carbon tether between the agonist head group and the aryl piperazine fragment. Compound (±)-**41** (K_i, D2 = 928 nM, D3 = 2.78 nM, D2/D3 = 333.8) contained a three-carbon linker and displayed an almost 2-fold increase in D3 selectivity compared to parent compound (±)-**40** (K_i, D2 = 852 nM, D3 = 4.59 nM, D2/D3 = 186). Compound (±)-**42** contains a four-carbon linker and affinity for both D2 and D3 receptors increased (K_i, D2 = 531 nM, D3 = 1.74 nM, D2/D3 = 305) compared to (±)-**40** and (±)-**41**. We also modified (±)-**45** to incorporate a hydroxyl substituent at the 5-position of indole. Hydroxyl substitution helped us to study the electronic effect of an electron-releasing group on the indole nucleus and a possible contribution of hydrogen-bond interactions in this region of D3 receptors. This modification produced compound **48**, which maintained micromolar D2 affinity of the parent compound, while D3 affinity decreased 4-fold (K_i, D2 = 1,079 nM, D3 = 16.8 nM, D2/D3 = 64.2). This result indicated that introduction of a 5-hydroxyl group on the indole nucleus did not have a significant effect on D2 affinity, while D3 affinity and selectivity was impacted unfavorably. Compound **49** was designed to combine a methylene unit, connecting piperazine to indole, with a 2-aminothiazole head group. This analog displayed increased affinity for D2 receptors, while D3 receptor affinity and selectivity was diminished compared to previous analogs with amide functionality in the aryl piperazine fragment (K_i, D2 = 132 nM, D3 = 8.07 nM, D2/D3 = 16.4). The binding affinity of **49**

reflected that of similar analogs, **9a-c**, which contained the 5-OH-aminotetralin head group in place of 2-aminothiazole, underscoring the importance of the amide functionality in the aryl piperazine fragment on D3 affinity and selectivity. Compounds (-)-**50** and (-)-**51** were designed as prodrugs of (-)-**45**, in order to examine the possibility of increasing CNS penetration and in the case of (-)-**51**, providing additional neuroprotective benefit by incorporating the disulfide antioxidant, *R*-(+)-lipoic acid. Although these studies are yet to be performed, they would be beneficial to our understanding of the neuroprotective action and *in vivo* activity of our lead compounds.

Table 4. Competitive binding of synthesized compounds with [³H]spiroperidol to cloned rat D2L and D3 receptors expressed in HEK-293 cells.

Compound	K_i (nM), D2L [³H]spiroperidol	K_i (nM), D3 [³H]spiroperidol	D2L/D3
(-)-5-OH-DPAT	58.8 ± 11.0	1.36 ± 0.28	43.2
D-237	26.0 ± 7.5	0.83 ± 0.13	31.5
D-301	269 ± 16	2.23 ± 0.60	121
D-264	264 ± 40	0.92 ± 0.23	253
9a	269 ± 183	4.17 ± 0.36	64.5
9b	183 ± 26	5.48 ± 0.86	33.4
9c	82.1 ± 7.1	3.20 ± 0.32	25.6
(±)-**19**	46.7 ± 6.6	1.92 ± 0.38	24.3
(-)-**19**	39 ± 5	2.19 ± 0.39	17.8
(+)-**19**	134 ± 12	15.9 ± 3.6	8.46

21	76.4 ± 2.4	10.4 ± 1.6	7.3
(±)-**40**	852 ± 209	4.59 ± 0.15	185.6
(-)-**40**	1,073 ± 92	1.84 ± 0.51	583
(+)-**40**	2,558 ± 112	54.1 ± 4.2	47.3
(±)-**41**	928 ± 152	2.78 ± 0.25	334
(±)-**42**	531 ± 119	1.74 ± 0.25	305
(±)-**45**	1,503 ± 67	4.17 ± 0.30	360
(-)-**45**	902 ± 130	1.09 ± 0.14	828
(+)-**45**	1,316 ± 244	48.2 ± 8.6	27.3
(±)-**46**	1,243 ± 130	4.10 ± 0.57	303
(-)-**46**	1,031 ± 182	1.40 ± 0.29	736
(+)-**46**	2,626 ± 229	52.8 ± 8.3	49.7
48	1,079 ± 139	16.8 ± 0.6	64.2
49	132 ± 22	8.07 ± 0.93	16.4

The next goal of our study was to investigate the functional activity of selected compounds at D2 and D3 receptors. The most and least selective D3 ligands, based on binding results, were selected for functional activity evaluation. Optically active lead compounds (−)-**19**, (−)-**40**, (−)-**45**, and (−)-**46** were tested in the [^{35}S]GTPγS functional assay to characterize their ability to stimulate D2 and D3 receptors in comparison to the endogenous ligand DA and parent compounds D-264 and D-301. Compounds (−)-**40**, (−)-**45**, and (−)-**46** each displayed higher functional potency and selectivity for D3

receptor in comparison to D-264 and DA (Table 5). In particular, (−)-**40** maintained high functional selectivity for D3 receptor (EC$_{50}$, D2 = 114 nM, D3 = 0.26 nM, D2/D3 = 438), correlating well with binding data and exhibited full agonist activity at both D2 and D3 receptors (E_{max} close to 100%). Compound (−)-**40** demonstrated a 5-fold increase in functional potency ((EC$_{50}$, D3 = 1.51 vs 0.26 for D-264 vs (−)-**40**)) and an almost 20-fold increase in functional selectivity ((D2/D3 = 22.1 vs 438 nM for D-264 vs (−)-**40**)) for D3 receptor when compared to D-264. Compounds (−)-**45** (EC$_{50}$, D2 = 86.4 nM, D3 = 0.87 nM, D2/D3 = 99.3) and (−)-**46** (EC$_{50}$, D2 = 70.7 nM, D3 = 0.56 nM, D2/D3 = 126) each exhibited full agonist activity (Emax not significantly different from 100%) at D2 and D3 receptors, while their selectivity for D3 receptor dropped considerably when compared to binding data. In contrast to the above-mentioned indoleacyl derivatives, compound (−)-**19** was exceptionally potent at both D2 (EC$_{50}$, D2 = 2.96 nM and D3 = 1.26 nM) and D3 receptor. Thus, (−)-**19** was indiscriminate in its activation of D2 and D3 receptors.

Table 5. Stimulation of [^{35}S]GTPγS binding to cloned human D2 and D3 receptor expressed in CHO cells.

Compound	CHO-D2		CHO-D3		
	EC$_{50}$ (nM) [^{35}S]GTPγS	% E$_{max}$	EC$_{50}$ (nM) [^{35}S]GTPγS	% E$_{max}$	D2/D3
DA	227 ± 11	100	8.57	100	26.5
D-301	116 ± 16	88.4 ± 3.9	0.82 ± 0.20	102 ± 2	141
D-264	33.1 ± 6.6	104 ± 5	1.51 ± 0.22	90.0 ± 4.3	22.1
(-)-**40**	114 ± 12	101 ± 5	0.26 ± 0.07	103 ± 10	438
(-)-**45**	86.4 ± 6.2	91.6 ± 5.9	0.87 ± 0.11	100 ± 6	99.3
(-)-**46**	70.7 ± 14.9	107 ± 4	0.56 ± 0.14	98.1 ± 3.3	126
(-)-**19**	2.96 ± 0.3	107 ± 3	1.26 ± 0.2	93.1 ± 4.4	2.35

3.4   Antioxidant, Neuroprotection and Anti-aggregation studies

3.4.1 Evaluation of Free Radical Scavenging Activity

In our attempt to assess the multifunctional nature of our lead compounds, we first measured their radical scavenging capacity. The DPPH radical scavenging assay is known to reveal the intrinsic radical scavenging potency of a compound and correlates well with protective concentrations of antioxidants against neurotoxic insults in cell-based systems {Kraus, 2005}. Scavenging of the DPPH (1,1-diphenyl-2-picrylhydrazyl) radical by (±)-**40**, (±)-**45**, (±)-**46**, (±)-**19**, and ascorbic acid is shown in Figure 12. Each

compound inhibited DPPH radical activity dose dependently. Ascorbic acid had an IC_{50} of 24.9 µM in this assay procedure, whereas the IC_{50} for (±)-**19** was 14.5 µM. All other compounds tested exhibited potencies comparable to that of ascorbic acid. It is clear from the data that the radical scavenging capacity of (±)-**19** is nearly twice that of ascorbic acid in quenching the DPPH radical.
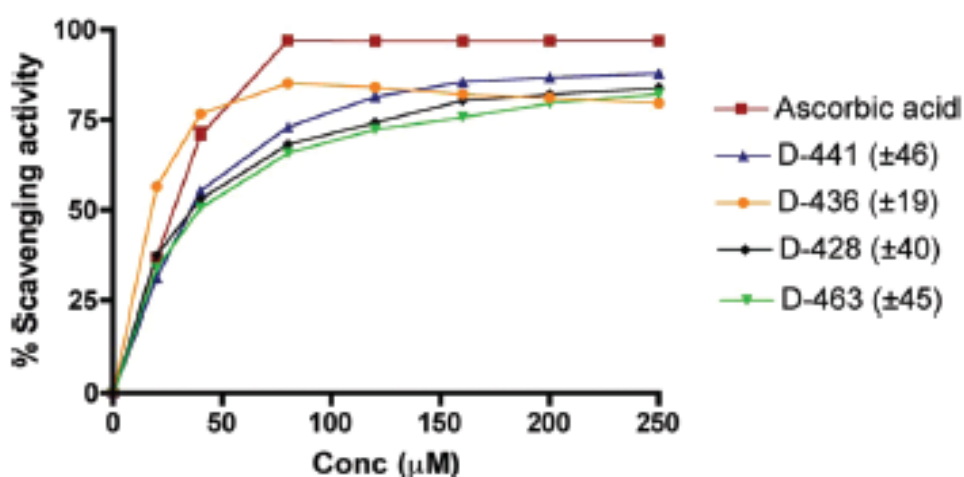
Figure 11. DPPH radical scavenging activity of (±)-**19**, (±)-**40**, (±)-**45**, (±)-**46** and ascorbic acid.

3.4.2 Neuroprotection Studies

3.4.2.1 Neuroprotection against 6-OHDA- and MPP+-induced cell death in MN9D cells

In order to further assess the multifunctional capability of our lead compounds, (-)-**19** (**D-512)** and (-)-**40** (**D-440**) were evaluated for their ability to protect dopaminergic cells from neurotoxic insults that mimic cell death in PD. The MN9D cell line was utilized for these experiments and is characterized as a hybridoma, derived via the somatic

fusion of rostral mesencephalic neurons from embryonic C57BL/6J (E14) mice and N18TG2 neuroblastoma cells {Choi, 1991}. MN9D cells are known to express high levels of TH and have high DA content. Furthermore, while exhibiting other similarities with DA neurons, the MN9D cell line represents one of the most suitable models for *in vitro* study of PD. In our initial studies, we carried out experiments to study the effect of (-)-**19** and (-)-**40** on the toxicity to MN9D cells caused by 6-OHDA and MPP$^+$. The neurotoxins, 6-OHDA and MPP+, are known to cause DA cell death possibly via different mechanisms. The toxicity of 6-OHDA is initiated by ROS production, following its transport into the cytosol via DAT. Oxidation of 6-OHDA is known to produce *p*-quinones and free radicals such as hydrogen peroxide, superoxide and hydroxyl radical, each of which induce apoptosis in cells {Bové, 2005; Breese, 1970}. The metabolism of MPTP by MAO-B produces MPP+, a neurotoxin that selectively destroys the nigrostriatal dopaminergic pathway and produces parkinsonian syndrome with massive loss of nigral DA neurons {Jackson-Lewis, 2007; Langston, 1983b; Przedborski, 2000}. The toxicity of MPP+ originates with its inhibition of mitochondrial complex I, thereby increasing oxidative stress and ultimately causing cell death {Przedborski, 2000}.
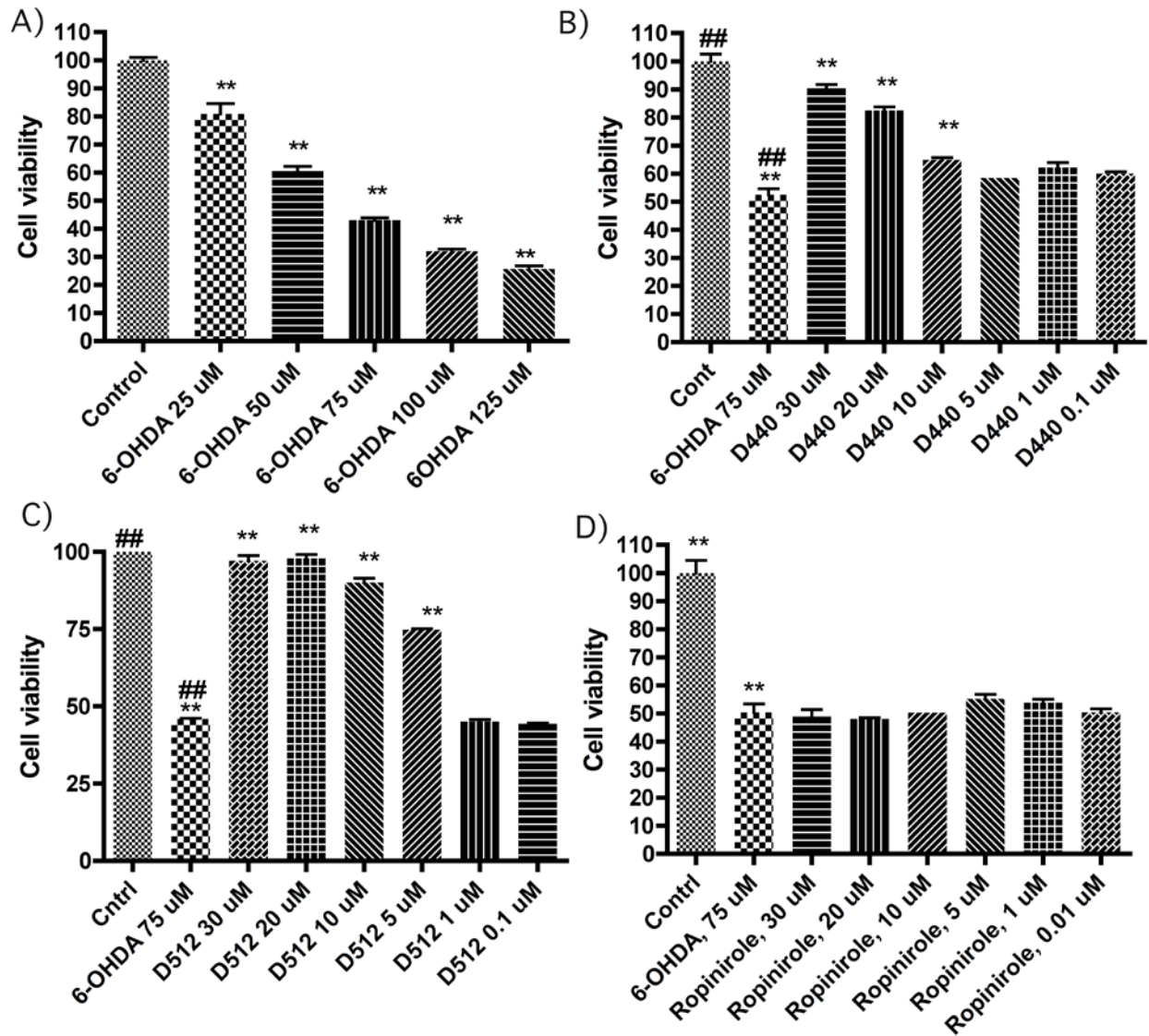
Figure 12. Dose-dependent effect of pre-treatment and co-treatment with D-512, D-440 and ropinirole on cell viability of 6-OHDA-treated MN9D cells. A: MN9D cells were treated with different concentrations of 6-OHDA (25 µM - 125 µM). B-D: MN9D cells were pre-treated with D-440, D-512 and ropinirole for 1 h followed by co-treatment with 75 µM 6-OHDA. One way ANOVA analysis followed by Tukey's Multiple Comparison post hoc test were performed. (**$p<0.001$ compared to the 6-OHDA group. ##$p<0.001$ compared to the control group).
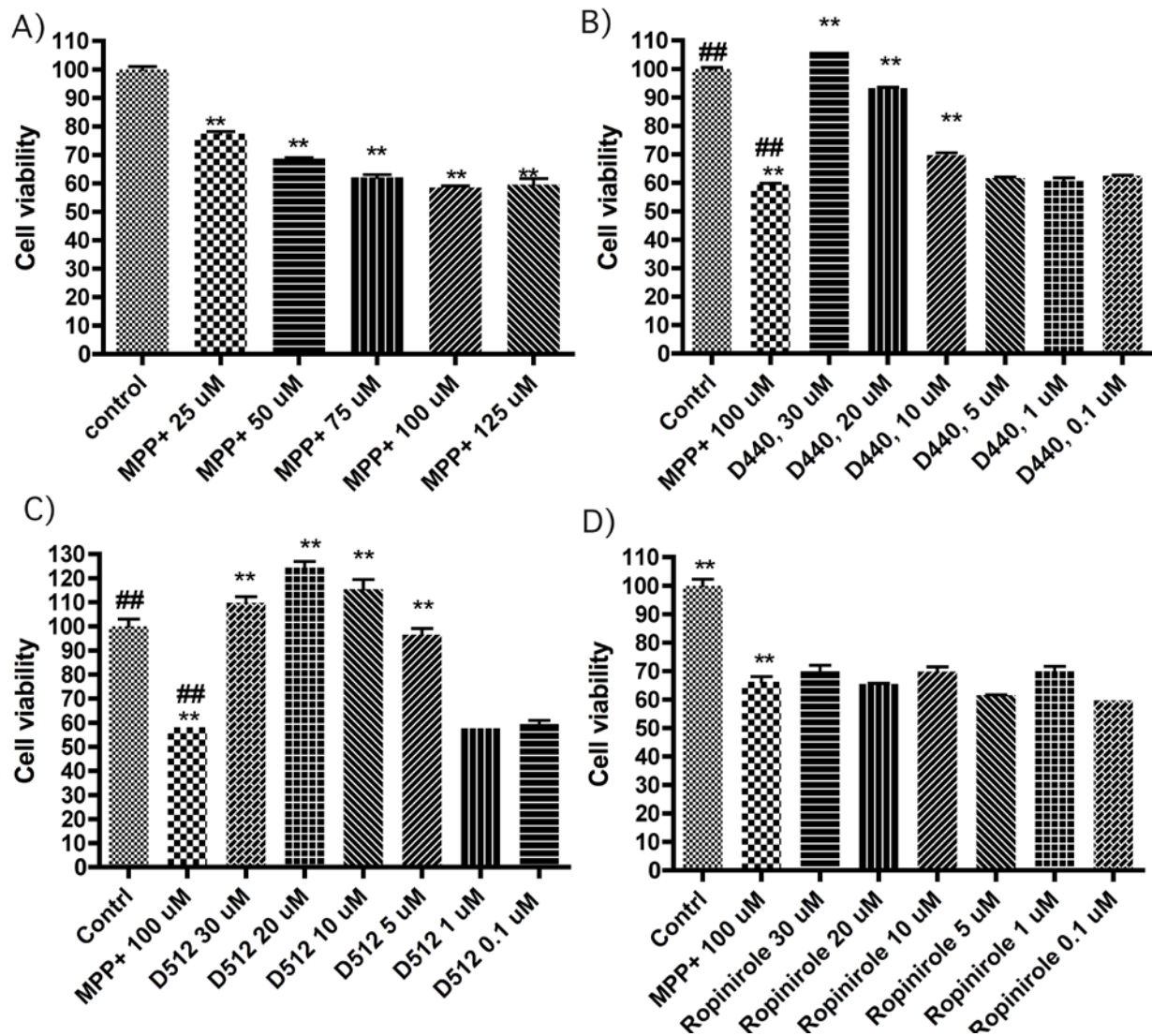
Figure 13. Dose-dependent effect of pre-treatment and co-treatment with D-512, D-440 and ropinirole on cell viability of MPP+-treated MN9D cells. A: MN9D cells were treated with different concentrations of MPP+ (25 μM - 125 μM). B-D: MN9D cells were pre-treated with D-440, D-512 and ropinirole for 1 h followed by co-treatment with 100 μM 6-OHDA. One way ANOVA analysis followed by Tukey's Multiple Comparison post hoc test were performed. (**p<0.001 compared to the MPP+ group. ##p<0.001 compared to the control group).

In order to demonstrate the ability of each neurotoxin to produce dose dependent cell death, we performed control experiments to determine the LD_{50} dose for 6-OHDA and MPP+ in MN9D cells (Figure 12A & 13A). The dose response profile of each neurotoxin revealed LD_{50} values of 75 µM and 100 µM for 6-OHDA and MPP+, respectively. Treatment of MN9D cells with (-)-**19** and (-)-**40** reversed the toxicity induced by 75 µM 6-OHDA. In the case of 6-OHDA, at doses between 5-30 µM, both (-)-**19** and (-)-**40** increased cell viability significantly. Compound (-)-**19** demonstrated potent (5 µM) neuroprotection and fully reversed 6-OHDA-induced toxicity at 20 and 30 µM (Figure 12C). Compound (-)-**40** exhibited a similar protection profile compared to (-)-**19**, although it exhibited somewhat lower potency in reversing 6-OHDA-induced toxicity (Figure 12B).

The neuroprotective effect of (-)-**19** and (-)-**40** in reversing the toxicity of MPP+ in MN9D cells is demonstrated in Figure 13. Data obtained from the MTT assay indicate that both (-)-**19** and (-)-**40** are able to protect MN9D cells from MPP+-induced neurotoxicity in a dose dependent manner. The results depicted in Figure 13C demonstrate that at doses of 5-30 µM, (-)-**19** conferred significant protection against MPP+-induced toxicity. Furthermore, at 10 and 20 µM dose, (-)-**19** not only reversed the toxicity of MPP+, but also induced cell proliferation compared to control. Compound (-)-**40** exhibited significant neuroprotection in the dose range of 10-30 µM and, at a dose of 30 µM, was able to fully protect MN9D cells from MPP+-induced toxicity. However, unlike (-)-**19**, (-)-**40** did not produce additional cell proliferation (Figure 13B). As shown in the case of 6-OHDA, (-)-**19** was more effective in reversing MPP+-induced toxicity compared to (-)-**40**. Next, we wanted to compare the neuroprotective effect of (-)-**19**

and (-)-**40** to the clinically approved PD drug, ropinirole. Interestingly, ropinirole did not demonstrate any significant neuroprotection against the toxicity of either 6-OHDA or MPP+ (Figure 12D & 13D). The cell morphology under different treatment regimes is depicted in Figure 14. These results underscore the neuroprotective potential of our lead compounds and demonstrate the inability of ropinirole to counteract the pathways involved in 6-OHDA- and MPP+-induced neurotoxicity.

3.4.2.2 Inhibition of 6-OHDA-Induced Caspase-Induction in MN9D cells

A possible mechanism behind the neuroprotective effect of (-)-**19** and (-)-**40** may involve reduction of 6-OHDA- and MPP+-induced oxidative stress. In order to further delineate the mechanisms involved in the neuroprotective effect of our lead compounds, we next examined the effect of (-)-**19** and (-)-**40** on the induction of caspase-3 and caspase-7 in 6-OHDA-treated MN9D cells. The caspases are a family of cysteine proteases that are known to play a critical role in apoptosis. Among the caspases, caspase-3, -6 and -7 are thought to trigger the execution phase of apoptosis via cleavage of several structural and repair proteins {Slee, 2001}. Previous studies indicate that 6-OHDA causes increased ROS production in MN9D cells and as a result, cell death arises via an intrinsic apoptotic pathway that involves caspase activation. Morphological changes accompanying 6-OHDA-induced cell death in MN9D cells include cytoplasmic membrane shrinkage, preservation of intracellular organelles and perinuclear chromatin condensation. In contrast, MPP+-induced cell death in MN9D cells has been shown to not involve significant ROS generation or caspase activation and to be accompanied by mitochondrial swelling and irregularly scattered

heterochromatin, characteristic of necrosis {Choi, 1999}. In order to evaluate whether (-)-**19** promotes cell survival in 6-OHDA-treated MN9D cells via inhibition of caspase activity, we carried out the fluorometric caspase 3/7 assay. The results from such experiments demonstrate that 6-OHDA treatment triggers a significant induction of caspase-3 activity, while (-)-**19** dose dependently inhibits 6-OHDA-induced caspase 3/7 activation in MN9D cells (Figure 15).

Figure 14. Morphological changes of MN9D cells treated with control, 75 µM 6-OHDA (24 h), 20 µM D-512 + 75 µM 6-OHDA (1 h pre-treatment/24 co-treatment), 100 µM MPP+ (24 h), 20 µM D-512 + 100 µM MPP+ (1 h pre-treatment/24 co-treatment) and 20 µM D-512 (24 h) detected under light micrograph (Magnification: 200X).

Control

6-OHDA 75uM

D512 20uM +
6-OHDA 75uM

MPP+ 100uM

D512 20uM +
MPP+ 100uM

D512 20uM
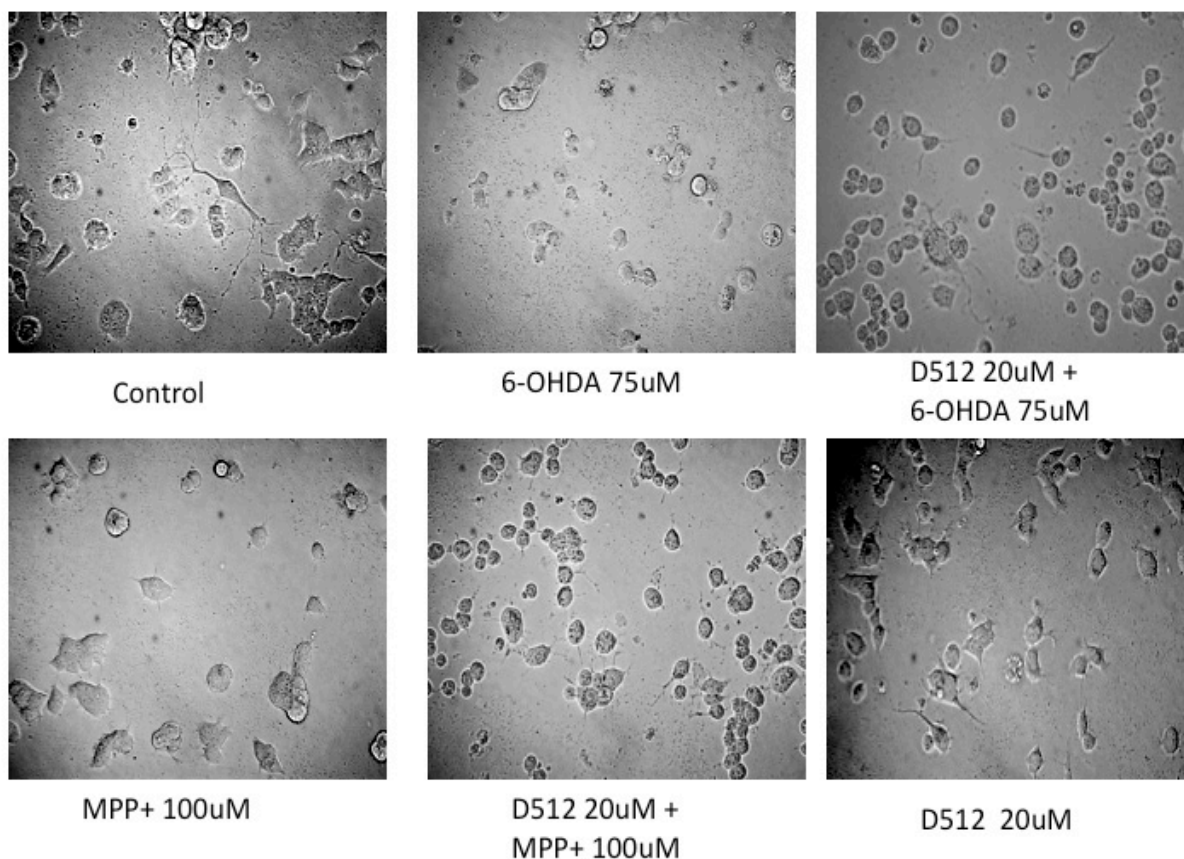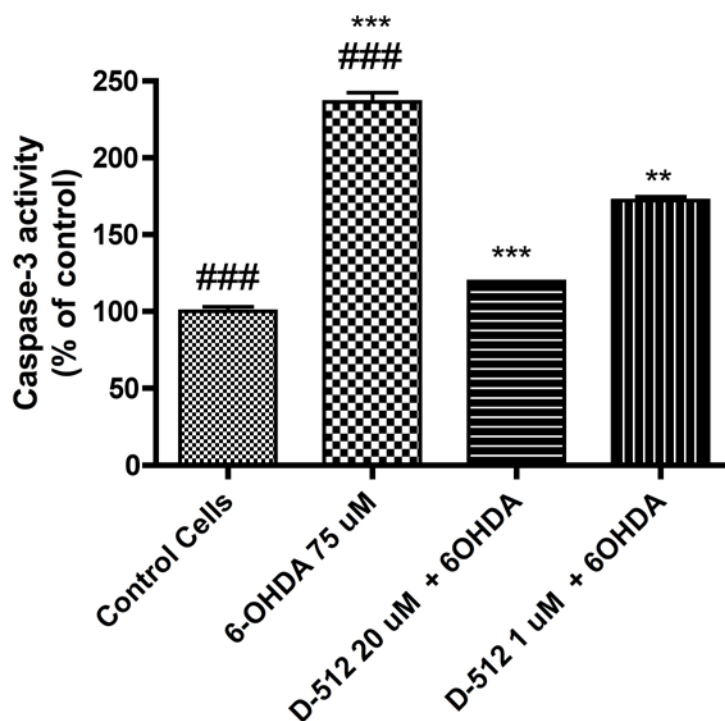
Figure 15. Dose-dependent inhibition of caspase-3 activity in 6-OHDA-treated MN9D cells by D-512. One way ANOVA analysis followed by Tukey's Multiple Comparison post hoc test were performed. (##p <0.01 control compared to 6-OHDA treated alone group. ***p <0.01 6-OHDA alone treated group compared to 6-OHDA + D-512 groups).

3.4.2.3 Restoration of TH level in 6-OHDA-treated MN9D cells

Tyrosine hydroxylase (TH) is the rate-limiting enzyme for DA biosynthesis and via immunohistochemistry, it has been widely utilized as a biomarker of dopaminergic neurons {Margolis, 2010}. Previous *in vivo* studies have established that 6-OHDA administration causes a parkinsonian condition that is accompanied by both reduced TH expression and DA content {Lotharius, 1999}. Due to the high levels of TH and DA in MN9D cells and owing to the importance of TH as a biomarker and in the integrity of dopaminergic neurons, we sought to determine the effect of (-)-**19** on TH levels in 6-OHDA-treated MN9D cells. Treatment of MN9D cells with 6-OHDA produced a

significant reduction in TH level. Our results illustrate the ability of (-)-**19** to restore TH

level in 6-OHDA-treated MN9D cells. Interestingly, treatment of MN9D cells with (-)-**19**,

in the absence of 6-OHDA, upregulated the level of TH compared to control (Figure 16).

The results obtained from neuroprotection studies suggest that our lead compounds

have the potential to act as neuroprotective, disease-modifying therapeutic agents for

PD.
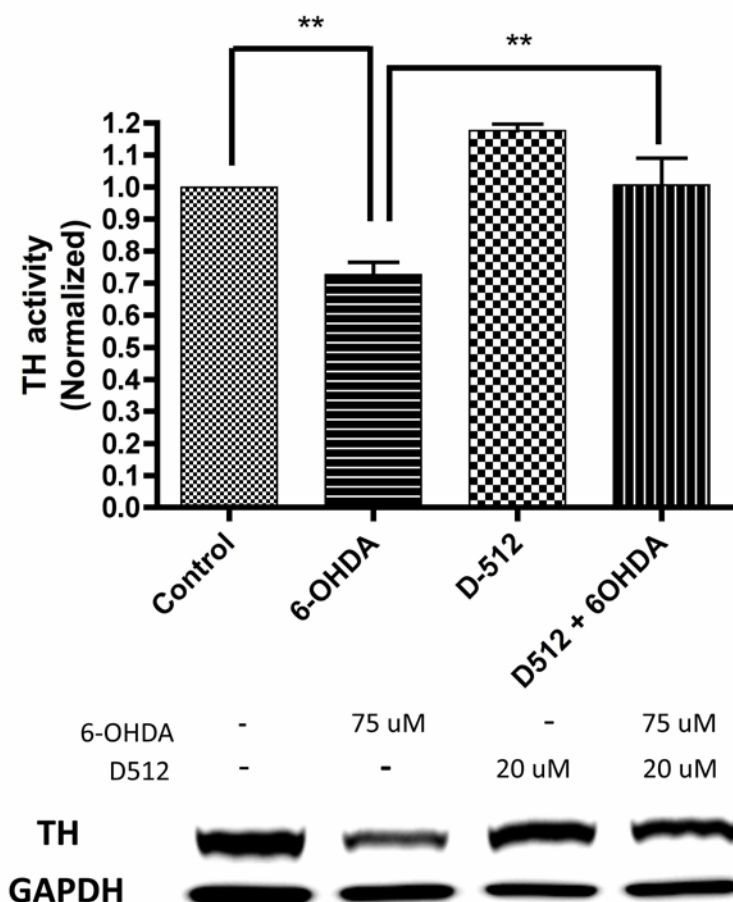
Figure 16. TH protein level in MN9D cells determined by Western blot analysis. MN9D cells were pretreated with 20 µM D-512 for 1 h and co-treated with 75 µM 6-OHDA for 24 h. MN9D cells were also treated with control vehicle, D-512 and 6-OHDA alone. For quantification purpose protein level was normalized with respect to GAPDH protein. One way ANOVA analysis followed by Tukey's Multiple Comparison post hoc test were performed. (**$p<0.05$ control compared to the 6-OHDA group. **$p<0.05$ 6-OHDA compared to the D-512 + 6-OHDA group).

3.4.3 Anti-Aggregation Studies

As mentioned previously, α-synuclein aggregation is thought to play a prominent role in PD pathogenesis. The mechanisms by which aggregation and associated neurotoxicity occur is not yet fully understood, although several factors, including DA and its oxidized by-prodcuts, as well as oxidative stress-inducing metals, seem to play a role in the aggregation process. Owing to the significant role of α-synuclein aggregation in the neurodegenerative process and to further study the multifunctional capability of (-)-**19**, we sought to evaluate the ability of our lead compound to modify α-synuclein aggregation in a cell-free system. Our initial experiment examined the ability of (±)-**19** to modify DA-induced, α-synuclein aggregation. In these studies, we utilized silver staining and transmission electron microscopy (TEM) to monitor the course of aggregation (Figures 17 & 18). We were able to demonstrate the formation of DA-induced oligomers, with a time-dependent increase in proportion of higher molecular weight aggregates (Figure 17A). Under identical experimental conditions, (±)-**19** was observed to drastically modify the DA-induced, α-synuclein aggregation process. In the case of (±)-**19**, we observed a rapid decrease in lower molecular weight forms of α-synuclein, although formation of discrete oligomeric aggregates was inhibited, in comparison to DA treatment alone (Figure 17C). Standard antioxidant, ascorbic acid, while slightly reducing the kinetics and nucleation of α-synuclein, was unable to significantly modify DA-induced α-synuclein aggregation (Figure 17B).

Transmission electon microscope images show morphological and physical characteristics of aggregates formed under different treatment regimes (Figure 18A-C).

A.
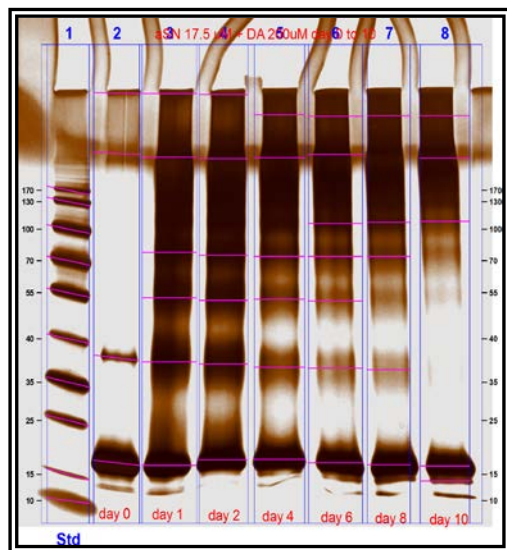
B.
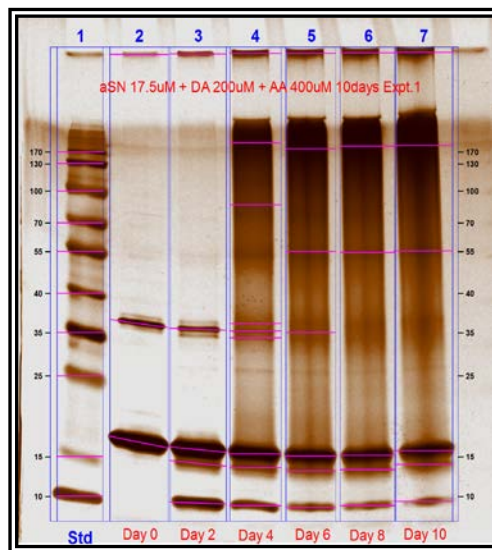
C.
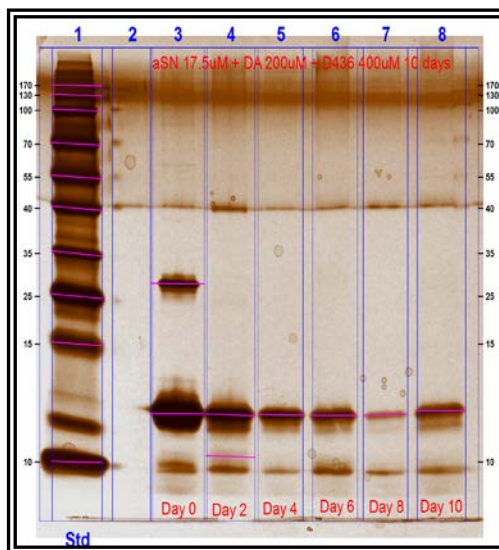
Figure 17. Silver staining of SDS-PAGE gels for aggregation experiments ran at 1400 rpm, 37 °C and under the following conditions: A. ASN (17.5 µM) + DA (200 µM) B. ASN (17.5 µm) + DA (200 µm) + ascorbic acid (400 µm) C. ASN (17.5 µm) + DA (200 µm) + (±)-19 (400 µm).

A.

B.
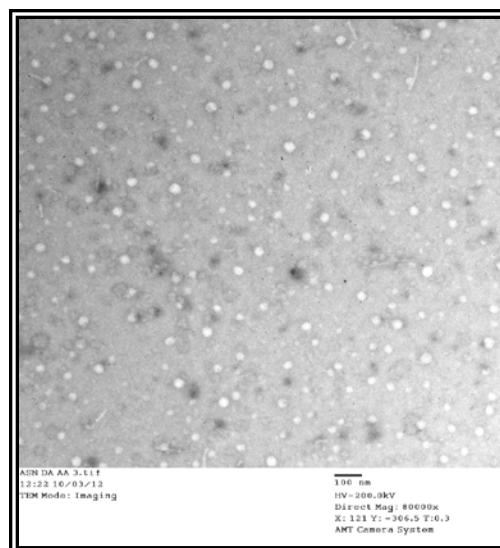
C.
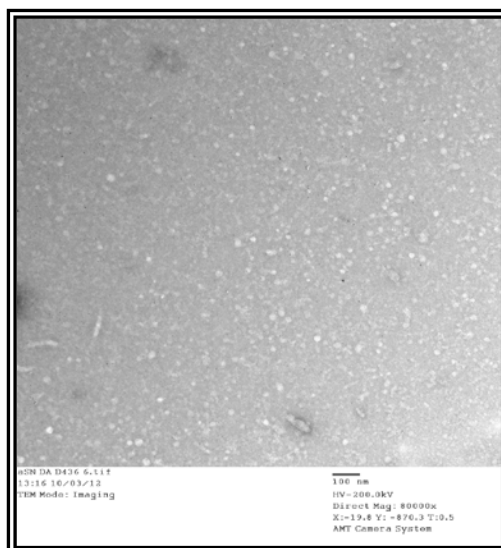
Figure 18. Transmission electron microscopy images at 80000x magnification to detect the morphology and physical characteristics of ASN samples taken from experiments ran under the following conditions: A. ASN (17.5 µM) + DA (200 µM) B. ASN (17.5 µm) + DA (200 µm) + ascorbic acid (400 µm) C. ASN (17.5 µm) + DA (200 µm) + (±)-19 (400 µm).

In comparison to ASN + DA treatment (Figure 18A), in which small globular and larger aggregates can be seen, co-incubation with (±)-**19** demonstrated a reduction in the size and number of aggregates (Figure 18C). Additionally, ascorbic acid co-treatment was able to modify DA-induced ASN aggregation slightly, with TEM imaging showing an increase in size and number of small, globular oligomers and a decrease in the number of large aggregates (Figure 18B).

3.5   *In vivo* Efficacy of Lead Compounds in PD Animal Models

3.5.1   Reversal of Reserpine-Induced Hypolocomotion in Rats

Reserpine induces depletion of catecholamines in nerve terminals, resulting in a cataleptic condition in rats and is a well established animal model for PD {Carlsson, 1957}. Reserpine irreversibly blocks the vesicular monamine transporter (VMAT) in the cytoplasm of presynaptic neurons, thereby inhibiting the intracellular storage of monamines and leaving them vulnerable to metabolism. Therefore, reserpine-induced DA depletion leads to reduced DA levels in the synaptic cleft, resulting in akinesia {Carlsson, 1975; Colpaert, 1987}. All clinically approved anti-parkinsonian drugs used to date, including L-dopa and DA agonists, are known to attenuate motor deficits in reserpine-treated rats {Menzaghi, 1997}. A significant reduction of locomotion was observed in the animals 18 h after the administration of reserpine (5 mg/kg, sc), indicating the development of akinesia. Compound (-)-**19** (5 µmol/kg, sc) was efficacious in significantly reversing akinesia in rats, compared to reserprine treatment alone (Figure 19). Treatment with reference drug, ropinirole (5 µmol/kg, sc), produced

significant locomotor activation, reaching higher levels of locomotion, but much shorter

duration of action compared to (-)-**19**. On the other hand, compounds (-)-**46** and (-)-**40**

(10 µmol/kg, sc) each failed to produce any appreciable reversal of akinesia in

reserpine-treated rats.
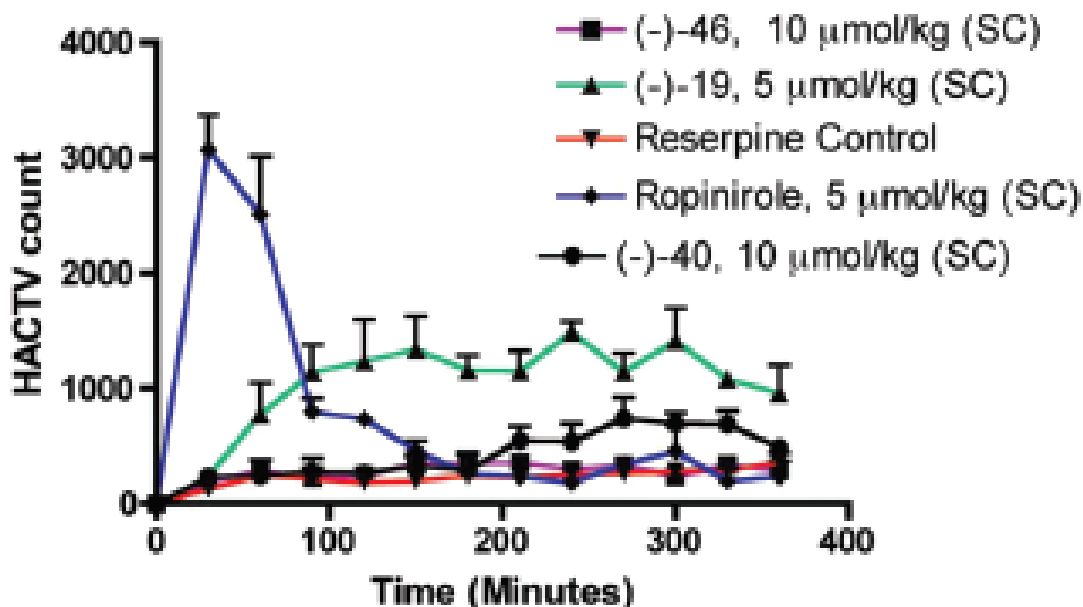
Figure 19. Effect of different drugs (administered sc) upon reserpine-induced (5.0 mg/kg) hypolocomotion in rats. Each point represents the mean ± SEM for three to six rats. Horizontal activity was measured as described in Materials and Methods section. Representation of horizontal locomotor activity is at discrete 30 min. intervals after the administration of (-)-19 (5 µMol/kg), (-)-46 (10 µMol/kg), (-)-40 (10 µMol/kg), and Ropinirole (5 µMol/kg) compared to control rats, 18 h after reserpine treatment. Differences among treatments were significant by one-way ANOVA analysis ($F(4.95)$ = 6.69 ($P < 0.0001$): (**) $P < 0.01$ ((-)-19) or (*) $P < 0.05$ (Ropinirole) compared to reserpine control (Dunnett's analysis after one-way ANOVA).

3.4.2 Induction of Contralateral Rotation in 6-OHDA-Lesioned Rats

In order to further determine the efficacy of (-)-**19** and (-)-**40** *in vivo*, lead

compounds were evaluated in rats carrying a unilateral lesion in the medial forebrain

bundle, induced by application of 6-OHDA (Figure 20). The 6-OHDA-lesioned rat model

is considered one of the standard preclinical models for early screening of PD drugs. In this model, administration of 6-OHDA causes degeneration of dopaminergic cell bodies and fibers in the nigrostriatal pathway and the development of supersensitivity of DA receptors on the lesioned side ensues {Deumens, 2002}. These unilaterally lesioned rats are known to produce rotations contralateral to their lesion when challenged with direct-acting DA agonists, such as apomorphine {Ungerstedt, 1971}. Our results show that D2 and D3 potent agonist, (-)-**19**, produces dose dependent rotations with long duration of action. In the case of (-)-**19**, the highest number of rotations (contralateral rotations = 4555) occurred at the highest dose of the drug (10 µMol/ kg). The D3 receptor-selective agonist, (-)-**40**, also produced dose dependent rotations of long duration, with the highest number of rotations (contralateral rotations = 4666) occurring at its highest dose (10 µMol/ kg).

Interestingly, although (-)-**40** failed to reverse reserpine-induced hypolocomotion in DA-depleted rats, it was able to produce contralateral rotation in 6-OHDA-lesioned rats. An explanation for this outcome rests on two main points. First, evidence suggests that D3 receptor number decreases in early stages of PD and similar studies have shown that nonresponders to antiparkinsonian medication correlate with a lower D3 receptor number (-48%). In contrast, PD cases that remain responsive to antiparkinsonian drugs correlate with elevated levels (+25%) of D3 receptor {Joyce, 2001b}. Furthermore, a post-mortem study of PD cases revealed that D3 receptor was reduced by 45% in the basal ganglia, while D2 receptor was elevated in similar regions by 15-25% {Ryoo, 1998}. Thus, it is hypothesized that in DA-depleted animals, D3 receptor number becomes significantly reduced and may cause lack of response to

antiparkinsonian medication. Second, in 6-OHDA-lesioned rats it has been shown that the motor stimulating effect of L-dopa and other D1 receptor agonists, such as apomorphine, measured as contraversive rotations, becomes enhanced upon repeated intermittent administration. The intensity of response to an L-dopa challenge increased 3- to 4-fold following chronic, L-dopa administration and progressively declined upon withdrawal of the treatment regime. Furthermore, the time course of the change in rotational behavior paralleled that of D3 receptor appearance and disappearance in the caudate putamen {Bordet, 1997}. It is hypothesized that repeated challenging of 6-OHDA-lesioned rats with apomorphine led to D3 receptor induction in the caudate putamen, and motor activation, when administered D3 receptor-selective agonist, (-)-**40**. Thus, each lead compound was efficacious in producing contralateral rotation in the 6-OHDA-lesioned rat model of PD.
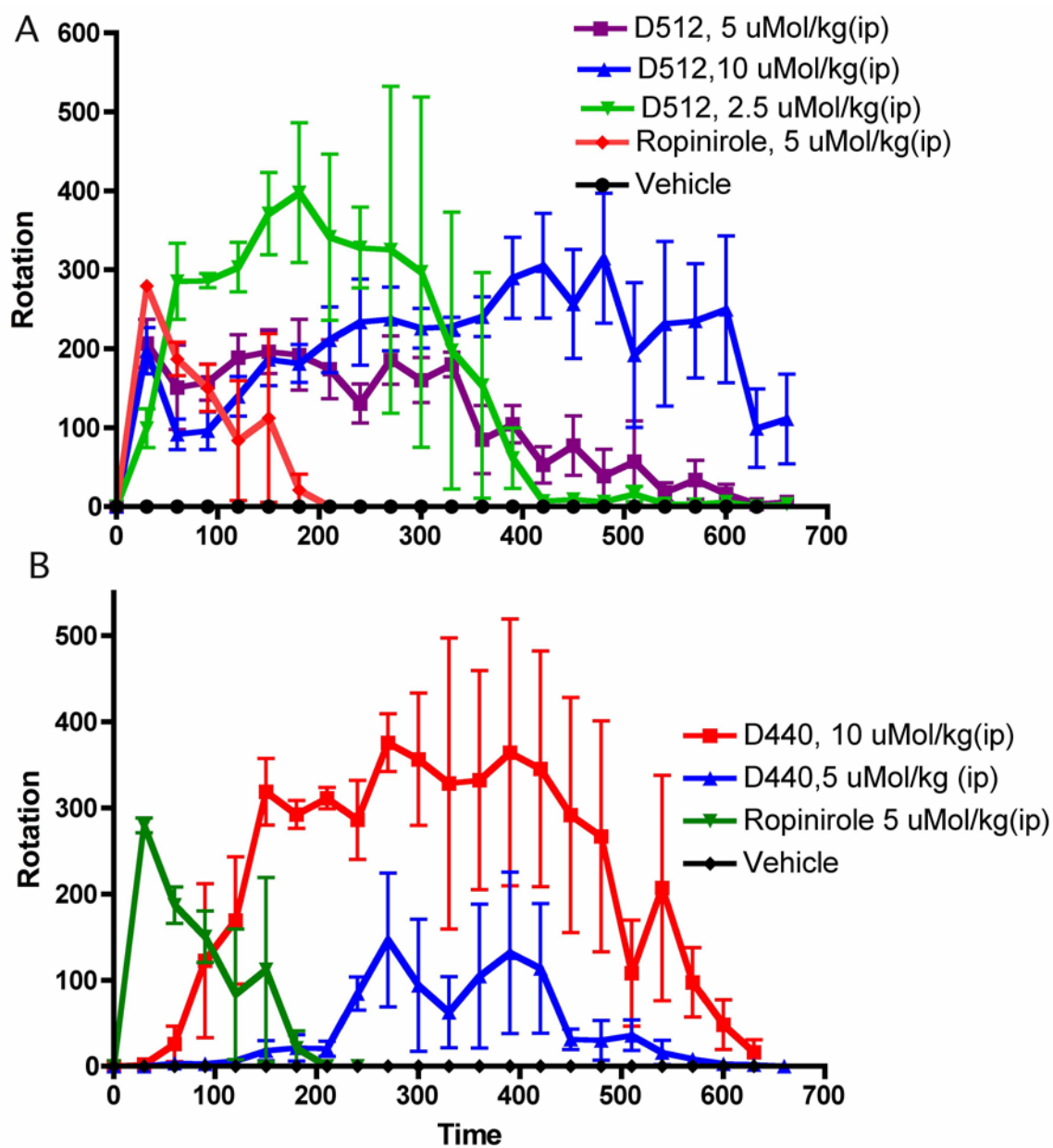
Figure 20. Effect on turning behavior of **D-512** ((-)-**19**), **D-440** ((-)-**40**) and ropinirole in 6-OHDA unilaterally lesioned rats.

CHAPTER 4

SUMMARY

Parkinson's disease (PD) is a progressive, neurodegenerative disorder that results from the death of DA-producing cells in the SNc region of the midbrain. Common symptoms include: resting tremor, muscular rigidity, bradykinesia, along with postural instability and cognitive psychiatric complications. In PD, the progressive loss of dopaminergic neurons in the SNc results in a depletion of DA in the basal ganglia and striatum. Low DA levels cause dysregulation of the motor circuits that project through this brain region, leading to the clinical manifestations of the disease. Although the etiology of PD is not yet clear, oxidative stress and mitochondrial dysfunction are thought to play a central role in the pathology of the disease. A reduction in natural antioxidant defenses, along with increased free iron levels have also been tied to PD disease progression and susceptibility. In addition, protein aggregation, namely that of α-synuclein, is thought to be intimately associated with disease pathogenesis.

DA receptor agonists have been employed more extensively in the treatment of Parkinson's disease than any other type of pharmacotherapy. L-dopa, the immediate precursor to endogenous DA, is the current gold-standard treatment option for PD. Although initially beneficial in reducing motor symptoms, chronic L-dopa therapy inevitably leads to a number of side effects including, wearing off, "on" and "off" episodes, production of involuntary movements and may even exacerbate the progression of the disease. The replacement of L-dopa by DA agonists has the

potential of alleviating these undesirable side effects, while also acting as both a symptomatic and neuroprotective therapeutic agent.

Utilizing our previously developed hybrid structure template, we have designed novel, D3 receptor-preferring agonists. These hybrid compounds contain an agonist binding moiety, consisting of either 5-OH-aminotetralin or 2-aminothiazole, linked to an aryl piperazine fragment via methylene linkage. These compounds have demonstrated high affinity and potency for D3 receptor. Additionally, antioxidant moieties have been incorporated into these molecules in order to confer radical scavenging capacity and the potential to protect dopaminergic cells from neurotoxic insults. These properties are hypothesized to address a number of the shortcomings of existing therapeutic agents for PD.

After synthesis we sought to characterize our compounds using *in vitro* radioligand binding and GTPγS functional assays. Binding results pointed to (±)-**19**, (±)-**40**, (±)-**45** and (±)-**46** as lead compounds due to high affinity binding of (±)-**19** to D2 and D3 receptors, as well as high selectivity of (±)-**40**, (±)-**45** and (±)-**46** for D3 receptor. Next, we synthesized and evaluated both the (+) and (-)-isomeric forms of each lead compound and determined the (-)-isomeric form to confer the highest biological activity. Going forward with the (-)-isomeric form of each compound, functional studies characterized each of these molecules as full agonists at both D2 and D3 receptors. The functional potency of (-)-**19** for D2 and D3 receptors remained high and correlated with binding affinity, while only the D3 selectivity of (-)-**40** correlated well with binding data.

Next, our lead molecules were further evaluated for the antioxidant, neuroprotective and anti-aggregation properties. The DPPH radical scavenging assay was used to reveal the intrinsic radical scavenging potency of our compounds. In this assay procedure, (±)-**19** demonstrated an IC_{50} of 14.5 µM, compared to that of 24.9 µM in the case of ascorbic acid. It was clear from the data that the radical scavenging capacity of (±)-**19** is nearly twice that of ascorbic acid in quenching the DPPH radical.

In order to further assess the multifunctional capability of our lead compounds, (-)-**19** and (-)-**40** were evaluated for their ability to protect dopaminergic cells from neurotoxic insults that mimic cell death in PD. Treatment of MN9D cells with (-)-**19** and (-)-**40** reversed the toxicity induced by 75 µM 6-OHDA. Additionally, data obtained show that both (-)-**19** and (-)-**40** are able to protect MN9D cells from MPP+-induced neurotoxicity in a dose dependent manner. Furthermore, at 10 and 20 µM dose, (-)-**19** not only reversed the toxicity of MPP+, but also induced cell proliferation. Interestingly, clinically approved PD drug, ropinirole, did not demonstrate any significant neuroprotection against the toxicity of either 6-OHDA or MPP+.

In order to further delineate the mechanisms involved in the neuroprotective effect of our lead compounds, we next examined the effect of (-)-**19** and (-)-**40** on the induction of caspase-3 and caspase-7 in 6-OHDA-treated MN9D cells. In order to evaluate whether (-)-**19** promotes cell survival in 6-OHDA-treated MN9D cells via inhibition of caspase activity, we carried out the fluorometric caspase 3/7 assay. The results from such experiments demonstrate that 6-OHDA treatment triggers a significant induction of caspase-3 activity, while (-)-**19** dose dependently inhibits 6-OHDA-induced caspase 3/7 activation in MN9D cells.

Tyrosine hydroxylase (TH) is the rate-limiting enzyme for DA biosynthesis and via immunohistochemistry, it has been widely utilized as a biomarker of dopaminergic neurons. Due to high levels of TH and DA in MN9D cells and owing to the importance of TH as a biomarker and in the integrity of dopaminergic neurons, we sought to determine the effect of (-)-**19** on TH levels in 6-OHDA-treated MN9D cells. Treatment of MN9D cells with 6-OHDA alone indicated a significant reduction in TH level. Furthermore, our results demonstrate the ability of (-)-**19** to restore TH level in 6-OHDA-treated cells. Interestingly, treatment of MN9D cells with (-)-**19**, in the absence of 6-OHDA, upregulated the level of TH.

Next, we sought to determine the *in vivo* efficacy of our lead compounds in PD animal models. Reserpine induces depletion of catecholamines in nerve terminals, resulting in a cataleptic condition in rats and is a well established animal model for PD. A significant reduction of locomotion was observed in the animals 18 h after the administration of reserpine (5 mg/kg, sc), indicating the development of akinesia. Compound (-)-**19** (5 μM/kg, sc) was efficacious in significantly reversing akinesia in rats, compared to reserprine treatment alone. Treatment with the reference drug, ropinirole (5 μM/kg, sc), produced significant locomotor activation, but much shorter duration of action compared to (-)-**19**.

We also evaluated the efficacy of (-)-**19** and (-)-**40** in rats carrying a unilateral lesion in the medial forebrain bundle, induced by application of 6-OHDA. In this model, administration of 6-OHDA causes degeneration of dopaminergic cell bodies and fibers in the nigrostriatal pathway and development of supersensitivity to DA receptors on the lesioned side ensues. These unilaterally lesioned rats are known to produce rotations

contralateral to their lesion when challenged with direct-acting DA agonists. Our results show that both (-)-**19** and (-)-**40** produce dose dependent rotations with long duration of action. Interestingly, although (-)-**40** failed to reverse reserpine-induced hypolocomotion in DA-depleted rats, it was able to produce contralateral rotation in 6-OHDA-lesioned rats. An explanation for this outcome rests on two main points. First, evidence suggests that it in DA-depleted animals D3 receptor number is significantly reduced, which may cause a lack of response to antiparkinsonian medication. Second, the repeated challenge of 6-OHDA-lesioned rats with apomorphine may have led to D3 receptor induction in the caudate putamen, causing motor activation upon administration of D3 receptor-selective agonist, (-)-**40**. Therefore, both lead compounds were efficacious in producing contralateral rotation in the 6-OHDA-lesioned rat model of PD. Taken together, the results obtained from *in vitro* binding and functional studies, as well as antioxidant, neuroprotection, anti-aggregation and *in vivo* PD animal model studies suggest that our lead compounds have the potential to act both as symptomatic and disease-modifying therapeutic agents for PD.

CHAPTER 5

MATERIALS AND METHODS

5.1 Chemistry

5-methoxy-N-propyl-1,2,3,4-tetrahydronaphthalen-2-amine (2). Into a stirring solution of *n*-propylamine (14.9 mL, 181.6 mmol) and ketone **1** (12.8 g, 72.6 mmol), in CH_2Cl_2 (70 mL), was added glacial acetic acid (17.3 mL, 290.5 mmol). After stirring for 0.5 h, $NaCNBH_3$ (11.4 g, 181.6 mmol) was added portion wise at 0 °C, followed by methanol (20 mL). The mixture was allowed to reach room temperature and stirred overnight. The reaction mixture was quenched with a saturated $NaHCO_3$ solution at 0 °C and extracted with ethyl acetate (3 x 100 mL). The combined organic layer was washed with water, brine and dried over Na_2SO_4. Solvent was removed under reduced pressure. Crude product was purified by column chromatography (EtOAc/MeOH, 9:1) to give compound **2** (11.1 g, 70%).^{1}H NMR (CDCl$_3$, 400 MHz): δ 0.96 (t, *J* = 7.2 Hz, 3H), 1.54-1.65 (m, 3H), 2.09-2.16 (m, 1H), 2.52-2.74 (m, 4H), 2.88-3.07 (m, 3H), 3.81 (s, 3H), 6.66 (d, *J* = 8.0 Hz, 1H), 6.71 (d, *J* = 8.4 Hz, 1H), 7.09 (t, *J* = 8.4 Hz, 1H).

4-(2-Hydroxy-ethyl)piperazine-1-carboxylic acid *tert*-butyl ester (5). A mixture of compound **4** (10.0 g, 53.7 mmol), 2-bromoethanol (10.1 g, 80.6 mmol) and K_2CO_3 (22.3 g, 161.1 mmol) in CH_3CN (100 mL) was refluxed for 14 h according to procedure D. The crude material was purified by silica gel column chromatography (EtOAc/MeOH, 20:1) to give compound **5** (7.12 g, 58%). ^{1}H NMR (CDCl$_3$, 400 MHz): δ 1.40 (s, 9H), 2.40 (t, *J* = 4.8 Hz, 4H), 2.50 (t, *J* = 5.2, 2H), 3.38 (t, *J* = 4.8 Hz, 4H), 3.58 (t, *J* = 5.2 Hz, 2H).

Procedure A. 4-(2-Oxo-ethyl)piperazine-1-carboxylic acid *tert*-butyl ester (6). Into a stirring solution of oxalyl chloride (5.5 g, 43.3 mmol) in CH_2Cl_2 (80 mL) at -78 $^{\circ}$C, DMSO (6.2 mL, 78.7 mmol) was added. The reaction mixture was stirred for 0.5 h, followed by addition of compound **5** (5.0 g, 21.7 mmol, solution in 20 mL of CH_2Cl_2). The reaction mixture was stirred at the same temperature for 0.5 h, followed by addition of Et_3N (18.2 mL, 179.4 mmol) and stirring was continued for 1.5 h, while allowing the reaction mixture to reach room temperature. The reaction mixture was quenched by addition of a saturated solution of $NaHCO_3$ and extracted with CH_2Cl_2 (3 x 100 mL). The combined organic layer was dried using Na_2SO_4 and the solvent was removed under reduced pressure. The crude product was purified by silica gel column chromatography (EtOAc/MeOH, 20:1) to give compound **6** (4.96 g, ~100%).

Procedure B. 4-{2-[(5-Methoxy-1,2,3,4-tetrahydro-naphthalen-2-yl)propyl amino]ethyl}piperazine-1-carboxylic acid *tert*-butyl ester (7). Into a stirring solution of amine **2** (4.76 g, 21.7 mmol) in CH_2Cl_2 (50 mL), aldehyde **6** (4.96 g, 21.7 mmol) was added. After stirring for 1 h, $NaBH(OAc)_3$ (8.29 g, 39.1 mmol) was added portion wise and the mixture was stirred for 48 h at room temperature. The reaction mixture was quenched with a saturated solution of $NaHCO_3$ at 0 $^{\circ}$C and extracted with ethyl acetate (3 x 100 mL). The combined organic layer was dried over Na_2SO_4 and the solvent was removed under reduced pressure. Crude product was purified by column chromatography (EtOAc/MeOH, 20:1) to give compound **7** (6.46 g, 69%). ^{1}H NMR (CDCl_3, 400 MHz): δ 0.86 (t, $J = 7.6$ Hz, 3H), 1.20 (s, 9H), 1.30-1.52 (m, 3H), 1.90-2.12 (m, 1H), 2.20-3.06 (m, 13H), 3.20-3.60 (m, 6H), 3.77 (s, 3H), 6.61 (d, $J = 8$ Hz, 1H), 6.67 (d, $J = 8$ Hz, 1H), 7.05 (t, $J = 7.6$ Hz, 1H).

6-[(2-piperazin-1-yl-ethyl)-propyl amino]-5,6,7,8-tetrahydronaphthalen-1-ol (8). A mixture of compound **7** (6.46 g, 14.9 mmol) and 48% aq. HBr (40 ml) was refluxed at 125 °C for 12 h. The reaction mixture was evaporated to dryness and a saturated solution of $NaHCO_3$ was added into it at 0 °C. The reaction mixture was then extracted with ethyl acetate (3 x 100 mL). The combined organic layer was dried over Na_2SO_4, filtered, and concentrated under reduced pressure to yield compound **8** (3.80 g, 80%). ^{1}H NMR (CD_3OD, 400 MHz): δ 1.06 (t, J = 7.2 Hz, 3H), 1.80-2.02 (m, 3H), 2.36-2.48 (m, 1H), 2.60- 2.80 (m, 1H), 2.96-4.02 (m, 18H), 6.61 (d, J = 8 Hz, 1H), 6.66 (d, J = 8 Hz, 1H), 6.96 (t, J = 8 Hz, 1H).

6-({2-[4-(1H-indol-5-ylmethyl)piperazin-1-yl]ethyl}propyl amino)-5,6,7,8-tetrahydro naphthalen-1-ol (9a). Amine **8** (200 mg, 0.63 mmol) was reacted with 1*H*-indole-5-carbaldehyde (91 mg, 0.63 mmol) and $NaBH(OAc)_3$ (240 mg, 1.13 mmol) in CH_2Cl_2 (15 mL) using procedure B. The crude residue was purified by column chromatography (MeOH/EtOAc, 1:6) to afford compound **9a** (220 mg, 79%). ^{1}H NMR ($CDCl_3$, 400 MHz): δ 0.86 (t, J = 7.2 Hz, 3H), 1.30-1.52 (m, 3H), 1.90-2.10 (m, 1H), 2.46-3.02 (m, 19H), 3.76 (s, 2H), 6.51 (d, J = 8 Hz, 1H), 6.67 (d, J = 8 Hz, 1H), 6.94 (t, J = 7.6 Hz, 1H), 7.06-7.25 (m, 3H), 7.36 (d, J = 8 Hz, 1H), 7.72 (d, J = 8.2 Hz, 1H), 8.26 (bs, 1H). [13]C ($CDCl_3$, 100 MHz): δ 12.0, 22.3, 24.0, 25.7, 29.9, 32.4, 47.9, 52.8, 53.5, 53.6, 53.8, 57.4, 58.7, 111.2, 112.2, 119.6, 121.4, 122.1, 123.6, 124.2, 126.3, 128.2, 136.5, 138.5, 154.2, 171.4. The free base was converted to its hydrochloride salt. M.p. 165-169 °C. Anal. calculated for $C_{30}H_{46.5}Cl_{3.5}N_4O$: C, H, N.

6-({2-[4-(1H-indol-2-ylmethyl)piperazin-1-yl]ethyl}propyl amino)-5,6,7,8-tetrahydro naphthalen-1-ol (9b). Amine **8** (200 mg, 0.63 mmol) was reacted with 1H-Indole-2-

carbaldehyde (91 mg, 0.63 mmol) and $NaBH(OAc)_3$ (240 mg, 1.13 mmol) in CH_2Cl_2 (15 mL) using procedure B. The crude residue was purified by column chromatography (MeOH/EtOAc, 1:6) to afford compound **9b** (225 mg, 81%). ^{1}H NMR ($CDCl_3$, 400 MHz): δ 0.90 (t, J = 7.2 Hz, 3H), 1.40-1.71 (m, 3H), 1.96-2.10 (m, 1H), 2.36-3.08 (m, 19H), 3.77 (s, 2H), 5.36 (bs, 2H), 6.39 (s, 1H), 6.60 (dd, J = 7.2 Hz, 1H), 6.95 (t, J = 7.6 Hz, 1H), 7.04-7.12 (m, 2H), 7.17 (t, J = 7.6 Hz, 1H), 7.36 (d, J = 8.4 Hz, 1H), 7.56 (d, J = 8.4 Hz, 1H). ^{13}C ($CDCl_3$, 100 MHz): δ 12.1, 21.6, 24.0, 25.4, 28.4, 30.0, 31.8, 47.5, 52.5, 52.8, 53.2, 53.6, 55.5, 57.2, 57.8, 103.0, 111.3, 119.9, 120.5 122.0, 123.7, 126.0, 128.3, 133.8, 136.7, 137.6, 154.6, 178.0. The free base was converted to its hydrochloride salt. M.p. 180-185 ºC. Anal. calculated for $C_{28}H_{47}Cl_4N_4O_{3.5}$: C, H, N.

6-({2-[4-(1H-indol-3-ylmethyl)piperazin-1-yl]ethyl}propyl amino)-5,6,7,8-tetrahydro naphthalen-1-ol (9c). Amine **8** (200 mg, 0.63 mmol) was reacted with 1*H*-indole-3-carbaldehyde (91 mg, 0.63 mmol) and $NaBH(OAc)_3$ (240 mg, 1.13 mmol) in CH_2Cl_2 (15 mL) using procedure B. The crude residue was purified by column chromatography (MeOH/EtOAc, 1:6) to afford compound **9c** (213 mg, 77%). ^{1}H NMR ($CDCl_3$, 400 MHz): δ 0.85 (t, J = 7.2 Hz, 3H), 1.20-1.56 (m, 2H), 1.80-2.04 (m, 1H), 2.20-3.00 (m, 18H), 3.20-3.45 (m, 2H), 3.74 (s, 2H), 6.48 (d, J = 7.6 Hz, 1H), 6.57 (d, J = 7.6 Hz, 1H), 6.93 (t, J = 7.2 Hz, 1H), 7.02-7.25 (m, 3H), 7.35 (d, J = 7.6 Hz, 1H), 7.71 (d, J = 7.6, 1H), 8.24 (s, 1H). ^{13}C ($CDCl_3$, 100 MHz): 12.0, 22.5, 25.4, 26.0, 26.7, 29.9, 48.4, 52.9, 53.7, 58.3, 58.6, 63.6, 102.6, 111.0, 117.5, 121.7, 124.0, 124.7, 128.1, 128.8, 135.5, 145.2, 165.9. The free base was converted to its hydrochloride salt. M.p. 180-185 ºC. Anal. calculated for $C_{28}H_{47}Cl_4N_4O_{3.5}$: C, H, N.

5-Bromo-1-(triisopropylsilyl)-1*H*-indole (11). Into a stirring solution of NaH (4.03 g, 170.0 mmol) in dry THF (150 mL), compound **10** (16.44 g, 83.9 mmol) was added portion wise at 0 °C. The reaction mixture was allowed to stir at room temperature for 1 h, followed by dropwise addition of triisopropylsilyl chloride (20 g, 103.7 mmol). The reaction mixture was stirred for 12 h and then filtered through celite. The crude residue was purified by column chromatography using hexane as solvent to afford compound **11** (22 g, 75%). ^{1}H NMR (CDCl$_3$, 400 MHz): δ 1.23 (s, 18H), 1.74 (heptet, J = 7.6 Hz, 3H), 6.64 (d, J = 3.2 Hz, 1H), 7.07 (d, J = 6 Hz, 1H), 7.14 (s, 1H), 7.31 (d, J = 3.2 Hz, 1H), 7.45 (d, J = 8.8, 1H).

tert-**Butyl   4-(1-(triisopropylsilyl)-1H-indol-5-yl)piperazine-1-carboxylate   (12).** A mixture of compound **11** (22.0 g, 63.0 mmol), **4** (11.71 g, 63.0 mmol), PdCl$_2$[P(O-tol)$_3$]$_2$ (2.47 g, 3.1 mmol) and NaO*t*Bu (9.08 g, 94.4 mmol) in xylenes (175 mL) was heated at 110 ^{o}C for 12 h. The reaction mixture was filtered through celite and concentrated in vacuo. The crude residue was purified by column chromatography (EtOAc/hexane, 1:20) to afford compound **12** (13.22 g, 46%). ^{1}H NMR (CDCl$_3$, 400 MHz): δ 1.19 (s, 18H), 1.55 (s, 9H), 1.74 (heptet, J = 6.8 Hz, 3H), 3.14 (bs, 4H), 3.67 (bs, 4H), 6.60 (t, J = 6 Hz, 1H), 6.94 (d, J = 8.8, 1H), 7.19 (s, 1H), 7.26 (t, J = 2.8 Hz, 1H), 7.47 (d, J = 8.8 Hz, 1H).

Procedure C. 5-Piperazin-1-yl-1*H*-indole (13). To a stirring solution of compound **12** (7.70 g, 16.8 mmol) in CH$_2$Cl$_2$ (15 mL), TFA (15 mL) was added slowly at room temperature and the reaction mixture was stirred for 2 h. Unreacted TFA and solvent were removed under reduced pressure and the salt was washed with diethylether. A saturated solution of NaHCO$_3$ was added to the salt, followed by extraction with CH$_2$Cl$_2$

(3 x 50 mL). The combined organic layer was dried over Na_2SO_4, filtered and evaporated in vacuo to provide compound **13** (2.88 g, 85%). ^{1}H NMR ($CDCl_3$, 400 MHz): δ 1.85 (bs, 1H), 2.80-3.28 (m, 8H), 6.85-7.10 (m, 1H), 7.02-7.40 (m, 4H), 8.31 (bs, 1H).

Procedure D. 5-{4-[2-(tert-butyl-dimethyl-silanyloxy)ethyl]piperazin-1-yl}-1H-indole (14). A mixture of compound **13** (2.88 g, 14.3 mmol), (2-bromoethoxy)-*tert*-butyl-dimethylsilane (3.42 g, 14.3 mmol) and K_2CO_3 (5.93 g, 42.9 mmol) in CH_3CN (50 mL) was refluxed for 14 hours. After filtration, acetonitrile was evaporated under reduced pressure and the crude material was purified by silica gel column chromatography (EtOAc/hexane, 3:1) to give compound **14** (4.01 g, 78%).^{1}H NMR ($CDCl_3$, 400 MHz): δ 0.02 (s, 6H), 0.83 (s, 9H), 2.30-2.80 (m, 6H), 2.82-3.30 (m, 4H), 3.52-3.82 (m, 2H), 6.25-6.48 (m, 1H), 6.75-7.30 (m, 4H), 8.09 (s, 1H).

5-{4-[2-(tert-butyl-dimethyl-silanyloxy)ethyl]piperazin-1-yl}indole-1-carboxylic acid tert-butyl ester (15). Amine **14** (4.0 g, 11.1 mmol) was reacted with (Boc)$_2$O (2.68 g, 12.2 mmol) and DMAP (1.49 g, 12.2 mmol) in THF (50 mL) at room temperature using procedure G. The crude material was purified by column chromatography over silica gel (EtOAc/hexane, 1:1) to give compound **15** (5.2 g, ~100%). ^{1}H NMR ($CDCl_3$, 400 MHz): δ 0.08 (s, 6H), 0.95 (s, 9H), 1.65 (s, 9H), 2.61 (t, $J = 6.4$ Hz, 2H), 2.73 (t, $J = 4.8$ Hz, 4H), 3.19 (t, $J = 4.8$ Hz, 4H), 3.81 (t, $J = 6.4$ Hz, 2H), 6.47 (d, $J = 3.6$ Hz, 1H), 7.01 (dd, $J = 6.4$, 2.4 Hz, 1H), 7.06 (dd, $J = 6.4$, 2.4 Hz, 1H), 7.53 (s, 1H), 8.00 (s, 1H).

Procedure E. 5-[4-(2-hydroxy-ethyl)piperazin-1-yl]indole-1-carboxylic acid tert-butyl ester (16). Into a stirring solution of compound **15** (2.0 g, 4.3 mmol) in THF (30 mL), *n*-tetrabutylammonium fluoride (1.14 g, 4.3 mmol, 1.0 M solution in THF) was

added at 0 °C. The reaction mixture was then stirred at room temperature for 1 h. THF was evaporated in vacuo, the residue was diluted with CH_2Cl_2 (50 mL) and washed with water. The water layer was extracted with CH_2Cl_2 (3 x 75 mL). The combined organic layer was washed with brine, dried over Na_2SO_4, and evaporated. The crude product was purified by silica gel column chromatography (EtOAc/MeOH, 20:1) to yield compound **16** (1.49 g, 99%). ^{1}H NMR (CDCl_3, 400 MHz): δ 1.65 (s, 9 H), 2.61 (t, J = 5.2 Hz, 2H), 2.70 (t, J = 4.8 Hz, 4H), 3.19 (t, J = 4.8 Hz, 4H), 3.67 (t, J = 5.2 Hz, 2H), 6.47 (d, J = 3.6 Hz, 1H), 7.01 (dd, J = 6.8, 2 Hz, 1H), 7.06 (d, J = 2 Hz, 1H), 7.53 (s, 1H), 8.00 (s, 1H).

5-[4-(2-Oxo-ethyl)piperazin-1-yl]indole-1-carboxylic acid tert-butyl ester (17). Compound **16** (1.49 g, 4.3 mmol) was reacted with oxalyl chloride (0.75 mL, 8.6 mmol), DMSO (1.23 mL, 17.3 mmol) and Et_3N (3.6 mL, 25.8 mmol) in CH_2Cl_2 (40 mL) using procedure A. The crude residue was purified by column chromatography using ethyl acetate as solvent to afford compound **17** (1.23 g, 83%).

 5-(4-{2-[(2-Amino-4,5,6,7-tetrahydrobenzothiazol-6-yl)propyl amino]ethyl}piperazin-1-yl)indole-1-carboxylic acid tert-butyl ester [(±)-18]. Compound **17** (175 mg, 0.51 mmol) was reacted with (±)-pramipexole (108 mg, 0.51 mmol) and NaBH(OAc)_3 (194 mg, 0.92 mmol) in CH_2Cl_2 (15 mL) according to procedure B. The crude product was purified by silica gel column chromatography (EtOAc/MeOH, 20:1) to yield compound (±)-**18** (150 mg, 55%). ^{1}H NMR (CDCl_3, 400 MHz): δ 0.91 (t, J = 6.8 Hz, 1H), 1.35-1.60 (m, 2H), 1.67 (s, 9H), 1.89-2.10 (m, 1H), 2.30-3.30 (m, 20H), 4.94 (bs, 2H), 6.67 (t, J = 3.2 Hz, 1H), 7.09 (dd, J = 8.8, 2.8 Hz, 1H), 7.28 (dd, J = 3.2 Hz, 1H), 7.59 (s, 1H), 7.97 (d, J = 6.4 Hz, 1H).

(*S*)-5-(4-{2-[(2-Amino-4,5,6,7-tetrahydro benzothiazol-6-yl)propyl amino]ethyl} piperazin-1-yl)indole-1-carboxylic acid tert-butyl ester [(-)-18]. Compound **17** (175 mg, 0.51 mmol) was reacted with (-)-pramipexole (108 mg, 0.51 mmol) and NaBH(OAc)$_3$ (194 mg, 0.92 mmol) in CH$_2$Cl$_2$ (15 mL) using procedure B. The crude residue was purified by column chromatography (EtOAc/MeOH, 20:1) to afford compound (-)-**18** (161 mg, 59%). ^{1}H NMR (CDCl$_3$, 400 MHz): δ 0.93 (t, J = 6.8 Hz, 1H), 1.35-1.60 (m, 2H), 1.68 (s, 9H), 1.89-2.10 (m, 1H), 2.30-3.30 (m, 20H), 4.94 (bs, 2H), 6.67 (t, J = 3.2 Hz, 1H), 7.09 (dd, J = 8.8, 2.8 Hz, 1H), 7.28 (dd, J = 3.2 Hz, 1H), 7.60 (s, 1H), 7.97 (d, J = 6.4 Hz, 1H).

(*R*)-5-(4-{2-[(2-Amino-4,5,6,7-tetrahydro-benzothiazol-6-yl)propyl amino]ethyl}piperazin-1-yl)indole-1-carboxylic acid tert-butyl ester [(+)-18]. Compound **17** (175 mg, 0.51 mmol) was reacted with (+)-pramipexole (108 mg, 0.51 mmol) and NaBH(OAc)$_3$ (194 mg, 0.92 mmol) in CH$_2$Cl$_2$ (15 mL) using procedure B. The crude residue was purified by column chromatography using (EtOAc/MeOH, 20:1) to afford compound (+)-**18** (164 mg, 60%). ^{1}H NMR (CDCl$_3$, 400 MHz): δ 0.91 (t, J = 6.8 Hz, 1H), 1.37-1.60 (m, 2H), 1.67 (s, 9H), 1.89-2.10 (m, 1H), 2.30-3.30 (m, 20H), 4.94 (bs, 2H), 6.67 (t, J = 3.2 Hz, 1H), 7.10 (dd, J = 8.8, 2.8 Hz, 1H), 7.28 (dd, J = 3.2 Hz, 1H), 7.59 (s, 1H), 7.98 (d, J = 6.4 Hz, 1H).

N^6-{2-[4-(1H-Indol-5-yl)piperazin-1-yl]ethyl}-N^6-propyl-4,5,6,7-tetrahydro benzothiazole-2,6-diamine [(±)-19]. Compound (±)-**18** (150 mg, 0.28 mmol) was reacted with TFA (10 mL) in CH$_2$Cl$_2$ (10 mL) using procedure C. Unreacted TFA and solvent were removed in vacuo and the salt was washed with diethylether and recrystallized from ethanol to afford compound (±)-**19** (106 mg, 38%). ^{1}H NMR (CD$_3$OD,

400MHz): δ 0.99 (t, *J* = 7.2 Hz, 3H), 1.52-1.74 (m, 2H), 1.76-2.04 (m, 1H), 2.19 (d, *J* = 9.2 Hz, 1H), 2.52-2.84 (m, 6H), 3.10-3.58 (m, 13H), 6.50 (d, *J* = 3.2 Hz, 1H), 7.05 (d, *J* = 8.8 Hz, 1H), 7.29 (d, *J* = 3.2 Hz, 1H), 7.34 (d, *J* = 8.8 Hz, 2H). ^{13}C (CD$_3$OD, 100 MHz): δ 12.0, 22.2, 24.0, 25.1, 47.0, 51.1, 54.4, 54.8, 59.2, 101.4, 101.5, 111.8, 115.3, 116.1, 127.8, 129.7, 135.1, 136.0, 140.7, 171.0. M.p. 110-115 ºC. Anal. calculated for C$_{30}$H$_{40}$F$_9$N$_6$O$_{7.5}$S: C, H, N.

(*S*)-*N*^{6}-{2-[4-(1H-Indol-5-yl)piperazin-1-yl]ethyl}-*N*^{6}-propyl-4,5,6,7-tetrahydro benzothiazole-2,6-diamine [(-)-19]. Compound (-)-**18** (150 mg, 0.28 mmol) was reacted with TFA (10 mL) in CH$_2$Cl$_2$ (10 mL) using procedure C. Unreacted TFA and solvent were removed in vacuo and the salt was washed with diethylether and recrystallized from ethanol to afford compound (-)-**19** (120 mg, 43%). ^{1}H NMR (CD$_3$OD, 400MHz): δ 0.98 (t, *J* = 7.2 Hz, 3H), 1.54-1.74 (m, 2H), 1.76-2.04 (m, 1H), 2.19 (d, *J* = 9.2 Hz, 1H), 2.52-2.84 (m, 6H), 3.10-3.58 (m, 13H), 6.51 (d, *J* = 3.2 Hz, 1H), 7.05 (d, *J* = 8.8 Hz, 1H), 7.29 (d, *J* = 3.2 Hz, 1H), 7.34 (d, *J* = 8.8 Hz, 2H). ^{13}C (CD$_3$OD, 100 MHz): δ 12.0, 22.3, 24.0, 25.1, 47.0, 51.1, 54.5, 54.8, 59.2, 101.4, 101.6, 111.8, 115.3, 116.1, 127.8, 129.7, 135.1, 136.0, 140.8, 171.0. [α]$^{25}_D$ = −11.0° (*c* = 1.0, CH$_3$OH). M.p. 115-120 ºC. Anal. calculated for C$_{31}$H$_{37.5}$F$_{10.5}$N$_6$O$_7$S: C, H, N.

(*R*)-*N*^{6}-{2-[4-(1H-Indol-5-yl)-piperazin-1-yl]ethyl}-*N*^{6}-propyl-4,5,6,7-tetrahydro benzothiazole-2,6-diamine [(+)-19]. Compound (+)-**18** (150 mg, 0.28 mmol) was reacted with TFA (10 mL) in CH$_2$Cl$_2$ (10 mL) using procedure C. Unreacted TFA and solvent were removed in vacuo and the salt was washed with diethylether and recrystalized from ethanol to afford compound (+)-**19** (140 mg, 50%). ^{1}H NMR (CD$_3$OD, 400MHz): δ 0.98 (t, *J* = 7.2 Hz, 3H), 1.54-1.78 (m, 2H), 1.76-2.04 (m, 1H), 2.20 (d, *J* =

9.2 Hz, 1H), 2.52-2.84 (m, 6H), 3.10-3.58 (m, 13H), 6.51 (d, *J* = 3.2 Hz, 1H), 7.05 (d, *J* = 8.8 Hz, 1H), 7.29 (d, *J* = 3.2 Hz, 1H), 7.34 (d, *J* = 8.8 Hz, 2H). ^{13}C (CD$_3$OD, 100 MHz): δ 12.2, 22.3, 24.0, 25.1, 47.0, 51.2, 54.5, 54.8, 59.2, 101.4, 101.6, 111.8, 115.3, 116.1, 127.8, 129.7, 135.1, 136.2, 140.8, 171.0. $[α]^{25}_D$ = +15.5° (*c* = 1.0, CH$_3$OH). M.p. 115-120 °C. Anal. calculated for C$_{31}$H$_{37.9}$F$_{10.5}$N$_6$O$_{7.2}$S: C, H, N.

***tert*-Butyl 5-(4-(2-((5-methoxy-1,2,3,4-tetrahydronaphthalen-2-yl)(propyl)amino)ethyl) piperazin-1-yl)-1*H*-indole-1-carboxylate (20).** Aldehyde **17** (320 mg, 0.93 mmol) was reacted with amine **2** (204 mg, 0.93 mmol) and NaBH(OAc)$_3$ (355 mg, 1.68 mmol) in CH$_2$Cl$_2$ (20 mL) using procedure B. The crude material was purified by column chromatography over silica gel (EtOAc/hexane, 1:1) to give compound **20** (190 mg, 38%). ^{1}H NMR (CDCl$_3$, 400 MHz): δ 0.91 (t, *J* = 7.2 Hz, 3H), 1.33-1.75 (m, 13H), 1.95-2.13 (m, 1H), 2.35-3.23 (m, 18H), 3.81 (s, 3H), 6.55-6.77 (m, 3H), 7.03-7.15 (m, 3H), 7.58 (d, *J* = 2.4 Hz, 1H), 7.96 (d, *J* = 6.8 Hz, 1H).

6-({2-[4-(1H-Indol-5-yl)piperazin-1-yl]-ethyl}propyl amino)-5,6,7,8-tetrahydro naphthalen-1-ol (21). A mixture of compound **20** (60 mg, 0.11 mmol) and 48% aq. HBr (10 ml) was refluxed for 5 h. The reaction mixture was evaporated to dryness and the residue was washed with diethylether. Finally, the HBr salt was recrystalized from ethanol to furnish compound **21** (50 mg, 60%). ^{1}H NMR (CD$_3$OD, 400 MHz): δ 0.95 (t, *J* = 7.2 Hz, 3H), 1.41-1.57 (m, 3H), 2.00-2.22 (m, 1H), 2.58-3.18 (m, 19H), 6.61 (d, *J* = 8 Hz, 1H), 6.75 (d, *J* = 8 Hz, 1H), 7.08 (t, *J* = 7.6 Hz, 1H), 7.19-7.38 (m, 3H), 7.51 (d, *J* = 8 Hz, 1H), 7.90 (d, *J* = 8.2 Hz, 1H), 8.50 (bs, 1H). M.p. 250-260 ºC. Anal. calculated for C$_{27}$H$_{41.4}$Br$_4$N$_4$O$_{1.7}$: C, H, N.

Procedure F. 4-(1H-indole-2-carbonyl)piperazine-1-carboxylic acid tert-butyl ester

(23). To a stirring solution of EDCI.HCl (15.45 g, 80.6 mmol) in CH_2Cl_2 (150 mL), acid derivative **22** (10.39 g, 64.5 mmol) was added at room temperature. The reaction mixture was stirred for 0.5 h, followed by addition of amine **4** (10.0 g, 53.7 mmol), HOBt (10.89 g, 80.6 mmol) and Et_3N (22.46 g, 161.2 mmol). The reaction mixture was stirred for 3 h, followed by addition of a saturated solution of $NaHCO_3$. The aqueous layer was extracted with CH_2Cl_2 (3 x 150 mL). The combined organic layer was dried over Na_2SO_4, evaporated under reduced pressure and the crude product was purified by flash column chromatography (CH_2Cl_2/MeOH, 50:1) to afford compound **23** (15.6 g, 88%). ^{1}H NMR ($CDCl_3$, 400 MHz): δ 1.49 (s, 9H), 3.56 (t, $J = 5.6$ Hz, 4H), 3.74-4.04 (m, 4H), 6.78 (s, 1H), 7.15 (t, $J = 7.6$ Hz, 1H), 7.30 (t, $J = 7.6$ Hz, 1H), 7.43 (d, $J = 8.4$ Hz, 1H), 7.65 (d, $J = 8.4$ Hz, 1H), 9.14 (bs, 1H).

(1H-Indol-2-yl)-piperazin-1-yl-methanone (24). Compound **23** (12 g, 36.4 mmol) was reacted with TFA (20 mL) in CH_2Cl_2 (20 mL) using procedure C to provide compound **24** (7.85 g, 94%). ^{1}H NMR ($CDCl_3$, 400 MHz): δ 2.52-3.04 (m, 4H), 3.60-4.06 (m, 4H), 6.77 (s, 1H), 7.14 (t, $J = 7.6$ Hz, 1H), 7.27 (d, $J = 6.8$ Hz, 1H), 7.43 (d, $J = 6.8$ Hz, 1H), 7.65 (d, $J = 6.8$ Hz, 1H), 9.50 (bs, 1H).

{4-[2-(tert-Butyldimethylsilanyloxy)ethyl]piperazin-1-yl}-(1H-indol-2-yl)methanone

(25). Compound **24** (2.50 g, 10.9 mmol) was reacted with (2-bromo-ethoxy)-*tert*-butyl-dimethylsilane (3.13 g, 13.1 mmol) and K_2CO_3 (4.52 g, 32.7 mmol) in CH_3CN (50 mL) using procedure D. The crude material was purified by silica gel column chromatography using ethyl acetate as solvent to give compound **25** (3.55 g, 84%). ^{1}H NMR ($CDCl_3$, 400 MHz): δ 0.09 (s, 6H), 0.92 (s, 9H), 2.02-2.80 (m, 6H), 3.01-4.20 (m,

6H), 6.77 (s, 1H), 7.11 (t, J = 7.6 Hz, 1H), 7.25 (t, J = 7.6 Hz, 1H), 7.44 (d, J = 8.0 Hz, 1H), 7.63 (d, J = 8 Hz, 1H), 10.4 (bs, 1H).

{4-[3-(tert-Butyldimethylsilanyloxy)propyl]piperazin-1-yl}-(1H-indol-2-yl)methanone (26). Compound **24** (2.50 g, 10.9 mmol) was reacted with (3-bromo-propoxy)-*tert*-butyl-dimethylsilane (3.31 g, 13.1 mmol) and K_2CO_3 (4.52 g, 32.7 mmol) in CH_3CN (50 mL) using procedure D. The crude material was purified by silica gel column chromatography (EtOAc/hexane, 1:1) to give compound **26** (3.33 g, 76%). ^{1}H NMR ($CDCl_3$, 400 MHz): δ 0.06 (s, 6H), 0.90 (s, 9H), 1.52-1.86 (m, 2H), 2.45-2.70 (m, 6H), 3.68 (t, J = 12 Hz, 2H), 3.72-4.20 (m, 4H), 6.78 (s, 1H), 7.14 (t, J = 7.6 Hz, 1H), 7.20-7.32 (m, 2H), 7.43 (d, J = 7.6 Hz, 1H), 7.64 (d, J = 7.6 Hz, 1H), 9.35 (s, 1H).

{4-[4-(tert-Butyldimethylsilanyloxy)butyl]piperazin-1-yl}-(1H-indol-2-yl)methanone (27). Compound **24** (2.50 g, 10.9 mmol) was reacted with (4-bromo-butoxy)-*tert*-butyl-dimethylsilane (3.50 g, 13.1 mmol) and K_2CO_3 (4.52 g, 32.7 mmol) in CH_3CN (50 mL) using procedure D. The crude material was purified by silica gel column chromatography (EtOAc/hexane, 2:3) to give compound **27** (4.31 g, 95%). ^{1}H NMR ($CDCl_3$, 400 MHz): δ 0.05 (s, 6H), 0.90 (s, 9H), 1.47-1.75 (m, 4H), 2.40 (t, J = 6.4 Hz, 2H), 2.53 (t, J = 4.4 Hz, 4H), 3.64 (t, J = 5.6 Hz, 2H), 3.80-4.05 (m, 4H), 6.77 (s, 1H), 7.12 (t, J = 6.8 Hz, 1H), 7.26 (t, J = 7.2 Hz, 1H), 7.43 (d, J = 8.4 Hz, 1H), 7.63 (d, J = 8 Hz, 1H), 10.00 (s, 1H).

Procedure G. 2-{4-[3-(tert-Butyldimethylsilanyloxy)ethyl]piperazine-1-carbonyl}indole-1-carboxylic acid tert-butyl ester (28). To a stirring solution of amine **25** (3.55 g, 9.2 mmol) in THF (50 mL), (Boc)$_2$O (2.21 g, 10.1 mmol) and DMAP (1.23 g, 10.1 mmol) were added at room temperature. The reaction mixture was stirred at the

same temperature for 12 h. The crude mixture was evaporated under reduced pressure, followed by extraction with CH_2Cl_2 (3 x 100 mL) in water. The combined organic layer was dried over Na_2SO_4, filtered, and concentrated in vacuo. The crude material was purified by column chromatography over silica gel using ethyl acetate as solvent to give compound **28** (4.46 g, ~100%). ^{1}H NMR (CDCl₃, 400 MHz): δ 0.05 (s, 6H), 0.09 (s, 9H), 1.62 (s, 9H), 2.48 (t, *J* = 4 Hz, 2H), 2.56 (t, *J* = 6 Hz, 2H), 2.63 (t, *J* = 4 Hz, 2H), 3.38 (t, *J* = 4 Hz, 2H), 3.76 (t, *J* = 6 Hz, 4H), 6.60 (s, 1H), 7.20-7.28 (m, 1H), 7.34 (t, *J* = 7.2 Hz, 1H), 7.53 (d, *J* = 7.6 Hz, 1H), 8.16 (d, *J* = 7.6 Hz, 1H).

2-{4-[3-(tert-Butyldimethylsilanyloxy)propyl]piperazine-1-carbonyl}indole-1-carboxylic acid tert-butyl ester (29). Amine **26** (3.33 g, 8.3 mmol) was reacted with (Boc)₂O (2.00 g, 9.1 mmol) and DMAP (1.11 g, 9.1 mmol) in THF (50 mL) using procedure G. The crude material was purified by column chromatography over silica gel (EtOAc/hexane, 1:1) to give compound **29** (4.04 g, 97%). ^{1}H NMR (CDCl₃, 400 MHz): δ 0.002 (s, 6H), 0.84 (s, 9H), 1.57 (s, 9H), 1.50-1.80 (m, 2H), 2.20-2.70 (m, 6H), 3.30-3.45 (m, 2H), 3.62 (t, *J* = 12 Hz, 2H), 3.66-3.80 (m, 2H), 6.55 (s, 1H), 7.18 (t, *J* = 7.6 Hz, 1H), 7.29 (t, *J* = 7.6 Hz, 1H), 7.48 (d, *J* = 7.6 Hz, 1H), 8.12 (d, *J* = 8.4 Hz, 1H).

2-{4-[4-(tert-Butyldimethylsilanyloxy)butyl]piperazine-1-carbonyl}-indole-1-carboxylic acid tert-butyl ester (30). Amine **27** (4.31 g, 10.4 mmol) was reacted with (Boc)₂O (2.50 g, 11.4 mmol) and DMAP (1.39 g, 11.4 mmol) in THF (50 mL) using procedure G. The crude material was purified by column chromatography over silica gel (EtOAc/hexane, 1:3) to give compound **30** (4.92 g, 92%). ^{1}H NMR (CDCl₃, 400 MHz): δ 0.001 (s, 6H), 0.84 (s, 9H), 1.25-1.70 (m, 13H), 2.15-2.40 (m, 4H), 2.42-2.55 (m, 2H),

3.25-3.45 (m, 2H), 3.47-3.65 (m, 2H), 3.67-3.85 (m, 2H), 6.54 (s, 1H), 7.18 (t, J = 7.2

Hz, 1H), 7.29 (t, J = 7.6 Hz, 1H), 7.48 (d, J = 7.6 Hz, 1H), 8.12 (d, J = 8.4 Hz, 1H).

2-[4-(2-Hydroxyethyl)piperazine-1-carbonyl]indole-1-carboxylic acid tert-butyl

ester (31). Compound **28** (4.46 g, 9.2 mmol) was reacted with *n*-tetrabutylammonium

fluoride (2.39 g, 9.2 mmol, 1.0 M solution in THF) in THF (30 mL) using procedure E.

The crude product was purified by silica gel column chromatography (EtOAc/MeOH,

9:1) to yield compound **31** (3.08 g, 90%). ^{1}H NMR (CDCl$_3$, 400 MHz): δ 1.62 (s, 9H),

2.46 (t, J = 4.8 Hz, 2H), 2.54-2.68 (m, 4H), 3.41 (t, J = 5.2 Hz, 2H), 3.64 (t, J = 5.2 Hz,

2H), 3.72-3.78 (m, 2H), 6.60 (s, 1H), 7.21-7.28 (m, 1H), 7.35 (t, J = 8.4 Hz, 1H), 7.54 (d,

J = 7.6 Hz, 1H), 8.14 (d, J = 7.6 Hz, 1H).

2-[4-(3-Hydroxypropyl)piperazine-1-carbonyl]indole-1-carboxylic acid tert-butyl

ester (32). Compound **29** (4.04 g, 8.1 mmol) was reacted with *n*-tetrabutylammonium

fluoride (2.11 g, 8.1 mmol, 1.0 M solution in THF) in THF (30 mL) using procedure E.

The crude product was purified by silica gel column chromatography (EtOAc/MeOH,

9:1) to yield compound **32** (2.84 g, 91%). ^{1}H NMR (CDCl$_3$, 400 MHz): δ 1.30-1.75 (m,

11H), 2.33 (m, 2H), 2.47 (t, J = 4.4 Hz, 4H), 3.29 (m, 2H), 3.63 (t, J = 4.8 Hz, 4H), 6.50

(s, 1H), 7.13 (t, J = 7.6 Hz, 1H), 7.24 (t, J = 7.2 Hz, 1H), 7.43 (d, J = 7.6 Hz, 1H), 8.05

(d, J = 8.4 Hz, 1H).

2-[4-(4-Hydroxybutyl)piperazine-1-carbonyl]indole-1-carboxylic acid tert-butyl

ester (33). Compound **30** (4.92 g, 9.5 mmol) was reacted with *n*-tetrabutylammonium

fluoride (2.50 g, 9.5 mmol, 1.0 M solution in THF) in THF (30 mL) using procedure E.

The crude product was purified by silica gel column chromatography (EtOAc/MeOH,

9:1) to yield compound **33** (3.72 g, 97%). ^{1}H NMR (CDCl$_3$, 400 MHz): δ 0.95-1.70 (m,

13H), 2.30 (t, *J* = 6 Hz, 4H), 2.37-2.65 (m, 2H), 3.15-3.36 (m, 2H), 3.37-3.55 (m, 2H), 3.55-3.82 (m, 2H), 6.48 (s, 1H), 7.12 (t, *J* = 7.6 Hz, 1H), 7.23 (t, *J* = 8 Hz, 1H), 7.42 (d, *J* = 8 Hz, 1H), 8.05 (d, *J* = 8 Hz, 1H).

2-[4-(2-Oxoethyl)piperazine-1-carbonyl]indole-1-carboxylic acid tert-butyl ester (34). Compound **31** (1.0 g, 2.7 mmol) was reacted with oxalyl chloride (0.47 mL, 5.4 mmol), DMSO (0.76 mL, 10.7 mmol) and Et$_3$N (2.2 mL, 16.1 mmol) in CH$_2$Cl$_2$ (40 mL) using procedure A. The crude residue was purified by column chromatography (EtOAc/MeOH, 20:1) to afford compound **34** (0.81 g, 81%).

2-[4-(3-Oxopropyl)piperazine-1-carbonyl]indole-1-carboxylic acid tert-butyl ester (35). Compound **32** (0.8 g, 2.1 mmol) was reacted with oxalyl chloride (0.36 mL, 4.1 mmol), DMSO (0.59 mL, 8.3 mmol) and Et$_3$N (1.73 mL, 12.4 mmol) in CH$_2$Cl$_2$ (40 mL) using procedure A. The crude residue was purified by column chromatography (EtOAc/MeOH, 20:1) to afford compound **35** (0.62 g, 78%).

2-[4-(4-Oxobutyl)piperazine-1-carbonyl]indole-1-carboxylic acid tert-butyl ester (36). Compound **33** (1.0 g, 2.5 mmol) was reacted with oxalyl chloride (0.43 mL, 5.0 mmol), DMSO (0.71 mL, 10.0 mmol) and Et$_3$N (2.08 mL, 15.0 mmol) in CH$_2$Cl$_2$ (40 mL) using procedure A. The crude residue was purified by column chromatography (EtOAc/MeOH, 20:1) to afford compound **36** (0.75 g, 75%).

2-(4-{2-[(2-Amino-4,5,6,7-tetrahydro-benzothiazol-6-yl)propyl amino]ethyl}piperazine-1-carbonyl)indole-1-carboxylic acid tert-butyl ester [(±)-37]. Aldehyde **34** (480 mg, 1.3 mmol) was reacted with (±)-pramipexole (273 mg, 1.3 mmol) and NaBH(OAc)$_3$ (451 mg, 2.3 mmol) in CH$_2$Cl$_2$ (25 mL) using procedure B. The crude material was purified by column chromatography over silica gel (EtOAc/MeOH,

9:1) to give compound (±)-**37** (0.52 g, 71%). ^{1}H NMR (CDCl$_3$, 400 MHz): δ 0.85 (t, J = 3.6 Hz, 3H), 1.30-1.65 (m, 2H), 1.60 (s, 9H), 1.95 (d, J = 10.8 Hz, 1H), 2.20-3.10 (m, 16H), 3.15-3.82 (m, 4H), 4.94 (bs, 2H), 6.58 (s, 1H), 7.24 (d, J = 8.4 Hz, 1H), 7.33 (t, J = 6.8 Hz, 1H), 7.53 (d, J = 6 Hz, 1H), 8.13 (d, J = 6 Hz, 1H).

(*R*)-2-(4-{2-[(2-Amino-4,5,6,7-tetrahydro-benzothiazol-6-yl)propyl amino]ethyl} piperazine-1-carbonyl)indole-1-carboxylic acid tert-butyl ester [(+)-37]. Aldehyde **34** (200 mg, 0.54 mmol) was reacted with (+)-pramipexole (114 mg, 0.54 mmol) and NaBH(OAc)$_3$ (205 mg, 0.97 mmol) in CH$_2$Cl$_2$ (25 mL) using procedure B. The crude material was purified by column chromatography over silica gel (EtOAc/MeOH, 9:1) to yield compound (+)-**37** (186 mg, 61%). ^{1}H NMR (CDCl$_3$, 400 MHz): δ 0.86 (t, J = 3.6 Hz, 3H), 1.30-1.65 (m, 2H), 1.61 (s, 9H), 1.95 (d, J = 10.8 Hz, 1H), 2.20-3.10 (m, 16H), 3.15-3.82 (m, 4H), 4.94 (bs, 2H), 6.58 (s, 1H), 7.25 (d, J = 8.4 Hz, 1H), 7.33 (t, J = 6.8 Hz, 1H), 7.53 (d, J = 6 Hz, 1H), 8.13 (d, J = 6 Hz, 1H).

(*S*)-2-(4-{2-[(2-Amino-4,5,6,7-tetrahydro benzothiazol-6-yl)propyl amino]ethyl} piperazine-1-carbonyl)indole-1-carboxylic acid tert-butyl ester [(-)-37]. Aldehyde **34** (300 mg, 0.81 mmol) was reacted with (-)-pramipexole (170 mg, 0.81 mmol) and NaBH(OAc)$_3$ (308 mg, 1.45 mmol) in CH$_2$Cl$_2$ (25 mL) using procedure B. The crude material was purified by column chromatography over silica gel (EtOAc/MeOH, 9:1) to yield compound (-)-**37** (284 mg, 62%). ^{1}H NMR (CDCl$_3$, 400 MHz): δ 0.83 (t, J = 3.6 Hz, 3H), 1.30-1.65 (m, 2H), 1.61 (s, 9H), 1.95 (d, J = 10.8 Hz, 1H), 2.20-3.10 (m, 16H), 3.15-3.82 (m, 4H), 4.94 (bs, 2H), 6.58 (s, 1H), 7.25 (d, J = 8.4 Hz, 1H), 7.33 (t, J = 6.8 Hz, 1H), 7.53 (d, J = 6 Hz, 1H), 8.14 (d, J = 6 Hz, 1H).

2-(4-{3-[(2-Amino-4,5,6,7-tetrahydro benzothiazol-6-yl) propyl amino] propyl} piperazine-1-carbonyl) indole-1-carboxylic acid tert-butyl ester (38). Aldehyde **35** (220 mg, 0.57 mmol) was reacted with (±)-pramipexole (121 mg, 0.57 mmol) and NaBH(OAc)$_3$ (218 mg, 1.03 mmol) in CH_2Cl_2 (25 mL) using procedure B. The crude material was purified by column chromatography over silica gel (EtOAc/MeOH, 9:1) to give compound **38** (215 mg, 65%). ^{1}H NMR (CDCl$_3$, 400 MHz): δ 0.86 (t, J = 7.2 Hz, 3H), 1.15-1.85 (m, 13H), 1.96 (d, J = 7.2 Hz, 1H), 2.10-2.85 (m, 15H), 2.90-3.15 (m, 1H), 3.20-3.50 (m, 2H), 3.55-3.95 (m, 2H), 6.58 (s, 1H), 7.23 (t, J = 7.6 Hz, 1H), 7.33 (t, J = 7.6 Hz, 1H), 7.52 (d, J = 7.6 Hz, 1H), 8.13 (d, J = 8 Hz, 1H).

2-(4-{4-[(2-Amino-4,5,6,7-tetrahydro benzothiazol-6-yl) propyl amino] butyl}piperazine 1-carbonyl) indole-1-carboxylic acid tert-butyl ester (39). Aldehyde **36** (233 mg, 0.58 mmol) was reacted with (±)-pramipexole (123 mg, 0.58 mmol) and NaBH(OAc)$_3$ (222 mg, 1.05 mmol) in CH_2Cl_2 (25 mL) using procedure B. The crude material was purified by column chromatography over silica gel (EtOAc/MeOH, 20:1) to yield compound **39** (190 mg, 55%). ^{1}H NMR (CDCl$_3$, 400 MHz): δ 0.87 (t, J = 7.2 Hz, 3H), 1.10-1.78 (m, 15H), 1.96 (d, J = 11.2 Hz, 1H), 2.12-2.85 (m, 15H), 2.90-3.15 (m, 1H), 3.25-3.50 (m, 2H), 3.65-3.92 (m, 2H), 4.78 (s, 2H), 6.60 (s, 1H), 7.25 (t, J = 7.6 Hz, 1H), 7.35 (t, J = 7.6 Hz, 1H), 7.54 (d, J = 7.6 Hz, 1H), 8.15 (d, J = 8.4 Hz, 1H).

(4-{2-[(2-Amino-4,5,6,7-tetrahydro-benzothiazol-6-yl) propyl amino] ethyl} piperazin-1-yl)-(1H-indol-2-yl) methanone [(±)-40]. Compound (±)-**37** (200 mg, 0.35 mmol) was reacted with TFA (20 mL) in CH_2Cl_2 (20 mL) using procedure C. Unreacted TFA and solvent were removed under reduced pressure. The TFA salt was converted

to the free base by extraction using CH_2Cl_2 (3 × 100 mL) and a saturated solution of $NaHCO_3$. The crude material was purified by column chromatography over silica gel to afford compound (±)-**40** (228 mg, 80%). ^{1}H NMR (CD$_3$OD, 400 MHz): δ 1.04 (t, J = 7.2 Hz, 3H), 1.70-1.88 (m, 2H), 2.01-2.18 (m, 1H), 2.32 (d, J = 10.8 Hz, 1H), 2.60-3.60 (m, 13H), 3.72-4.20 (m, 6H), 6.85 (s, 1H), 7.07 (t, J = 8 Hz, 1H), 7.23 (t, J = 8 Hz, 1H), 7.44 (d, J = 8 Hz, 1H), 7.62 (d, J = 8 Hz, 1H). [13]C (CD$_3$OD, 100 MHz): δ 14.1, 23.0, 26.0, 26.7, 27.0, 56.6, 57.0, 57.8, 63.1, 109.2, 115.7, 116.3, 124.1, 125.4, 127.9, 131.3, 132.7, 137.4, 137.5, 167.8, 174.4. The free base was converted to its hydrochloride salt. M.p. 270-275 °C. Anal. calculated for $C_{25}H_{40}Cl_4N_6O_2S$: C, H, N.

(*R*)-(4-{2-[(2-Amino-4,5,6,7-tetrahydro-benzothiazol-6-yl) propyl amino] ethyl} piperazin-1-yl)-(1H-indol-2-yl) methanone [(+)-40]. Compound (+)-**37** (150 mg, 0.26 mmol) was reacted with TFA (15 mL) in CH_2Cl_2 (15 mL) using procedure C. Unreacted TFA and solvent were removed in vacuo and the salt was washed with diethylether and recrystallized from ethanol to afford compound (+)-**40** (160 mg, 75%). ^{1}H NMR (CD$_3$OD, 400 MHz): δ 1.05 (t, J = 7.2 Hz, 3H), 1.70-1.88 (m, 2H), 2.01-2.18 (m, 1H), 2.34 (d, J = 10.8 Hz, 1H), 2.60-3.60 (m, 13H), 3.72-4.20 (m, 6H), 6.85 (s, 1H), 7.07 (t, J = 8 Hz, 1H), 7.23 (t, J = 8 Hz, 1H), 7.44 (d, J = 8 Hz, 1H), 7.63 (d, J = 8 Hz, 1H). [13]C (CD$_3$OD, 100 MHz): δ 14.1, 23.0, 26.2, 26.7, 27.0, 56.6, 57.0, 57.8, 63.1, 109.3, 115.7, 116.3, 124.1, 125.4, 127.9, 131.3, 132.7, 137.4, 137.6, 167.8, 174.4. $[\alpha]^{25}_D$ = +25.2° (c = 1.0, CH$_3$OH). M.p. 100-110 °C. Anal. calculated for $C_{31}H_{38 \cdot 2}F_9N_6O_{7 \cdot 6}S$: C, H, N.

(*S*)-(4-{2-[(2-Amino-4,5,6,7-tetrahydrobenzothiazol-6-yl) propyl amino]ethyl}piperazin-1-yl)-(1H-indol-2-yl)methanone [(-)-40]. Compound (-)-**37** (200 mg, 0.35 mmol) was reacted with TFA (20 mL) in CH_2Cl_2 (20 mL) using procedure C.

Unreacted TFA and solvent were removed in vacuo and the salt was washed with diethylether and recrystallized from ethanol to afford compound (-)-**40** (237 mg, 83%). ^{1}H NMR (CD$_3$OD, 400 MHz): δ 1.02 (t, J = 7.2 Hz, 3H), 1.73-1.88 (m, 2H), 2.01-2.18 (m, 1H), 2.32 (d, J = 10.8 Hz, 1H), 2.60-3.60 (m, 13H), 3.72-4.20 (m, 6H), 6.85 (s, 1H), 7.08 (t, J = 8 Hz, 1H), 7.23 (t, J = 8 Hz, 1H), 7.44 (d, J = 8 Hz, 1H), 7.62 (d, J = 8 Hz, 1H). ^{13}C (CD$_3$OD, 100 MHz): δ 14.3, 23.0, 26.2, 26.7, 27.0, 56.6, 57.0, 57.8, 63.1, 109.3, 115.7, 116.3, 124.1, 125.4, 127.9, 131.3, 132.7, 137.4, 137.5, 167.8, 174.4. $[α]^{25}_D$ = −31.2° (c = 1.0, CH$_3$OH). M.p. 110-115 ºC. Anal. calculated for C$_{31}$H$_{40}$F$_9$N$_6$O$_{8.5}$S: C, H, N.

(4-{3-[(2-Amino-4,5,6,7-tetrahydrobenzothiazol-6-yl)propylamino]propyl}piperazin-1-yl)-(1H-indol-2-yl)methanone [(±)-41)]. Compound **38** (200 mg, 0.34 mmol) was reacted with TFA (20 mL) in CH$_2$Cl$_2$ (20 mL) using procedure C. Unreacted TFA and solvent were removed under reduced pressure, followed by washing of the salt with diethylether and recrystallization from ethanol to afford compound (±)-**41** (266 mg, 94%). ^{1}H NMR (CD$_3$OD, 400 MHz): δ 1.04 (t, J = 7.6 Hz, 3H), 1.65-1.90 (m, 2H), 1.95-2.18 (m, 1H), 2.20-2.48 (m, 3H), 2.56-3.70 (m, 12H), 3.78-4.40 (m, 5H), 6.90 (s, 1H), 7.08 (t, J = 8 Hz, 1H), 7.23 (t, J = 8 Hz, 1H), 7.44 (d, J = 8.4 Hz, 1H), 7.62 (d, J = 8.4 Hz, 1H). ^{13}C (CD$_3$OD, 100 MHz): δ 10.0, 18.4, 20.1, 21.8, 22.3, 22.7, 51.8, 53.1, 53.6, 59.2, 104.4, 105.7, 111.8, 120.2, 121.6, 124.2, 127.4, 128.2, 133.7, 136.9, 163.8, 170.5. M.p. 115-120 ºC. Anal. calculated for C$_{32}$H$_{42}$F$_9$N$_6$O$_{8.5}$S: C, H, N.

(4-{4-[(2-Amino-4,5,6,7-tetrahydrobenzothiazol-6-yl)propylamino]butyl}piperazin-1-yl)-(1H-indol-2-yl)methanone [(±)-42)]. Compound **39** (175 mg, 0.29 mmol) was reacted with TFA (20 mL) in CH$_2$Cl$_2$ (20 mL) using procedure C. Unreacted TFA and

solvent were removed under reduced pressure, followed by washing of the salt with diethylether and recrystallization from ethanol to afford compound (±)-**42** (175 mg, 71%). ^{1}H NMR (CD$_3$OD, 400 MHz): δ 1.03 (t, J = 7.2 Hz, 3H), 1.50-2.02 (m, 6H), 2.03-2.20 (m, 1H), 2.35 (d, J = 10.8 Hz, 1H), 2.54-3.70 (m, 18H), 3.74-4.01 (m, 1H), 6.90 (s, 1H), 7.08 (t, J = 7.6 Hz, 1H), 7.23 (t, J = 7.6 Hz, 1H), 7.44 (d, J = 8.4 Hz, 1H), 7.62 (d, J = 8.4 Hz, 1H). ^{13}C (CD$_3$OD, 100 MHz): δ 10.0, 18.4, 21.0, 21.7, 22.0, 22.2, 22.7, 51.6, 56.0, 59.1, 105.7, 105.7, 111.8, 120.3, 121.6, 124.2, 127.4, 128.2, 133.2, 136.9, 163.8, 170.6. M.p. 100-105 ºC. Anal. calculated for C$_{35}$H$_{43.6}$F$_{12}$N$_6$O$_{9.8}$S: C, H, N.

4-{2-[(2-Amino-4,5,6,7-tetrahydro-benzothiazol-6-yl)propylamino]ethyl}piperazine-1-carboxylic acid tert-butyl ester [(±)-43]. Aldehyde **6** (2.4 g, 10.5 mmol) was reacted with (±)-pramipexole (2.22 g, 10.5 mmol) and NaBH(OAc)$_3$ (4.01 g, 18.9 mmol) in CH$_2$Cl$_2$ (40 mL) using procedure B. The crude material was purified by column chromatography over silica gel (EtOAc/MeOH, 20:1) to yield compound (±)-**43** (3.34 g, 75%). ^{1}H NMR (CDCl$_3$, 400 MHz): δ 0.81 (t, J = 7.2 Hz, 3H), 1.10-1.75 (m, 10H), 1.91 (d, J = 9.6, 1H), 2.10-2.75 (m, 15H), 2.97 (m, 1H), 3.36 (m, 4H), 5.29 (bs, 2H).

(*R*)-4-{2-[(2-Amino-4,5,6,7-tetrahydro-benzothiazol-6-yl)propylamino]-ethyl}piperazine-1-carboxylic acid tert-butyl ester [(+)-43]. Compound **6** (1.2 g, 5.25 mmol) was reacted with (+)-pramipexole (1.11 g, 5.25 mmol) and NaBH(OAc)$_3$ (2.0 g, 9.46 mmol) in CH$_2$Cl$_2$ (25 mL) using procedure B. The crude material was purified by column chromatography over silica gel (EtOAc/MeOH, 20:1) to give compound (+)-**43** (1.63 g, 73%). ^{1}H NMR (CDCl$_3$, 400 MHz): δ 0.83 (t, J = 7.2 Hz, 3H), 1.10-1.75 (m, 10H), 1.91 (d, J = 9.6 Hz, 1H), 2.10-2.75 (m, 15H), 2.98 (m, 1H), 3.36 (m, 4H), 5.29 (bs, 2H).

(*S*)-4-{2-[(2-Amino-4,5,6,7-tetrahydro-benzothiazol-6-yl)propylamino]ethyl}piperazine-1-carboxylic acid tert-butyl ester [(-)-43]. Compound **6** (1.2 g, 5.25 mmol) was reacted with (S)-(-)-pramipexole (1.11 g, 5.25 mmol) and NaBH(OAc)$_3$ (2.0 g, 9.46 mmol) in CH$_2$Cl$_2$ (25 mL) using procedure B. The crude material was purified by column chromatography over silica gel (EtOAc/MeOH, 20:1) to give compound (-)-**43** (1.61 g, 71%). ^{1}H NMR (CDCl$_3$, 400 MHz): δ 0.80 (t, *J* = 7.2 Hz, 3H), 1.10-1.75 (m, 10H), 1.91 (d, *J* = 9.6 Hz, 1H), 2.12-2.75 (m, 15H), 2.97 (m, 1H), 3.36 (m, 4H), 5.29 (bs, 2H).

N^6-(2-Piperazin-1-yl-ethyl)-N^6-propyl-4,5,6,7-tetrahydrobenzothiazole-2,6-diamine [(±)-44]. Compound (±)-**43** (3.34 g, 7.88 mmol) was reacted with TFA (20 mL) in CH$_2$Cl$_2$ (20 mL) using procedure C to give compound (±)-**44** (2.30 g, 90%). ^{1}H NMR (CDCl$_3$, 400 MHz): δ 0.79 (t, *J* = 7.2 Hz, 3H), 1.25-1.48 (m, 2H), 1.50-1.72 (m, 1H), 1.88 (d, *J* = 11.2 Hz, 1H), 2.08-3.07 (m, 19H), 5.40 (bs, 2H).

(*R*)-N^6-(2-Piperazin-1-yl-ethyl)-N^6-propyl-4,5,6,7-tetrahydrobenzothiazole-2,6-diamine [(+)-44]. Compound (+)-**43** (1.63 g, 3.84 mmol) was reacted with TFA (15 mL) in CH$_2$Cl$_2$ (15 mL) using procedure C to yield compound (+)-**44** (1.16 g, 93%). ^{1}H NMR (CDCl$_3$, 400 MHz): δ 0.80 (t, *J* = 7.2 Hz, 3H), 1.25-1.48 (m, 2H), 1.52-1.72 (m, 1H), 1.88 (d, *J* = 11.2 Hz, 1H), 2.08-3.07 (m, 19H), 5.40 (bs, 2H).

(*S*)-N^6-(2-Piperazin-1-yl-ethyl)-N^6-propyl-4,5,6,7-tetrahydrobenzothiazole-2,6-diamine [(-)-44]. Compound (-)-**43** (1.61 g, 3.80 mmol) was reacted with TFA (15 mL) in CH$_2$Cl$_2$ (15 mL) using procedure C to afford compound (-)-**44** (1.16 g, 94%). ^{1}H NMR (CDCl$_3$, 400 MHz): δ 0.79 (t, *J* = 7.2 Hz, 3H), 1.25-1.48 (m, 2H), 1.50-1.72 (m, 1H), 1.89 (d, *J* = 11.2 Hz, 1H), 2.08-3.07 (m, 19H), 5.41 (bs, 2H).

(4-{2-[(2-Amino-4,5,6,7-tetrahydrobenzothiazol-6-yl)propylamino]ethyl}piperazin-1-yl)-(1H-indol-3-yl)methanone [(±)-45]. Indole-3-carboxylic acid (54 mg, 0.33 mmol) was reacted with compound (±)-**44** (90 mg, 0.28 mmol) in the presence of EDCI.HCl (80 mg, 0.42 mmol), TEA (0.12 mL, 0.83 mmol) and HOBt (56 mg, 0.41 mmol) in CH_2Cl_2 (10 mL) using procedure F. The crude product was purified by flash column chromatography (EtOAc/MeOH, 4:1) to afford compound (±)-**45** (83 mg, 64%). ^{1}H NMR (CDCl$_3$, 400 MHz): δ 0.87 (t, J = 7.6 Hz, 3H), 1.30-1.52 (m, 2H), 1.55-1.80 (m, 1H), 1.95 (d, J = 11.6, 1H), 2.20-2.80 (m, 13H), 2.85-3.10 (m, 1H), 3.50-3.82 (m, 4H), 4.86 (bs, 2H), 7.0-7.38 (m, 4H), 7.60-7.76 (m, 1H), 9.77 (s, 1H). ^{13}C (CDCl$_3$, 100 MHz): δ 12.0, 14.4, 21.3, 22.5, 25.4, 26.1, 26.8, 48.6, 53.7, 54.2, 58.3, 58.8, 60.6, 111.5, 112.1, 117.6, 120.4, 121.2, 122.8, 125.6, 127.5, 135.9, 145.3, 165.8, 167.2. The free base was converted to its hydrochloride salt. M.p. 170-175 °C. Anal. calculated for $C_{25}H_{38.6}Cl_4N_6O_{1.3}S$: C, H, N.

(*R*)-(4-{2-[(2-Amino-4,5,6,7-tetrahydrobenzothiazol-6-yl)propylamino]ethyl}piperazin-1-yl)-(1H-indol-3-yl)methanone [(+)-45)]. Indole-3-carboxylic acid (54 mg, 0.33 mmol) was reacted with compound (+)-**44** (90 mg, 0.28 mmol) in the presence of EDCI.HCl (80 mg, 0.42 mmol), TEA (0.12 mL, 0.83 mmol) and HOBT (56 mg, 0.41 mmol) in CH_2Cl_2 (10 mL) using procedure F. The crude material was purified by column chromatography over silica gel (EtOAc/MeOH, 4:1) to yield compound (+)-**45** (87 mg, 67%). ^{1}H NMR (CDCl$_3$, 400 MHz): δ 0.89 (t, J = 7.6 Hz, 3H), 1.30-1.52 (m, 2H), 1.57-1.80 (m, 1H), 1.95 (d, J = 11.6 Hz, 1H), 2.20-2.80 (m, 13H), 2.85-3.10 (m, 1H), 3.50-3.82 (m, 4H), 4.87 (bs, 2H), 7.0-7.38 (m, 4H), 7.60-7.76 (m, 1H), 9.77 (s, 1H). ^{13}C (CDCl$_3$, 100 MHz): δ 12.0, 14.4, 21.4, 22.5, 25.4, 26.1, 26.9, 48.6,

53.7, 54.2, 58.3, 58.8, 60.6, 111.6, 112.1, 117.6, 120.4, 121.2, 122.8, 125.6, 127.5, 135.9, 145.3, 165.9, 167.2. $[\alpha]^{25}_D$ = +37.4° (c = 1.0, CH_3OH). The free base was converted to its hydrochloride salt. M.p. 185-190 °C. Anal. calculated for $C_{25}H_{40}Cl_4N_6O_2S$: C, H, N.

(S)-(4-{2-[(2-Amino-4,5,6,7-tetrahydrobenzothiazol-6-yl)propylamino]ethyl}piperazin-1-yl)-(1H-indol-3-yl)methanone   [(-)-45)]. Indole-3-carboxylic acid (54 mg, 0.33 mmol) was reacted with compound (-)-**44** in the presence of EDCI.HCl (80 mg, 0.42 mmol), TEA (0.12 mL, 0.83 mmol) and HOBT (56 mg, 0.41 mmol) in CH_2Cl_2 (10 mL) using procedure F. The crude material was purified by column chromatography over silica gel (EtOAc/MeOH, 4:1) to give compound (-)-**45** (93 mg, 72%). ^{1}H NMR ($CDCl_3$, 400 MHz): δ 0.85 (t, J = 7.6 Hz, 3H), 1.30-1.52 (m, 2H), 1.55-1.80 (m, 1H), 1.95 (d, J = 11.6 Hz, 1H), 2.20-2.80 (m, 13H), 2.85-3.10 (m, 1H), 3.50-3.82 (m, 4H), 4.86 (bs, 2H), 7.0-7.38 (m, 4H), 7.60-7.76 (m, 1H), 9.77 (s, 1H). ^{13}C ($CDCl_3$, 100 MHz): δ 12.0, 14.4, 21.3, 22.5, 25.4, 26.1, 26.8, 48.6, 53.8, 54.2, 58.3, 58.8, 60.6, 111.5, 112.1, 117.7, 120.4, 121.2, 122.8, 125.6, 127.5, 135.9, 145.3, 165.8, 167.2. $[\alpha]^{25}_D$ = −33.6° (c = 1.0, CH_3OH). The free base was converted to its hydrochloride salt. M.p. 205-210 °C. Anal. calculated for $C_{25}H_{41.5}Cl_{4.5}N_6O_{2.5}S$: C, H, N.

(4-{2-[(2-Amino-4,5,6,7-tetrahydrobenzothiazol-6-yl)propylamino]ethyl}piperazin-1-yl)-(1H-indol-5-yl)methanone [(±)-46]. Indole-5-carboxylic acid (60 mg, 0.37 mmol) was reacted with compound (±)-**44** (100 mg, 0.31 mmol) in the presence of EDCI.HCl (89 mg, 0.46 mmol), TEA (0.13 mL, 0.93 mmol) and HOBT (63 mg, 0.46 mmol) in CH_2Cl_2 (15 mL) using procedure F. The crude material was purified by column chromatography over silica gel (EtOAc/MeOH, 4:1) to yield compound (±)-**46** (102 mg,

71%). ^{1}H NMR (CDCl$_3$, 400 MHz): δ 0.88 (t, J = 7.2 Hz, 1H), 1.40-1.54 (m, 2H), 1.60-1.81 (m, 1H), 1.97 (d, J = 11.2 Hz, 1H), 2.20-2.72 (m, 14H), 2.90-3.15 (m, 1H), 3.30-4.02 (m, 4H), 4.89 (bs, 2H), 6.57 (s, 1H), 7.15-7.29 (m, 1H), 7.35 (d, J = 8.4 Hz, 1H), 7.71 (s, 1H), 8.84 (s, 1H). ^{13}C (CDCl$_3$, 100 MHz): δ 12.0, 22.5, 25.3, 26.0, 26.7, 48.5, 53.7, 58.3, 58.7, 103.1, 111.4, 117.3, 120.4, 121.4, 125.9, 127.0, 127.5, 136.7, 145.1, 166.1, 172.2. The free base was converted to its hydrochloride salt. M.p. 185-190 ºC. Anal. calculated for C$_{25}$H$_{41}$Cl$_4$N$_6$O$_{2.5}$S: C, H, N.

(*R*)-(4-{2-[(2-Amino-4,5,6,7-tetrahydrobenzothiazol-6-yl)propylamino]ethyl}piperazin-1-yl)-(1H-indol-5-yl)methanone [(+)-46]. Indole-5-carboxylic acid (60 mg, 0.37 mmol) was reacted with compound (+)-**44** (100 mg, 0.31 mmol) in the presence of EDCI.HCl (89 mg, 0.46 mmol), TEA (0.13 mL, 0.93 mmol) and HOBT (63 mg, 0.46 mmol) in CH$_2$Cl$_2$ (15 mL) using procedure F. The crude material was purified by column chromatography over silica gel (EtOAc/MeOH, 4:1) to furnish compound (+)-**46** (94 mg, 65%). ^{1}H NMR (CDCl$_3$, 400 MHz): δ 0.89 (t, J = 7.2 Hz, 1H), 1.40-1.54 (m, 2H), 1.60-1.81 (m, 1H), 1.97 (d, J = 11.2 Hz, 1H), 2.20-2.72 (m, 14H), 2.90-3.15 (m, 1H), 3.30-4.03 (m, 4H), 4.89 (bs, 2H), 6.57 (s, 1H), 7.16-7.29 (m, 1H), 7.35 (d, J = 8.4 Hz, 1H), 7.71 (s, 1H), 8.84 (s, 1H). ^{13}C (CDCl$_3$, 100 MHz): δ 12.0, 22.5, 25.3, 26.0, 26.7, 48.5, 53.7, 58.3, 58.7, 103.1, 111.4, 117.3, 120.4, 121.4, 125.9, 127.0, 127.5, 136.7, 145.1, 166.1, 172.2. [α]$^{25}_D$ = +38.6° (*c* = 1.0, CH$_3$OH). The free base was converted to its hydrochloride salt. M.p. 200-205 ºC. Anal. calculated for C$_{25}$H$_{40}$Cl$_4$N$_6$O$_2$S: C, H, N.

(*S*)-(4-{2-[(2-Amino-4,5,6,7-tetrahydrobenzothiazol-6-yl)propylamino]ethyl}piperazin-1-yl)-(1H-indol-5-yl)methanone [(-)-46]. Indole-5-

carboxylic acid (60 mg, 0.37 mmol) was reacted with compound (-)-**44** (100 mg, 0.31 mmol) in the presence of EDCI.HCl (89 mg, 0.46 mmol), TEA (0.13 mL, 0.93 mmol) and HOBT (63 mg, 0.46 mmol) in CH_2Cl_2 (15 mL) using procedure F. The crude material was purified by column chromatography over silica gel (EtOAc/MeOH, 4:1) to yield compound (-)-**46** (95 mg, 66%). ^{1}H NMR (CDCl$_3$, 400 MHz): δ 0.86 (t, J = 7.2 Hz, 1H), 1.40-1.54 (m, 2H), 1.62-1.81 (m, 1H), 1.97 (d, J = 11.2 Hz, 1H), 2.20-2.72 (m, 14H), 2.90-3.15 (m, 1H), 3.30-4.02 (m, 4H), 4.89 (bs, 2H), 6.58 (s, 1H), 7.15-7.29 (m, 1H), 7.35 (d, J = 8.4 Hz, 1H), 7.71 (s, 1H), 8.84 (s, 1H). [13]C (CDCl$_3$, 100 MHz): δ 12.2, 22.5, 25.3, 26.1, 26.7, 48.5, 53.7, 58.3, 58.9, 103.1, 111.4, 117.3, 120.4, 121.4, 125.9, 127.1, 127.5, 136.7, 145.1, 166.1, 172.2. $[\alpha]^{25}_D$ = −34.4° (c = 1.0, CH$_3$OH). The free base was converted to its hydrochloride salt. M.p. 200-205 ^{o}C. Anal. calculated for $C_{25}H_{42.1}Cl_{4.5}N_6O_{2.8}S$: C, H, N.

(4-{2-[(2-Amino-4,5,6,7-tetrahydrobenzothiazol-6-yl)propylamino]ethyl}piperazin-1-yl)-(5-methoxy-1H-indol-3-yl)methanone (47). 5-methoxy-1*H*-indole-3-carboxylic acid (213 mg, 1.11 mmol) was reacted with compound (±)-**44** (300 mg, 0.93 mmol) in the presence of EDCI.HCl (267 mg, 1.40 mmol), TEA (0.39 mL, 2.78 mmol) and HOBT (188 mg, 1.40 mmol) in CH_2Cl_2 (25 mL) using procedure F. The crude material was purified by column chromatography over silica gel (EtOAc/MeOH, 6:1) to give compound **47** (280 mg, 61%). ^{1}H NMR (CDCl$_3$, 400 MHz): δ 0.85 (t, J = 7.2 Hz, 3H), 1.32-1.48 (m, 2H), 1.56-1.76 (m, 1H), 1.93 (d, J = 10 Hz, 1H), 2.26-2.78 (m, 1H), 2.90-3.10 (m, 1H), 3.52-3.77 (m, 4H), 3.77 (s, 3H), 5.21 (bs, 2H), 6.77 (d, J = 8.4 Hz, 1H), 6.90-7.22 (m, 3H), 10.3 (bs, 1H).

(4-{2-[(2-Amino-4,5,6,7-tetrahydrobenzothiazol-6-yl)propylamino]ethyl}piperazin-1-yl)-(5-hydroxy-1H-indol-3-yl)methanone (48). Compound **47** (140 mg, 0.28 mmol) was brought to -78 ^{o}C in CH_2Cl_2 (15 mL), followed by dropwise addition of BBr_3 (0.13 mL, 1.41 mmol). The reaction mixture was allowed to stir for 12 h, while gradually attaining room temperature. The reaction was quenched by the addition of a saturated solution of $NaHCO_3$ and extracted with CH_2Cl_2 (2 × 100 mL). The organic layer was dried over Na_2SO_4 and concentrated under reduced pressure. The crude material was purified by flash column chromatography over silica gel (EtOAc/MeOH, 2:1) to give compound **48** (80 mg, 59%). ^{1}H NMR (CD$_3$OD, 400 MHz): δ 0.91 (t, J = 7.6 Hz, 3H), 1.42-1.58 (m, 2H), 1.62-1.80 (m, 1H), 2.00 (d, J = 8.8 Hz, 1H), 2.40-2.85 (m, 15H), 3.00-3.22 (m, 1H), 3.60-3.88 (m, 4H), 6.74 (dd, J = 8, 1.6 Hz, 1H), 7.04 (d, J = 2.4 Hz, 1H), 7.24 (s, 1H), 7.53 (s, 1H). The free base was converted to its hydrochloride salt. M.p. 210-215 ^{o}C. Anal. calculated for $C_{25.8}H_{43.4}Cl_4N_6O_{3.9}S$: C, H, N.

N^6-{2-[4-(1H-Indol-5-ylmethyl)piperazin-1-yl]ethyl}-N^6-propyl-4,5,6,7-tetrahydrobenzothiazole-2,6-diamine (49). Amine (±)-**44** (80 mg, 0.25 mmol) was reacted with 1*H*-indole-5-carbaldehyde (36 mg, 0.25 mmol) and NaBH(OAc)$_3$ (94 mg, 0.45 mmol) in CH_2Cl_2 (15 mL) using procedure B. The crude residue was purified by column chromatography (EtOAc/MeOH, 4:1) to afford compound **49** (71 mg, 63%). ^{1}H NMR (CDCl$_3$, 400 MHz): δ 0.86 (t, J = 7.2 Hz, 3H), 1.32-1.54 (m, 2H), 1.60-1.78 (m, 1H), 1.95 (d, J = 10.4 Hz, 1H), 2.20-2.80 (m, 18H), 2.90-3.10 (m, 1H), 3.63 (s, 2H), 4.87 (bs, 2H), 6.51 (s, 1H), 7.16 (d, J = 8.4 Hz, 1H), 7.19 (s, 1H), 7.33 (d, J = 8.4 Hz, 1H), 7.55 (s, 1H), 8.45 (s, 1H). The free base was converted to its hydrochloride salt. M.p. 230-235 ^{o}C. Anal. calculated for $C_{27}H_{49}Cl_5N_6O_2S$: C, H, N.

(S)-N-[6-({2-[4-(1-Acetyl-1H-indole-3-carbonyl)-piperazin-1-yl]-ethyl}-propyl-amino)-4,5,6,7-tetrahydro-benzothiazol-2-yl]-acetamide [(-)-50]. Compound (-)-**45** (30 mg, 0.06 mmol) in CH_2Cl_2 (10 mL) was brought to 0 ^{o}C and Ac_2O (0.03 mL, 0.32 mmol) was added dropwise, along with DMAP (0.4 mg, 0.005 mmol). The reaction mixture was allowed to stir at room temperature for 12 h. The reaction was quenched by the addition of a saturated solution of $NaHCO_3$ and extracted with CH_2Cl_2. The organic layer was dried over Na_2SO_4 and concentrated under reduced pressure. The crude mixture was purified over silica gel (MeOH/EtOAc, 1:6) to yield compound (-)-**50** (26 mg, 73%). ^{1}H NMR (CDCl$_3$, 400 MHz): δ 0.86 (t, J = 7.6 Hz, 3H), 1.40-1.62 (m, 2H), 1.64-1.84 (m, 1H), 2.20 (s, 3H), 2.36-2.94 (m, 16H), 2.96-3.20 (m, 1H), 3.40-3.86 (m, 3H), 7.18-7.50 (m, 2H), 7.56 (d, J = 8.4 Hz, 1H), 7.74 (s, 1H), 8.44 (d, J = 8.4 Hz, 1H).

5-[1,2]Dithiolan-3-yl-pentanoic acid [6-({2-[4-(1H-indole-3-carbonyl)-piperazin-1-yl]-ethyl}-propyl-amino)-4,5,6,7-tetrahydro-benzothiazol-2-yl]-amide [(-)-51]. DCC (26 mg, 0.12 mmol) and (R)-lipoic acid (26 mg, 0.12 mmol) in CH_2Cl_2 (10 mL) were stirred at room temperate for 0.5 h, followed by addition of (-)-**45** (48 mg, 0.10 mmol) dissolved in CH_2Cl_2. DMAP (3 mg, 0.024 mmol) was finally added and the reaction mixture was allowed to stir at room temperature for 12 h. Solvent was removed under reduced pressure and crude product was purified over silica gel (MeOH/EtOAc, 1:9) to afford compound (-)-**51** (44 mg, 66%). ^{1}H NMR (CDCl$_3$, 400 MHz): δ 0.81 (t, J = 7.6 Hz, 3H), 1.30-1.50 (m, 4H), 1.52-1.74 (m, 5H), 1.98 (d, J = 12 Hz, 1H), 2.25- 2.40 (m, 3H), 2.42-2.70 (m, 12H), 2.90-3.15 (m, 2H), 3.40-3.75 (m, 8H), 7.06-7.15 (m, 2H), 7.33 (d, J = 7.2 Hz, 1H), 7.43 (s, 1H), 7.54 (d, J = 7.2 Hz, 1H).

5.2 Experimental Procedures

Reagents and solvents were purchased from commercial suppliers and used as received, unless otherwise noted. Dry solvent was obtained following the standard procedure. All reactions were performed under N_2 atmosphere, unless otherwise indicated. Analytical silica gel 60 F_{254}-coated TLC plates were purchased from EMD Chemicals, Inc. and were visualized with UV light or by treatment with phosphomolybdic acid (PMA), Dragendorff's reagent or ninhydrin. Whatman Purasil® 60A silica gel 230-400 mesh was used for flash column, chromatographic purifications. Proton nuclear magnetic resonance (^{1}H NMR) spectra were measured on Varian 400 MHz FT NMR spectrometer, using tetramethylsilane (TMS) as an internal standard. The NMR solvent used was CDCl$_3$, unless otherwise indicated. Optical rotations were recorded on Perkin-Elmer 241 polarimeter. Mass spectra were recorded on Micromass QuattroLC triple quadrupole mass spectrometer. Melting points were recorded using MEL-TEMP II (Laboratory Devices Inc., USA), capillary melting point apparatus and were uncorrected. Elemental analyses were performed by Atlantic Microlab, Inc. and were within ± 0.4% of the theoretical value.

Evaluation of binding affinity to and activation of DA D2 and D3 receptors

Binding potency was measured by the ability of a test compound to inhibit [^{3}H]spiroperidol (15.0 Ci/mmole, Perkin-Elmer) binding to rat D2 and D3 receptors expressed in HEK-293 cells, in a buffer containing 0.9% NaCl. Functional activity in activating human D2 and D3 receptors expressed in CHO cells was measured by the

ability of a test compound to stimulate [^{35}S]GTPγS (1250 Ci/mmole, Perkin-Elmer) binding, in comparison to stimulation by the full agonist DA.

Evaluation of antioxidant activity

DPPH Radical Scavenging Assay. To a 96 well plate, 100 µL of methanolic drug solutions ranging from 20 µM to 250 µM were added. Next, 100 µL of 200 µM methanolic solution of DPPH (1,1-diphenyl-2-picryl-hydrazyl) was added and the plate was shaken vigorously at 30 °C for 20 min. Control wells received 100 µL of methanol and 100 µL of 200 µM methanolic DPPH solution. Wells containing only 200 µL of methanol served as a background correction. The change in absorbance of all samples and standard (ascorbic acid) were measured at 517 nm. Radical scavenging activity was expressed as inhibition percentage and was calculated using the following formula: % scavenging activity = [(absorbance of control - absorbance of sample)/(absorbance of control)] x 100.

Neuroprotection Studies

Materials

1-Methyl-4-phenylpyridinium (MPP$^+$), 6-Hydroxydopamine hydrochloride, Thiazolyl Blue Tetrazolium Bromide (MTT), Poly-L-lysine, Dulbecco's modified Eagle's Medium, Sodium Bicarbonate, Hydrochloric acid, DMSO, methanol, Dulbecco's phosphate buffer saline, Tissue culture grade water were obtained from Sigma-Aldrich. Pennicilin-Streptomycin and Trypsin were purchased from Invitrogen. Fetal Clone III bovine serum (Hyclone, Logan, UT) was purchased from Fisher Scientific. The 96 well plates were purchased from Greiner Bio-One. Apo-One^{TM} Homogeneous Caspase 3/7 reagent was

purchased from Promega Inc. (Madison, Wisconsin, USA). RIPA lysis buffer was purchased from the Santa Cruz Biotechnology Inc. (Santa Cruz, CA, USA). BCA protein assay reagents and horseradish peroxidase-conjugated rabbit secondary antibody were purchased from the Thermo Fisher Scientific Inc. (Rockford, IL, USA). TH primary antibody was purchased from the Cell Signaling Technology Inc. (Danvers, MA, USA). The anti-GAPDH antibody was purchased from BD Biosciences (San Jose, CA, USA). Compounds **D-512** ((-)-**19**) ((6S)-N6-(2-(4-(4-chloro-1H-indol-5-yl)piperazin-1-yl)ethyl)-N6-propyl-3a,4,5,6,7,7a-hexahydrobenzo[d]thiazole-2,6-diamine) and **D-440** ((-)-**40**) ((4-(2-(((6S)-2-amino-3a,4,5,6,7,7a-hexahydrobenzo[d]thiazol-6-yl)(propyl)amino)ethyl)piperazin-1-yl)(1H-indol-2-yl)methanone) were synthesized in our lab as described in our recent publication.

Cell Culture and Treatments

The hybridoma dopaminergic MN9D cells are derived from the somatic infusion of rostral mesencephalic neurons from embryonic C57BL/6J (E14) mice with N18TG2 mouse cells. They were cultured in T-75 flask (Greiner Bio One, Frickenhausen, Germany) coated with 1 mg/ml poly-L-lysine and maintained in DMEM (high glucose with phenol red) supplemented with 10% Fecal Clone III serum, penicillin (50 units/ml) and streptomycin (50 µg/ml) at 37 °C under 5% CO_2 atmosphere. Stock solution of **D-512**, **D-440** and ropinirole were prepared in DMSO and stored at -20 °C for the period of experiments. MN9D cells were pre-treated with various concentrations of **D-512**, **D-440** or ropinirole and then co-treated with 75 µM 6-OHDA (prepared freshly before addition from a stock solution in DMSO stored at -20 °C) or 100 µM MPP+ (prepared

freshly before addition from a stock solution in DMSO stored at -20 °C). The control cells were treated with the above medium having 0.01% DMSO only.

Assessment of Cell Viability

To evaluate the neuroprotection ability of the test compounds in the presence of the neurotoxins 6-OHDA and MPP^+, the quantitative and colorimetric MTT (3-4,5-dimethylthiazolyl-2)-2,5-diphenyltetrazoliumbromide) tetrazolium salt assay was used to assess cell viability. MN9D cells were seeded into poly-L-lysine coated 96-well plates at 1×10^4 cells/well in 100 µL medium. After the plate was equilibrated for 40 h, old medium was taken out from each well and 160 µL of fresh medium (containing 0.01% DMSO) was added to control wells, while 160 µL of fresh medium (without DMSO) was added to the wells which were to be treated with 6-OHDA or MPP^+. A solution of 160 µL of **D-512**, **D-440** or ropinirole, in the above medium without DMSO, in 30, 20, 10, 5, 1, 0.1 µM concentrations were added to wells which would be co-treated with 6-OHDA or MPP^+. The plate was incubated for 1 h at 37 °C under 5% CO_2 atmosphere. At the end of incubation, the required amount of 6-OHDA or MPP^+ was added to each well (except the control wells) to maintain a final concentration of 75 or 100 µM, respectively. The plate was then incubated for 24 h at 37 °C under 5% CO_2 atmosphere. The next day, 20 µL of MTT stock solution (prepared in Dulbecco's phosphate-buffered saline) was added to each well to maintain a final concentration of 0.5 mg/ml and the plate was incubated for another 3 h at 37 °C under 5% CO_2 atmosphere. Next, the plate was centrifuged at 1500 rpm for 10 min and the supernatants were removed carefully. The formazan crystals were dissolved in 100 µL of a 1:1 mixture of DMSO/Methanol solution by shaking gently at 400 rpm for 30 min at ambient temperature on a Thermomix R

shaker (Eppendorf, Hamburg, Germany). Finally, absorbance was measured at 570 nM and 690 nM using an Epoch microplate reader (BioTek, Winooski, VT, USA). Background corrected values (570 nM – 690 nM) values were used to plot the graph. Data from at least three experiments were analyzed using GraphPad software (Version 4, San Diego, USA).

Fluorometric Caspase-3/7 Assay

The caspase 3/7 activity was measured by the fluorometric Apo-ONE[TM] Homogeneous Caspase 3/7 assay kit following the specification provided by the manufacturer (Promega, Madison, WI, USA) with slight modification. Briefly, 10,000 MN9D cells/well were seeded in 90 µL DMEM (with phenol red, containing 10% Fecal Clone III FBS and Pen/Strep) in a cell-bind 96 well plate (PLL-coated) and incubated for 48 h at 37 °C under 5% CO_2. A solution of 10 µL fresh medium (as mentioned above) without DMSO was added to control cells, while 5 µL of fresh medium (as mentioned above) was added to the cells which would be treated with 6-OHDA alone. Next, the required amount of **D-512** was added to the cells which would be co-treated with 6-OHDA, to maintain a final concentration of 20 µM and 1 uM, respectively. The plate was shaken at 400 rpm for 3 min on an Eppendorf Thermomix shaker to ensure homogeneous mixing of the drug. The plate was then incubated for 1 h at 37 °C under 5% CO_2 atmosphere. Next, the required amount of 6-OHDA solution (prepared from a 1 M stock solution in DMSO) was added very quickly to the co-treated cells to maintain a final concentration of 75 µM. The plate was incubated for 24 h at 37 °C under 5% CO_2 atmosphere. Following incubation, old medium was taken out from each well and 75 µL of fresh DMEM medium (high glucose without serum and phenol red) was quickly

added to each well. Freshly prepared Caspase-3/7 reagent 75 µL (substrate + lysis buffer at 1:100 dilution) was added to each well. The addition of Caspase 3/7 reagent was performed in dark. The plate was covered with aluminum foil and shaken at 400 rpm on an Eppendorf Thermopmix R shaker. Fluorescence reading was taken each hour at excitation wavelength of 489 nM and emission wavelength of 535 nM on a BioTek Synergy H-1 fluorescence plate reader with sensitivity set to 65. The optimized result was obtained at 7 h after the addition of Caspase 3/7 reagent. The value from the blank well was substracted from control and treated wells. Data were analyzed using GraphPad software (Version 4, San Diego, USA).

Western Blot Analysis

A standard protocol was followed to perform Western blotting. In brief, MN9D cells were grown in 6-well plates coated with 1mg/ml PLL. After seeding for 24 h, the cells were pretreated with 20 µM **D-512** followed by co-treatment with 75 µM 6-OHDA for 24 h. Cells were then harvested by cell scraping and lysed in RIPA lysis buffer on ice for 30 min. The supernatant was collected and the protein concentration was determined using the BCA protein assay reagents. Samples containing 30 µg of total protein were electrophoresed on 12% SDS-polyacrylamide gels and transferred to PVDF membrane. The membrane was blocked in 10% nonfat milk in TBST for 1 h followed by probing with TH primary antibody overnight at 4 °C. The membrane was next treated with HRP (horseradish peroxidase)-conjugated rabbit secondary antibody for 1 h at ambient temperature. The image was visualized using ECL-Plus (PerkinElmer, Waltham, MA, USA) and ImageQuant LAS 4000 (GE Healthcare Biosciences, Pittsburgh, PA, USA).

GAPDH was used as a house keeping protein to monitor loading control and the GAPDH expression levels were determined with an anti-GAPDH antibody.

Anti-Aggregation Studies

α-syn

Locomotor Experiment

Drugs and chemicals:

The following commercially available drugs were used in the experiment: reserpine hydrochloride (Alfa Aesar) and ropinirole (Sigma Aldrich). The trifluoroacetate salt of (-)-**19** and (-)-**40** and the hydrochloride salt of (-)-**46** and ropinirole were dissolved in water. Reserpine was dissolved in 10-25 μL of glacial acetic acid and further diluted with 5.5% glucose solution. All compounds for this study were administered subcutaneously (sc), in a volume of 0.1-0.3 mL to each rat.

Animals:

In rodent studies, animals were male and female, Sprague-Dawley rats from Harlan (Indianapolis, IN) weighing 220-225 g, unless otherwise specified. Animals were maintained in sawdust-lined cages, in a temperature and humidity controlled environment at 22 ± 1°C and 60 ± 5% humidity, respectively. A 12 h light/dark cycle was maintained, with lights on from 6:00 AM to 6:00 PM. They were group-housed with unrestricted access to food and water. All experiments were performed during the light component. All animal use procedures were in compliance with the Wayne State University Animal Investigation Committee, consistent with AALAC guidelines.

Reversal of Reserpine-Induced Hypolocomotion in Rats:

Administration of reserpine induces catalepsy in rodents, primarily by blocking the vesicular monoamine trasporter (VMAT), which assists in the internalization of monoamines into vesicles. VMAT inhibition results in metabolism of unprotected monoamines in the cytosol, ultimately causing depletion of monoamines in the synapses of the peripheral sympathetic nerve terminals. The ability of compounds (-)-**19**, (-)-**40** and (-)-**46** to reverse reserpine-induced, hypolocomotion was investigated. Ropinirole was used as a reference compound in this study. Reserpine (5.0 mg/kg, sc) was administered 18 h before the injection of drug or vehicle (sc). The rats were placed individually in the chambers 1 h before administration of the test drug, standard drug or vehicle for acclimitization. Immediately after administration of drug or vehicle, animals were individually placed in versamax animal activity monitor chamber (45 cm × 30 cm × 20 cm) (AccuScan Instruments, Inc., Columbus, OH) to start measuring locomotor activity. Locomotion was monitored for 6 h. Consecutive interruption of two infrared beams, situated 24 cm apart and 4 cm above the cage floor, in the monitor chamber recorded movement. The data were presented as horizontal activity (HACTV). The effect of individual doses of drugs on locomotor activity was compared with respect to saline treated controls (mean ± S.E.M.). The data were analyzed by one-way analysis of variance (ANOVA) followed by Dunnett's post hoc test. The effect was considered significant if the difference from the control group was observed at $p < 0.05$.

Rotational Experiment

Drugs and chemicals:

The commercially available drug ropinirole (Sigma Aldrich) was used in the experiment. The trifluoroacetate salts of compounds **D-512** and **D-440** and the hydrochloride salt of ropinirole were dissolved in water. All compounds for this study were administered intraperitoneally (ip) in a volume of 0.5-0.8 mL to each rat.

Animals:

The lesioned rats (250-260 g) were purchased from Charles River (Wilmington, MA) and their unilateral lesion was checked twice by apomorphine challenge following the surgery. Animals were maintained in sawdust-lined cages in a temperature and humidity controlled environment at 22 ± 1°C and 60 ± 5 % respectively, with a 12-h light/dark cycle, with lights on from 6:00 AM to 6:00 PM. They were group housed with unrestricted access to food and water. All experiment was performed during the light component. All animal use procedures were in compliance with the Wayne State University Animal Investigation Committee consistent with AALAC guidelines.

In vivo Rotational experiment with 6-OH-DA lesioned rats

The first 7 days post-lesion challenge with apomorphine was done with lesioned animals to observe a complete rotation session post administration. In the second challenge with apomorphine (0.05 mg/kg) 21 days post lesion, contralateral rotations were recorded for 30 min; apomorphine produced rotations in all four rats (average rotation > 250) indicating successful unilateral lesion. In these rats, lesion was performed on the left side of the medial forebrain bundle in the brain and the coordinates used from Bregma are: IB +2.5 AP -1.5 ML +/- 1.8 DV -7.5 from the Dura

based on Paxinos-Watson Second Addition Atlas. The rotations produced upon agonist challenge occurred clockwise. The rats were brought to the test room 1 h before the administration of the test drug, standard drug or vehicle for acclimatization. The rotations were measured over 7-10 h. For control, vehicle was administered alone. Rotations were measured in the Rotomax Rotometry System (AccuScan Instruments, Inc. Columbus, Ohio) equipped with Rotomax Analyser, high resolution sensor and animal chambers with harnesses. Data were analyzed with Rotomax Window software program. Test drugs **D-512** (2.5, 5 and 10 μMol/kg), **D-440** (5 and 10 μMol/kg) and ropinirole (5 μMol/kg) were each administered ip. The rotations were measured in a rotational chamber immediately after administration of drugs. Data was collected at discrete 30 min. intervals. Data were analyzed by Graph Pad (Version 4, San Diego) program.

Statistical Analysis

The data were expressed as mean value ± standard error mean (SEM). For multiple groups statistical significance was determined using one way analysis of variance (ANOVA) followed Tukey's Multiple Comparison post hoc test. In all cases, $P < 0.05$ was considered statistically significant.

REFERENCES

Abramova, N. A., D. S. Cassarino, S. M. Khan, T. W. Painter and J. P. Bennett Jr. "Inhibition by R(+) or S(-) Pramipexole of Caspase Activation and Cell Death Induced by Methylpyridinium Ion or Beta Amyloid Peptide in SH-SY5Y Neuroblastoma." *Journal of Neuroscience Research* 67, no. 4 (2002): 494-500.

Akunne, H. C., P. Towers, G. J. Ellis, D. Dijkstra, H. Wikström, T. G. Heffner, L. D. Wise and T. A. Pugsley. "Characterization of Binding of [3H]PD 128907, a Selective Dopamine D3 Receptor Agonist Ligand, to CHO-K1 Cells." *Life Sciences* 57, no. 15 (1995): 1401-1410.

Andersen, J. K. "Oxidative Stress in Neurodegeneration: Cause or Consequence?" *Nature Medicine* 10, no. Suppl (2004): S18-S25.

Avenell, K. Y., I. Boyfield, M. S. Hadley, C. N. Johnson, D. J. Nash, G. J. Riley and G. Stemp. "Heterocyclic Analogues of 2-Aminotetralins with High Affinity and Selectivity for the Dopamine D3 Receptor." *Bioorganic & Medicinal Chemistry Letters* 9, no. 18 (1999): 2715-2720.

Bennett Jr., J. P. and M. F. Piercey. "Pramipexole--a New Dopamine Agonist for the Treatment of Parkinson's Disease." *Journal of the Neurological Sciences* 163, no. 1 (1999): 25-31.

Bézard, E., S. Ferry, U. Mach, H. Stark, L. Leriche, T. Boraud, C. Gross and P. Sokoloff. "Attenuation of Levodopa-Induced Dyskinesia by Normalizing Dopamine D3 Receptor Function." *Nature Medicine* 9, no. 6 (2003): 762-767.

Birkmayer, W. and O. Hornykiewicz. "The Effect of L-3,4-dihydroxyphenylalanine (= Dopa) on Akinesia in Parkinsonism. 1961." *Wiener klinische Wochenschrift* 113, no. 22 (2001): 851-854.

Biswas, S., S. Zhang, F. Fernandez, B. Ghosh, J. Zhen, E. Kuzhikandathil, M. E. Reith and A. K. Dutta. "Further Structure-Activity Relationships Study of Hybrid 7-{[2-(4-phenylpiperazin-1-yl)ethyl]propylamino}-5,6,7,8-tetrahydronaphthalen-2-ol Analogues: Identification of a High-Affinity D3-Preferring Agonist with Potent *in vivo* Activity with Long Duration of Action." *Journal of Medicinal Chemistry* 51, no. 1 (2008a): 101-117.

Biswas, S., S. Hazeldine, B. Ghosh, I. Parrington, E. Kuzhikandathil, M. E. Reith and A. K. Dutta. "Bioisosteric Heterocyclic Versions of 7-{[2-(4-phenyl-piperazin-1-yl)ethyl]propylamino}-5,6,7,8-tetrahydronaphthalen-2-ol: Identification of Highly Potent and Selective Agonists for Dopamine D3 Receptor with Potent *in vivo* Activity." *Journal of Medicinal Chemistry* 51, no. 10 (2008b): 3005-3019.

Blandini, F., M. T. Armentero, R. Fancellu, E. Blaugrund and G. Nappi. "Neuroprotective Effect of Rasagiline in a Rodent Model of Parkinson's Disease." *Experimental Neurology* 187, no. 2 (2004): 455-459.

Boeckler, F., H. Lanig and P. Gmeiner. "Modeling the Similarity and Divergence of Dopamine D2-Like Receptors and Identification of Validated Ligand-Receptor Complexes." *Journal of Medicinal Chemistry* 48, no. 3 (2005): 694-709.

Boeckler, F. and P. Gmeiner. "The Structural Evolution of Dopamine D3 Receptor Ligands: Structure-Activity Relationships and Selected Neuropharmacological Aspects." *Pharmacology and Therapeutics* 112, no. 1 (2006): 281-333.

Bordet, R., S. Ridray, S. Carboni, J. Diaz, P. Sokoloff and J. C. Schwartz. "Induction of Dopamine D3 Receptor Expression as a Mechanism of Behavioral Sensitization to Levodopa." *Proceeding of the National Academy of Sciences of the USA* 94, no. 7 (1997): 3363-3367.

Bové, J., D. Prou, C. Perier and S. Przedborski. "Toxin-Induced Models of Parkinson's Disease." *NeuroRx* 2, no. 3 (2005): 484-494.

Braak, H., K. Del Tredici, U. Rub, R. A. I. De Vos and E. N. H. J. Steur. "Staging of Brain Pathology Related to Sporadic Parkinson's Disease." *Neurobiology of Aging* 24, no. 2 (2003): 197-211.

Bredesen, D. E. "Neural Apoptosis." *Annals of Neurology* 38, no. 6 (1995): 839-851.

Breese, G. R. and T. D. Traylor. "Effect of 6-hydroxydopamine on Brain Norepinephrine and Dopamine Evidence for Selective Degeneration of Catecholamine Neurons." *Journal of Pharmacology and Experimental Therapeutics* 174, no. 3 (1970): 413-420.

Brown, D. A., M. Mishra, S. Zhang, S. Biswas, I. Parrington, T. Antonio, M. E. Reith and A. K. Dutta. "Investigation of Various N-Heterocyclic Substituted Piperazine Versions of 5/7-{[2-(4-aryl-piperazin-1-yl)-ethyl]-propyl-amino}-5,6,7,8-tetrahydro-naphthalen-2-ol: Effect on Affinity and Selectivity for Dopamine D3 Receptor." *Bioorganic & Medicinal Chemistry* 17, no. 11 (2009): 3923-3933.

Bunzow, J. R., H. H. Van Tol, D. K. Grandy, P. Albert, J. Salon, M. Christie, C. A. Machida, K. A. Neve and O. Civelli. "Cloning and Expression of a Rat D2 Dopamine Receptor cDNA." *Nature* 336, no. 6201 (1988): 783-787.

Cannon, J. G. "Structure-Activity Relationships of Dopamine Agonists." *Annual Review of Pharmacology and Toxicology* 23, (1983): 103-129.

Cappai, R., S. L. Leck, D. J. Tew, N. A. Williamson, D. P. Smith, D. Galatis, R. A. Sharpless, C. C. Curtain, F. E. Ali, R. A. Cherny, J. G. Culvenor, S. P. Bottomley, C. L. Masters, K. J. Barnham and A. F. Hill. "Dopamine Promotes Alpha-Synuclein Aggregation into SDS-Resistant Soluble Oligomers Via a Distinct Folding Pathway." *FASEB Journal* 19, no. 10 (2005): 1377-1379.

Carlsson, A., M. Lindqvist and T. Magnusson. "3,4-dihydroxyphenylalanine and 5-hydroxytryptophan as Reserpine Antagonists." *Nature* 180, no. 4596 (1957): 1200.

Carlsson, A. "Monoamine-Depleting Drugs." *Pharmacology and Therapeutics. Part B: General & Systematic Pharmacology* 1, no. 3 (1975): 393-400.

Carter, A. J. and R. E. Müller. "Pramipexole, a Dopamine D2 Autoreceptor Agonist, Decreases the Extracellular Concentration of Dopamine *in vivo*." *European Journal of Pharmacology* 200, no. 1 (1991): 65-72.

Carvey, P. M., L. R. Ptak, D. Lin, E. S. Lo, C. M. Buhrfiend, G. E. Drucker and J. Z. Fields. "Alterations in Striatal Neurotrophic Activity Induced by Dopaminergic Drugs." *Pharmacology, Biochemistry and Behavior* 46, no. 1 (1993a): 195-204.

Carvey, P. M., L. R. Ptak, S. T. Nath, D. K. Sierens, E. J. Mufson, C. G. Goetz and H. L. Klawans. "Striatal Extracts from Patients with Parkinson's Disease Promote Dopamine Neuron Growth in Mesencephalic Cultures." *Experimental Neurology* 120, no. 1 (1993b): 149-152.

Carvey, P. M., S. Pieri and Z. D. Ling. "Attenuation of Levodopa-Induced Toxicity in Mesencephalic Cultures by Pramipexole." *Journal of Neural Transmission* 104, no. 2-3 (1997): 209-228.

Carvey, P. M., S. O. McGuire and Z. D. Ling. "Neuroprotective Effects of D3 Dopamine Receptor Agonists." *Parkinsonism & Related Disorders* 7, no. 3 (2001): 213-223.

Cavalli, A., M. L. Bolognesi, A. Minarini, V.Tumiatti, M. Recanatini and C. Melchiorre. "Multi-Target-Directed Ligands to Combat Neurodegenerative Diseases." *Journal of Medicinal Chemistry* 51, no. 7 (2008): 2326-2326.

Chiueh, C. C., R. M. Wu, K. P. Mohanakumar, L. M. Sternberger, G. Krishna, T. Obata and D. L. Murphy. "*In vivo* Generation of Hydroxyl Radicals and MPTP-Induced Dopaminergic Toxicity in the Basal Ganglia." *Annals of the New York Academy of Sciences* 738, (1994): 25-36.

Choi, H. K., L. A. Won, P. J. Kontur, D. N. Hammond, A. P. Fox, B. H. Wainer, P. C. Hoffmann and A. Heller. "Immortalization of Embryonic Mesencephalic Dopaminergic Neurons by Somatic Cell Fusion." *Brain Research* 552, no. 1 (1991): 67-76.

Choi, W. S., S. Y. Yoon, T. H. Oh, E. J. Choi, K. L. O'Malley and Y. J. Oh. "Two Distinct Mechanisms Are Involved in 6-hydroxydopamine- and MPP+-Induced Dopaminergic Neuronal Cell Death: Role of Caspases, ROS, and JNK." *Journal of Neuroscience Research* 57, no. 1 (1999): 86-94.

Churchyard, A., C. J. Mathias, P. Boonkongchuen and A. J. Lees. "Autonomic Effects of Selegiline: Possible Cardiovascular Toxicity in Parkinson's Disease." *Journal of Neuorlogy, Neurosurgery and Psychiatry* 63, no. 2 (1997): 228-234.

Clarke, C. E. and M. Guttman. "Dopamine Agonist Monotherapy in Parkinson's Disease." *Lancet* 360, no. 9347 (2002): 1767-1769.

Colpaert, F. C. "Pharmacological Characteristics of Tremor, Rigidity and Hypokinesia Induced by Reserpine in Rat." *Neuropharmacology* 26, no. 9 (1987): 1431-1440.

Damsma, G., T. Bottema, B. H. Westerink, P. G. Tepper, D. Dijkstra, T. A. Pugsley, R. G. MacKenzie, T. G. Heffner and H. Wikström. "Pharmacological Aspects of R-(+)-7-OH-DPAT, a Putative Dopamine D3 Receptor Ligand." *European Journal of Pharmacology* 249, no. 3 (1993): R9-R10.

Dauer, W. and S. Przedborski. "Parkinson's Disease: Mechanisms and Models." *Neuron* 39, no. 6 (2003): 889-909.

Deumens, R., A. Blokland and J. Prickaerts. "Modeling Parkinson's Disease in Rats: An Evaluation of 6-OHDA Lesions of the Nigrostriatal Pathway." *Experimental Neurology* 175, no. 2 (2002): 303-317.

Du, F., R. Li, Y. Huang, X. Li and W. Le. "Dopamine D3 Receptor-Preferring Agonists Induce Neurotrophic Effects on Mesencephalic Dopamine Neurons." *European Journal of Neuroscience* 22, no. 10 (2005): 2422-2430.

Dutta, A. K., X. S. Fei and M. E. Reith. "A Novel Series of Hybrid Compounds Derived by Combining 2-Aminotetralin and Piperazine Fragments: Binding Activity at D2 and D3 Receptors." *Bioorganic & Medicinal Chemistry Letters* 12, no. 4 (2002): 619-622.

Dutta, A. K., S. K. Venkataraman, X. S. Fei, R. Kolhatkar, S. Zhang and M. E. Reith. "Synthesis and Biological Characterization of Novel Hybrid 7-[[2-(4-phenyl-piperazin-1-yl)-ethyl]-propyl-amino]-5,6,7,8-tetrahydro-naphthalen-2-ol and Their

Heterocyclic Bioisosteric Analogues for Dopamine D2 and D3 Receptors." *Bioorganic & Medicinal Chemistry* 12, no. 16 (2004): 4361-4373.

Eisenhofer, G., I. Lamensdorf, K. L. Kirk, M. Kawamura and S. Sato. "Oxidative Deamination of Monoamines and Biogenic Aldehydes in Neurodegeneration." In *Role of Quinone Species in Cellular Toxicity*, 103-145. Johnson City, TN: Creveling CR, 2000.

Eisenhofer, G., I. Kopin and D. S. Goldstein. "Catecholamine Metabolism: A Contemporary View with Implications for Physiology and Medicine." *Pharmacological Reviews* 56, no. 3 (2004): 331-349.

El-Agnaf, O. M., R. Jakes, M. D. Curran and A. Wallace. "Effects of the Mutations Ala30 to Pro and Ala53 to Thr on the Physical and Morphological Properties of Alpha-Synuclein Protein Implicated in Parkinson's Disease." *FEBS letters* 440, no. 1-2 (1998): 67-70.

Fahn, S. "Does Levodopa Slow or Hasten the Rate of Progression of Parkinson's Disease?" *Journal of Neurology* 252, no. Suppl 4 (2005): IV37-IV42.

Fahn, S. and G. Cohen. "The Oxidant Stress Hypothesis in Parkinson's Disease: Evidence Supporting It." *Annals of Neurology* 32, no. 6 (1992): 804-812.

Forno, L. S., J. W. Langston, L. E. Delanney and I. Irwin. "An Electron Microscopic Study of MPTP-Induced Inclusion Bodies in an Old Monkey." *Brain Research* 448, no. 1 (1988): 150-157.

Friedman, A. and J. Galazka-Friedman. "The History of the Research of Iron in Parkinsonian Substantia Nigra." *Journal of Neural Transmission* 119, no. 12 (2012): 1507-1510.

Fujita, Y., Y. Izawa, N. Ali, Y. Kanematsu, K. Tsuchiya, S. Hamano, T. Tamaki and M. Yoshizumi. "Pramipexole Protects against H2O2-Induced PC12 Cell Death." *Naunyn-Schmiedeberg's Archives of Pharmacology* 372, no. 4 (2006): 257-266.

Giros, B., M. P. Martres, P. Sokoloff and J. C. Schwartz. "[Gene Cloning of Human Dopaminergic D3 Receptor and Identification of its Chromosome]." *Comptes Rendus de l'Académie des Sciences. Série III* 311, no. 13 (1990): 501-508.

Gomez-Tortosa, E., K. Newell, M. C. Irizarry, M. Albert, J. H. Growdon and B. T. Hyman. "Clinical and Quantitative Pathologic Correlates of Dementia with Lewy Bodies." *Neurology* 53, no. 6 (1999): 1284-1291.

Grandy, D. K., M. A. Marchionni, H. Makam, R. E. Stofko, M. Alfano, L. Frothingham, J. B. Fischer, K. J. Burke-Howie, J. R. Bunzow, A. C. Server and O. Civelli. "Cloning of the cDNA and Gene for a Human D2 Dopamine Receptor." *Proceeding of the National Academy of Sciences of the USA* 86, no. 24 (1989): 9762-9766.

Hoehn, M. M. "Parkinsonism: Onset, Progression, and Mortality." *Neurology* 17, no. 5 (1998): 427-442.

Jackson-Lewis, V. and S. Przedborski. "Protocol for the MPTP Mouse Model of Parkinson's Disease." *Nature Protocols* 2, no. 1 (2007): 141-151.

Jenner, P. "Dopamine Agonists, Receptor Selectivity and Dyskinesia Induction in Parkinson's Disease." *Current Opinion in Neurology* 16, no. Suppl 1 (2003a): S3-S7.

Jenner, P. "Oxidative Stress in Parkinson's Disease." *Annals of Neurology* 53, no. 3 (2003b): S26-S36.

Jo, E., J. McLaurin, C. M. Yip, P. St. George-Hyslop and P. E. Fraser. "Alpha-Synuclein Membrane Interactions and Lipid Specificity." *Journal of Biological Chemistry* 275, no. 44 (2000): 34328-34334.

Joyce, J. N. "Dopamine D3 Receptor as a Therapeutic Target for Antipsychotic and Antiparkinsonian Drugs." *Pharmacology and Therapeutics* 90, no. 2-3 (2001a): 231-259.

Joyce, J. N., H. Ryoo, E. V. Gurevich, C. Adler and T. Beach. "Ventral Striatal D(3) Receptors and Parkinson's Disease." *Parkinsonism & Related Disorders* 7, no. 3 (2001b): 225-230.

Kirschner, P. B., B. G. Jenkins, J. B. Schulz, S. P. Finkelstein, R. T. Matthews, B. R. Rosen and M. F. Beal. "NGF, BDNF and NT-5, but not NT-3 Protect against MPP+ Toxicity and Oxidative Stress in Neonatal Animals." *Brain Research* 13, no. 1-2 (1996): 178-185.

Kowall, N. W., P. Hantraye, E. Brouillet, M. F. Beal, A. C. McKee and R. J. Ferrante. "MPTP Induces Alpha-Synuclein Aggregation in the Substantia Nigra of Baboons." *Neuroreport* 11, no. 1 (2000): 211-213.

Kraus, R. L., R. Pasieczny, K. Lariosa-Willingham, M. S. Turner, A. Jiang and J. W. Trauger. "Antioxidant Properties of Minocycline: Neuroprotection in an Oxidative Stress Assay and Direct Radical-Scavenging Activity." *Journal of Neurochemistry* 94, no. 3 (2005): 819-827.

Krobert, K., I. Lopez-Colberg and L. A. Cunningham. "Astrocytes Promote or Impair the Survival and Function of Embryonic Ventral Mesencephalon Co-Grafts: Effects of Astrocyte Age and Expression of Recombinant Brain-Derived Neurotrophic Factor." *Experimental Neurology* 145, no. 2 Pt 1 (1997): 511-523.

Kvernmo, T., S. Härtter and E. Burger. "A Review of the Receptor-Binding and Pharmacokinetic Properties of Dopamine Agonists." *Clinical Therapeutics* 28, no. 8 (2006): 1065-1078.

Langston, J. W., P. Ballard, J. W. Tetrud and I. Irwin. "Chronic Parkinsonism in Humans Due to a Product of Meperidine-Analog Synthesis." *Science* 219, no. 4587 (1983a): 979-980.

Langston, J. W. and P. A. Ballard Jr. "Parkinson's Disease in a Chemist Working with 1-methyl-4-phenyl-1,2,5,6-tetrahydropyridine." *New England Journal of Medicine* 309, no. 5 (1983b): 310.

Le, W. D., J. Jankovic, W. Xie and S. H. Appel. "Antioxidant Property of Pramipexole Independent of Dopamine Receptor Activation in Neuroprotection." *Journal of Neural Transmission* 107, no. 10 (2000): 1165-1173.

Le, W. D. and J. Jankovic. "Are Dopamine Receptor Agonists Neuroprotective in Parkinson's Disease?" *Drugs & Aging* 18, no. 6 (2001): 389-396.

Levant, B. "The D3 Dopamine Receptor: Neurobiology and Potential Clinical Relevance." *Pharmacological Reviews* 49, no. 3 (1997): 231-252.

Li, C., S. Biswas, X. Li, A. K. Dutta and W. Le. "Novel D3 Dopamine Receptor-Preferring Agonist D-264: Evidence of Neuroprotective Property in Parkinson's Disease Animal Models Induced by 1-methyl-4-phenyl-1,2,3,6-tetrahydropyridine and Lactacystin." *Journal of Neuroscience Research* 88, no. 11 (2010): 2513-2523.

Lieberman, A., A. Ranhosky and D. Korts. "Clinical Evaluation of Pramipexole in Advanced Parkinson's Disease: Results of a Double-Blind, Placebo-Controlled, Parallel-Group Study." *Neurology* 49, no. 1 (1997): 162-168.

Lieberman, A., C. W. Olanow, K. Sethi, P. Swanson, C. H. Waters, S. Fahn, H. Hurtig and M. Yahr. "A Multicenter Trial of Ropinirole as Adjunct Treatment for Parkinson's Disease. Ropinirole Study Group." *Neurology* 51, no. 4 (1998): 1057-1062.

Lipski, J., R. Nistico, N. Berretta, E. Guatteo, G. Bernadi and N. B. Mercuri. "L-Dopa: A Scapegoat for Accelerated Neurodegeneration in Parkinson's Disease?" *Progress in Neurobiology* 94, no. 4 (2011): 389-407.

Livingstone, C. D., P. G. Strange and L. H. Naylor. "Molecular Modelling of D2-Like Dopamine Receptors." *Biochemical Journal* 287, no. Pt 1 (1992): 277-282.

Lotharius, J., L. L. Dugan and K. L. O'Malley. "Distinct Mechanisms Underlie Neurotoxin-Mediated Cell Death in Cultured Dopaminergic Neurons." *Journal of Neuroscience* 19, no. 4 (1999): 1284-1293.

Lotharius, J. and P. Brundin. "Impaired Dopamine Storage Resulting from Alpha-Synuclein Mutations May Contribute to the Pathogenesis of Parkinson's Disease." *Human Molecular Genetics* 11, no. 20 (2002): 2395-2407.

Mallajosyula, J. K., D. Kaur, S. J. Shinta, S. Rajagopalan, A. Rane, D. G. Nicholls, D. A. Di Monte, H. Macarthur and J. K. Andersen. "MAO-B Elevation in Mouse Brain Astrocytes Results in Parkinson's Pathology." *PLoS One* 3, no. 2 (2008): e1616.

Malmberg, A., G. Nordvall, A. M. Johansson, N. Mohell and U. Hacksell. "Molecular Basis for the Binding of 2-Aminotetralins to Human Dopamine D2A and D3 Receptors." *Molecular Pharmacology* 46, no. 2 (1994): 299-312.

Mandel, S., E. Grunblatt, P. Riederer, M. Gerlach, Y. Levites and M. B. H. Youdim. "Neuroprotective Strategies in Parkinson's Disease: An Update on Progress." *CNS Drugs* 17, no. 10 (2003): 729-762.

Manning-Bog, A. B., A. L. McCormack, J. Lo, V. N. Uversky, A. L. Fink and D. A. Di Monte. "The Herbicide Paraquat Causes Up-Regulation and Aggregation of Alpha-Synuclein in Mice: Paraquat and Alpha-Synuclein." *Journal of Biological Chemistry* 277, no. 3 (2002): 1641-1644.

Margolis, E. B., A. R. Coker, J. R. Driscoll, A. I. Lemaître and H. L. Fields. "Reliability in the Identification of Midbrain Dopamine Neurons." *PLoS One* 5, no. 12 (2010): e15222.

Marsden, C. D. "Parkinson's Disease." *Lancet* 335, no. 8695 (1990): 948-952.

McCormack, A. L., M. Thiruchelvam, A. B. Manning-Bog, C. Thiggault, J. W. Langston, D. A. Cory-Slechta and D. A. Di Monte. "Environmental Risk Factors and Parkinson's Disease: Selective Degeneration of Nigral Dopaminergic Neurons Caused by the Herbicide Paraquat." *Neurobiology of Disease* 10, no. 2 (2002): 119-127.

McDermed, J. D., G. M. McKenzie and H. S. Freeman. "Synthesis and Dopaminergic Activity of (+/-)-, (+)-, and (-)-2-dipropylamino-5-hydroxy-1,2,3,4-tetrahydronaphthalene." *Journal of Medicinal Chemistry* 19, no. 4 (1976): 547-549.

Menzaghi, F., K. T. Whelan, V. B. Risbrough, T. S. Rao and G. K. Lloyd. "Interactions between a Novel Cholinergic Ion Channel Agonist, SIB-1765F and L-Dopa in the Reserpine Model of Parkinson's Disease in Rats." *Journal of Pharmacology and Experimental Therapeutics* 280, no. 1 (1997): 393-401.

Mierau, J., F. J. Schneider, H. A. Ensinger, C. L. Chio, M. E. Lajiness and R. M. Huff. "Pramipexole Binding and Activation of Cloned and Expressed Dopamine D2, D3 and D4 Receptors." *European Journal of Pharmacology* 290, no. 1 (1995): 29-36.

Monsma Jr., F. J., L. C. Mahan, L. D. McVittie, C. R. Gerfen and D. R. Sibley. "Molecular Cloning and Expression of a D1 Dopamine Receptor Linked to Adenylyl Cyclase Activation." *Proceeding of the National Academy of Sciences of the USA* 87, no. 17 (1990): 6723-6727.

Münchau, A. and K. P. Bhatia. "Pharmacological Treatment of Parkinson's Disease." *Postgraduate Medical Journal* 76, no. 900 (2000): 602-610.

Nayak, L. and C. Henchcliffe. "Rasagiline in Treatment of Parkinson's Disease." *Neuropsychiatric Disease and Treatment* 4, no. 1 (2008): 11-20.

Nutt, J. G., W. R. Woodward, R. M. Beckner, C. K. Stone, K. Berggren, J. H. Carter, S. T. Gancher, J. P. Hammerstad and A. Gordin. "Effect of Peripheral Catechol-O-Methyltransferase Inhibition on the Pharmacokinetics and Pharmacodynamics of Levodopa in Parkinsonian Patients." *Neurology* 44, no. 5 (1994): 913-919.

Olanow, C. W. "Rationale for Considering that Propargylamines might be Neuroprotective in Parkinson's Disease." *Neurology* 66, no. 10 Suppl 4 (2006): S69-S79.

Paulus, W. and K. Jellinger. "The Neuropathologic Basis of Different Clinical Subgroups of Parkinson's Disease." *Journal of Neuropathology and Experimental Neurology* 50, no. 6 (1991): 743-755.

Perachon, S., J. C. Schwartz and P. Sokoloff. "Functional Potencies of New Antiparkinsonian Drugs at Recombinant Human Dopamine D1, D2 and D3 Receptors." *European Journal of Pharmacology* 366, no. 2-3 (1999): 293-300.

Perez, R. G., J. C. Waymire, E. Lin, J. J. Liu, F. Guo and M. J. Zigmond. "A Role for Alpha-Synuclein in the Regulation of Dopamine Biosynthesis." *Journal of Neuroscience* 22, no. 8 (2002): 3090-3099.

Pilon, C., D. Lévesque, V. Dimitriadou, N. Griffon, M. P. Martres, J. C. Schwartz and P. Sokoloff. "Functional Coupling of the Human Dopamine D3 Receptor in a Transfected NG 108-15 Neuroblastoma-Glioma Hybrid Cell Line." *European Journal of Pharmacology* 268, no. 2 (1994): 129-139.

Pinter, M. M., O. Pogarell and W. H. Oertel. "Efficacy, Safety, and Tolerance of the Non-Ergoline Dopamine Agonist Pramipexole in the Treatment of Advanced Parkinson's Disease: A Double Blind, Placebo Controlled, Randomised, Multicentre Study." *Journal of Neuorlogy, Neurosurgery and Psychiatry* 66, no. 4 (1999): 436-441.

Przedborski, S., V. Jackson-Lewis, R. Djaldetti, G. Liberatore, M. Vila, S. Vukosavic and G. Almer. "The Parkinsonian Toxin MPTP: Action and Mechanism." *Restorative Neurology and Neuroscience* 16, no. 2 (2000): 135-142.

Recchia, A., P. Debetto, A. Negro, D. Guidolin, S. D. Skaper and P. Giusti. "Alpha-Synuclein and Parkinson's Disease." *FASEB Journal* 18, no. 6 (2004): 617-626.

Riddle, L. R., R. Kumar, S. A. Griffin, P. Grundt, A. H. Newman and R. R. Luedtke. "Evaluation of the D3 Dopamine Receptor Selective Agonist/Partial Agonist PG01042 on L-Dopa Dependent Animal Involuntary Movements in Rats." *Neuropharmacology* 60, no. 2-3 (2011): 284-294.

Ross, S. B. "Synaptic Concentration of Dopamine in the Mouse Striatum in Relationship to the Kinetic Properties of the Dopamine Receptors and Uptake Mechanism." *Journal of Neurochemistry* 56, no. 1 (1991): 22-29.

Ryoo, H. L., D. Pierrotti and J. N. Joyce. "Dopamine D3 Receptor Is Decreased and D2 Receptor Is Elevated in the Striatum of Parkinson's Disease." *Movement Disorders* 13, no. 5 (1998): 788-797.

Sautel, F., N. Griffon, D. Lévesque, C. Pilon, J. C. Schwartz and P. Sokoloff. "A Functional Test Identifies Dopamine Agonists Selective for D3 versus D2 Receptors." *Neuroreport* 6, no. 2 (1995): 329-332.

Savitt, J. M., V. L. Dawson and T. M. Dawson. "Diagnosis and Treatment of Parkinson Disease: Molecules to Medicine." *Journal of Clinical Investigation* 116, no. 7 (2006): 1744-1754.

Schapira, A. H. V., E. Bezard, J. Brotchie, F. Calon, G. L. Collingridge, B. Ferger, B. Hengerer, E. Hirsch, P. Jenner, N. Le Novére, J. A. Obeso, M. A. Schwarzschild, U. Spampinato and G. Davidai. "Novel Pharmacological Targets for

the Treatment of Parkinson's Disease." *Nature Reviews. Drug Discovery* 5, no. 10 (2006): 845-854.

Schrag, A. "Entacapone in the Treatment of Parkinson's Disease." *Lancet Neurology* 4, no. 6 (2005): 366-370.

Seeman, P., D. Nam, C. Ulpian, I. S. Liu and T. Tallerico. "New Dopamine Receptor, D2(Longer), with Unique TG Splice Site, in Human Brain." *Brain Research. Molecular Brain Research* 76, no. 1 (2000): 132-141.

Seeman, P. and D. Grigoriadis. "Dopamine Receptors in Brain and Periphery." *Neurochemistry International* 10, no. 1 (1987): 1-25.

Seiler, M. P. and R. Markstein. "Further Characterization of Structural Requirements for Agonists at the Striatal Dopamine D-1 Receptor. Studies with a Series of Monohydroxyaminotetralins on Dopamine-Sensitive Adenylate Cyclase and a Comparison with Dopamine Receptor Binding." *Molecular Pharmacology* 22, no. 2 (1982): 281-289.

Serpell, L. C., J. Berriman, R. Jakes, M. Goedert and R. A. Crowther. "Fiber Diffraction of Synthetic Alpha-Synuclein Filaments Shows Amyloid-Like Cross-Beta Conformation." *Proceedings of the National Academy of Sciences of the USA* 97, no. 9 (2000): 4897-4902.

Shapira, A. H. V., J. M. Cooper, D. Dexter, J. B. Clark, P. Jenner and C. D. Marsden. "Mitochondrial Complex I Deficiency in Parkinson's Disease." *Journal of Medicinal Chemistry* 54, no. 3 (1990): 823-827.

Sherer, T. B., R. Betarbet and J. T. Greenamyre. "Pathogensis of Parkinson's Disease." *Current Opinion in Investigational Drugs* 2, no. 5 (2001): 657-662.

Sherer, T. B., R. Betarbet and J. T. Grennamyre. "Environment, Mitochondria, and Parkinson's Disease." *Neuroscientist* 8, no. 3 (2002): 192-197.

Slee, E. A., C. Adrain and S. J. Martin. "Executioner Caspase-3, -6, and -7 Perform Distinct, Non-Redundant Roles During the Demolition Phase of Apoptosis." *Journal of Biological Chemistry* 276, no. 10 (2001): 7320-7326.

Smith, L. A., M. J. Jackson, G. Al-Barghouthy, S. Rose, M. Kuoppamaki, W. Olanow and P. Jenner. "Multiple Small Doses of Levodopa Plus Entacapone Produce Continuous Dopaminergic Stimulation and Reduce Dyskinesia Induction in MPTP-Treated Drug-Naive Primates." *Movement Disorders* 20, no. 3 (2005): 306-314.

Sokoloff, P., B. Giros, M. P. Martres, M. L. Bouthenet and J. C. Schwartz. "Molecular Cloning and Characterization of a Novel Dopamine Receptor (D3) as a Target for Neuroleptics." *Nature* 347, no. 6289 (1990): 146-151.

Spillantini, M. G., R. A. Crowther, R. Jakes, N. J. Cairns, P. L. Lantos and M. Goedert. "Filamentous Alpha-Synuclein Inclusions Link Multiple System Atrophy with Parkinson's Disease and Dementia with Lewy Bodies." *Neuroscience Letters* 251, no. 3 (1998a): 205-208.

Spillantini, M. G., R. A. Crowther, R. Jakes, M. Hasegawa and M. Goedert. "Alpha-Synuclein in Filamentous Inclusions of Lewy Bodies from Parkinson's Disease and Dementia with Lewy Bodies." *Proceedings of the National Academy of Sciences of the USA* 95, no. 11 (1998b): 6469-6473.

Stocchi, F., M. Tagliati and C. W. Olanow. "Treatment of Levodopa-Induced Motor Complications." *Movement Disorders* 23, no. Suppl 3 (2008): S599-S612.

Tuite, P. and J. Riss. "Recent Developments in the Pharmacological Treatment of Parkinson's Disease." *Expert Opinion on Investigational Drugs* 12, no. 8 (2003): 1335-1352.

Ungerstedt, U. "Postsynaptic Supersensitivity after 6-hydroxy-dopamine Induced Degeneration of the Nigro-Striatal Dopamine System." *Acta Physiologica Scandinavica. Supplementum* 367, (1971): 69-93.

Uversky, V. N., J. Li and A. L. Fink. "Metal-Triggered Structural Transformations, Aggregation, and Fibrillation of Human Alpha-Synuclein. A Possible Molecular NK between Parkinson's Disease and Heavy Metal Exposure." *Journal of Biological Chemistry* 276, no. 47 (2001a): 44284-44296.

Uversky, V. N., J. Li and A. L. Fink. "Pesticides Directly Accelerate the Rate of Alpha-Synuclein Fibril Formation: A Possible Factor in Parkinson's Disease." *FEBS letters* 500, no. 3 (2001b): 105-108.

Van den Buuse, M. and A. C. Lambrechts. "Effects of 7-hydroxy-N,N-di-n-propylaminotetralin on Behaviour and Blood Pressure of Spontaneously Hypertensive Rats." *European Journal of Pharmacology* 243, no. 2 (1993): 169-177.

Van Der Walt, J. M., K. K. Nicodemus, E. R. Martin, W. K. Scott, M. A. Nancy, R. L. Watts, J.P. Hubble, J. L. Haines, W. C. Koller, K. Lyons, R. Pahwa, M. B. Stern, A. Colcher, B. C. Hiner, J. Jankovic, W. G. Ondo, F. H. Allen, C. G. Goetz, G. W. Small, F. Mastaglia, J. M. Stajich, A. C. McLaurin, L. T. Middleton, B. L. Scott, D. E. Schmechel, M.A. Pericak-Vance and J. M. Vance. "Mitochondrial Polymorphisms Significantly Reduce the Risk of Parkinson Disease." *The American Journal of Human Genetics* 72, no. 4 (2003): 804-811.

Van Vliet, L. A., P. G. Tepper, D. Dijkstra, G. Damsma, H. Wikström, T. A. Pugsley, H. C. Akunne, T. G. Heffner, S. A. Glase and L. D. Wise. "Affinity for Dopamine D2, D3, and D4 Receptors of 2-Aminotetralins. Relevance of D2 Agonist Binding for Determination of Receptor Subtype Selectivity." *Journal of Medicinal Chemistry* 39, no. 21 (1996): 4233-4237.

Vincenzi, F. F. and T. R. Hinds. "Pramipexole Has Antioxidant Properties and Inhibits Lipid Peroxidation." *Proceedings of the Western Pharmacology Society* 41, (1998): 43-46.

Volles, M. J. and P. T. Landsbury Jr. "Vesicle Permeabilization by Protofibrillar Alpha-Synuclein Is Sensitive to Parkinson's Disease-Linked Mutations and Occurs by a Pore-Like Mechanism." *Biochemistry* 41, no. 14 (2002): 4595-4602.

Winner, B., R. Jappelli, S. K. Maji, P. A. Desplats, L. Boyer, S. Aigner, C. Hetzer, T. Loher, M. Vilar, S. Campioni, C. Tzitzilonis, A. Soragni, S. Jessberger, H. Mira, A. Consiglio, E. Pham, E. Masliah, F. H. Gage and R. Riek. "*In vivo* Demonstration That Alpha-Synuclein Oligomers Are Toxic." *Proceedings of the National Academy of Sciences of the USA* 108, no. 10 (2011): 4194-4199.

Wood, S. J., J. Wypych, S. Steavenson, J.-C. Louis, M. Citron and A. L. Biere. "Alpha-Synuclein Fibrillogenesis Is Nucleation-Dependent: Implications for the Pathogenesis of Parkinson's Disease." *Journal of Biological Chemistry* 274, no. 28 (1999): 19509-19512.

Xu, J., S. Y. Kao, F. J. Lee, W. Song, L. W. Jin and B. A. Yankner. "Dopamine-Dependent Neurotoxicity of Alpha-Synuclein: A Mechanism for Selective Neurodegeneration in Parkinson Disease." *Nature Medicine* 8, no. 6 (2002): 600-606.

Yang, L., R. T. Matthews, J. B. Schulz, T. Klockgether, A. W. Liao, J. C. Martinou, J. B. Penney Jr., B. T. Hyman and M. F. Beal. "1-Methyl-4-Phenyl-1,2,3,6-Tetrahydropyride Neurotoxicity Is Attenuated in Mice Overexpressing Bcl-2." *Journal of Neuroscience* 18, no. 20 (1998): 8145-8152.

Yi, H., W. Maruyama, Y. Akao, T. Takahashi, K. Iwasa, M. B. Youdim and M. Naoi. "N-Propargylamine Protects SH-SY5Y Cells from Apoptosis Induced by an Endogenous Neurotoxin, N-methyl(R)salsolinol, through Stabilization of Mitochondrial Membrane and Induction of Anti-Apoptotic Bcl-2." *Journal of Neural Transmission* 113, no. 1 (2006): 21-32.

Youdim, M. B. and M. Weinstock. "Molecular Basis of Neuroprotective Activities of Rasagiline and the Anti-Alzheimer Drug TV3326 [(N-propargyl-(3R)aminoindan-5-YL)-ethyl methyl carbamate]." *Cellular and Molecular Neurobiology* 21, no. 6 (2001): 555-573.

Zhou, Q. Y., D. K. Grandy, L. Thambi, J. A. Kushner, H. H. Van Tol, R. Cone, D. Pribnow, J. Salon, J. R. Bunzow and O. Civelli. "Cloning and Expression of Human and Rat D1 Dopamine Receptors." *Nature* 347, no. 6288 (1990): 76-80.

Zou, L., J. Jankovic, D. B. Rowe, W. Xie, S. H. Appel and W. Le. "Neuroprotection by Pramipexole against Dopamine- and Levodopa-Induced Cytotoxicity." *Life Sciences* 64, no. 15 (1999): 1275-1285.

"Effect of Deprenyl on the Progression of Disability in Early Parkinson's Disease. Parkinson Study Group." *New England Journal of Medicine* 321, no. 20 (1989): 1364-1371.

"Pramipexole vs Levodopa as Initial Treatment for Parkinson Disease: A Randomized Controlled Trial. Parkinson Study Group." *Journal of the American Medical Association* 284, no. 15 (2000): 1931-1938.

"Dopamine Transporter Brain Imaging to Assess the Effects of Pramipexole vs Levodopa on Parkinson Disease Progression. Parkinson Study Group." *Journal of the American Medical Association* 287, no. 13 (2002): 1653-1661.

ABSTRACT

PROGRESS TOWARDS DEVELOPMENT OF MULTIFUNCTIONAL, DOPAMINE D2/D3 RECEPTOR AGONISTS AS SYMPTOMATIC AND DISEASE-MODIFYING THERAPEUTIC AGENTS FOR PARKINSON'S DISEASE

by

MARK JOHNSON

August 2013

Advisor: Aloke Dutta, Ph. D.

Major: Pharmaceutical Sciences

Degree: Doctor of Philosophy

Parkinson's disease (PD) is a progressive, neurodegenerative disorder that arises primarily through the loss of dopaminergic neurons in the substantia nigra pars compacta, resulting in a diminished level of the neurotransmitter dopamine in the nigrostriatal pathway and ensuing loss of motor function. Common symptoms of PD include resting tremor, muscular rigidity, bradykinesia (slowness and decreased amplitude of movement), along with postural instability and cognitive psychiatric complications. PD affects 1% of the population $\geq$ 65 and is the second most prevalent neurodegenerative disorder next to Alzheimer's disease (AD). Although the etiology of PD is not yet clear and may be multifactorial, oxidative stress and mitochondrial dysfunction are thought to play a central role in the pathology of the disease. L-dopa, the biosynthetic precursor to DA, is the gold-standard treatment option for PD. Although initially beneficial in reducing motor symptoms, chronic L-dopa treatment causes pharmacoresistant involuntary movements, "on" and "off" phases and may even

exacerbate the progression of PD. It has become increasingly evident that for a complex disease such as PD, a drug aimed at one target site will only partially address the therapeutic need of the disease. Thus, it is hypothesized that multi-functional drugs, having multiple pharmacological activities, will be more effective in treating PD. Our approach in developing such agents involves alleviating symptoms of the disease, along with preventing or halting the neurodegeneration process. To this end, we have utilized our hybrid molecular template to design novel, D3-preferring agonists, with a range of selectivity for D3 receptor, while also incorporating antioxidant moieties to provide antioxidant capacity to the molecule. In this dissertation, we investigate the potential of our D3-preferring agonists to both alleviate motor dysfunction and modify the progression of PD.

AUTOBIOGRAPHICAL STATEMENT

MARK JOHNSON

Education

B.S. (Biomedical Sciences)   2006
Western Michigan University, Kalamazoo, MI

Professional Experience

Laboratory Technician/Technologist   2007-2008
Viral Immunological Testing Laboratory
American Red Cross, Detroit, MI

Awards and Honors

University Graduate Research Fellowship (UGRF) Dissertation Award   2011
Wayne State University, Detroit, MI

Graduate Student Professional Travel Award (GSPTA)   2011
Wayne State University, Detroit, MI

Publications

1. **Mark Johnson**, Tamara Antonio, Maarten Reith, Aloke Dutta; "Structure-activity-relationship study of N^6-(2-(4-(1H-indol-5-yl)piperazin-1-yl)ethyl)-N^6-propyl-4,5,6,7-tetrahydrobenzo[d]thiazole-2,6-diamine analogues: Development of highly selective D_3 dopamine receptor agonists along with a highly potent D_2/D_3 agonist and their pharmacological characterization" *J. Med. Chem.* 2012, 55, 5826-5840.

2. Bhaskar Gopishetty, Stuart Hazeldine, Soumava Santra, **Mark Johnson**, Gyan Modi, Solav Ali, Juan Zhen, Maarten Reith, Aloke Dutta; "Further structure-activity-relationship studies on 4-((((3S,6S)-6-benzhydryltetrahydro-2H-pyran-3-yl)amino)methyl)phenol: Identification of compounds with triple uptake inhibitory activity as potential antidepressant agents" *J. Med. Chem.* 2011, 54, 2924-2932.

Published Abstract and Presentation

1. **Mark Johnson**, Tamara Antonio, Maarten Reith, Aloke Dutta; "Structure-activity-relationship study of N^6-(2-(4-(1H-indol-5-yl)piperazin-1-yl)ethyl-N^6-propyl-4,5,6,7-tetrahydrobenzo[d]thiazole-2,6-diamine analogues: Development of highly selective D_3 dopamine receptor agonists and their pharmacological characterization" 243$^{rd.}$ American Chemical Society National Meeting and Exposition, San Diego, CA, USA, March 25-29, 2012.